Università degli Studi dell'Insubria
Department of Science and High Technology
PHD PROGRAM IN PHYSICS AND ASTROPHYSICS

Non-homogeneous random walks: from the transport properties to the statistics of occupation times

Doctoral Dissertation of:
Mattia Radice

Advisor:
Prof. Roberto Artuso

Supervisor of the Doctoral Program:
Prof. Giuliano Benenti

October 2020

Preface

This thesis embraces all the efforts that I put during the last three years as a PhD student at Università degli Studi dell' Insubria. I have been working under the supervision of Prof. Roberto Artuso, whom I firstly met as a teacher during my university years, and I have been collaborating with my longtime classmate Manuele Onofri, whom I owe many hours of discussions about our work. In this time frame I also had the wonderful opportunity of meeting a number of smart and interesting people, who encouraged me to explore the vast world of scientific research.

My research is all about *stochastic processes*, in particular *random walks*, focusing my attention on the effects of spatial inhomogeneity on the main properties of the dynamics. From a theoretical point of view, I found this topic very intriguing: indeed, although the theory of random walk in the presence of translational invariance has been well developed, little is known for system lacking this fundamental property, despite they represent the most typical case. This motivated me to pursue my objective of discovering as much as I could and sharing my findings, in order to improve, even for just a little bit, the knowledge on the matter.

By working on stochastic processes, I discovered their incredible importance in the modelling of physical systems - which I still find rather surprising. Indeed, even though Nature is ruled by deterministic laws of evolution, I have learnt that in many contexts the dynamics is so complex that it has to be understood in a statistical sense. Nevertheless, the fact that this approach can yield a good approximation of the behaviour of complex systems is far from being trivial, and, in my opinion, also very fascinating. Furthermore, the stochastic approach is also quite general and suitable not only for the physical context: from biology to chemistry, from finance to sociology, one finds that the analysis of stochastic processes helps in the solution of many problems, showing their unbelievably broad range of fields of application. This radically changed the way I look at things: I found my natural *thinking outside the box* attitude, which helped me improve as a person.

I am grateful to the humongous amount of people that, directly or indirectly, have contributed to my research, and, in particular, to this work. I must acknowledge support from whoever accompanied me during this three-years journey, which presented both bright and dark times. In particular, I thank my family for letting me focus entirely on my studies and develop my work in the best possible way. This thesis would have not been possible without their invaluable presence.

Mattia Radice
Como
January 2021

Abstract

This dissertation details our research on random walks seen as simple mathematical models useful to describe the complex dynamics of many physical systems. In particular, we focus on the role of spatial inhomogeneity in determining the deviations from the standard behaviour.

In the first chapter we present a general method that can be used to obtain the continuum limit for the evolution equations of a random walk with nearest neighbour jumps, from which one can derive the asymptotic properties and deduce the physical interpretation of the walk itself. Then in the following we adopt this method to discuss two particular models.

The first model, which we call *Gillis random walk*, is treated in the second chapter and consists in a random walk with space-dependent drift. Although lacking translational invariance, it provides one of the very few examples of a stochastic system allowing for a number of exact results. From the continuum limit, one deduces that this model provides a microscopical description for the problem of Brownian diffusion in a logarithmic potential, and indeed we compare the results regarding the diffusion problem already present in the literature with the behaviour of the Gillis random walk, finding good agreement.

The second model, which we have originally introduced in the literature and deal with in the third chapter, is a correlated random walk closely related to the *Lévy-Lorentz* gas, a stochastic system where a particle is scattered by static points arranged on a line in such a way that the distances between first neighbour scatterers are independent and identically distributed random variables, drawn from a heavy-tailed distribution. Our model results from a particular procedure of average over all possible arrangements of scatterers and it is mathematically described as a correlated random walk on the integer lattice, where at each step the particle can be either reflected or transmitted according to a space-dependent probability. We apply the continuum limit and derive the long-time properties of the system, which to some extent match those of the original Lévy-Lorentz gas.

In the fourth and last chapter we consider the problem of occupation times for one-dimensional random walks, showing that for a wide class of processes a single exponent related to a local property of the system is sufficient to describe the distributions of the variables of interests. We test our findings using the two stochastic models presented in the previous chapters and obtain good agreement with our theory. However, our result breaks down, for example, if we consider *continuous time random walk* models in which the distribution of waiting times between steps does not possess finite mean. Nevertheless, we show how also in this case the theory developed in the first part of the chapter is useful to obtain the statistics of occupation times. We revise some of the results already present in the literature in terms of our theory and test the results on a novel continuous time model based on the dynamics of the Gillis random walk, finding good agreement with both the literature and our theory.

Contents

List of Figures

List of Acronyms

Random walks and the connection with diffusion processes: the continuum limit 1

The elementary concepts of probability theory arose in the seventeenth century and found their first applications in the study of games of chance. Over time, the tools developed by the theory proved to be relevant in more complex contexts, and today their utility in the solution of scientific and technological problems is widely recognized. In particular, the theme of *random processes* plays an essential role, as it has found from its first introduction an enormous number of fields of applications, including physics, chemistry, biology, computer science, sociology, economics and finance.

In physics, the notion of random process grows from the need of describing the behaviour of complex systems by statistical equations of evolution. At first, this may seem unreasonable, since it is a matter of fact that the laws of physics are deterministic. However, there are many situations where the resulting motion, although produced by deterministic evolution equations, is sufficiently erratic that it may be regarded as random. A paradigmatic example is the case of *Brownian motion*, named after Robert Brown, the well-known British botanist who examined the motion of pollen grains in order to shed light on the mechanism by which the grains moved towards the ova when fertilising flowers [19]. According to Brown's first interpretation of the phenomenon, the erratic motion was a manifestation of life of the grains, but later experiments showed that the same jittery motion was observable also with apparently dead pollen, for example coming from inorganic matter.

For many years no satisfactory explanation to Brownian motion was provided. One of the first descriptions was given in 1880 by the Danish mathematician and astronomer Thorvald N. Thiele, in a paper on the method of least squares. Twenty years later Louis Bachelier derived and applied the equations of Brownian motion in his doctoral thesis, in which he studied the pricing fluctuations of shares and options in the stock market [4]. The first physical picture appeared in a famous paper by Einstein [36], in 1905, whose results were also obtained independently by Smoluchovski [109], responsible for much of the later development of the theory. The pioneering work of these two scientists was followed by many others - starting from Langevin in 1908 [73] - who contributed substantially in making clear the fundamental role of Brownian motion, and in general of stochastic processes, in the description and explanation of complex physical phenomena.

For the purposes of this thesis, it is worth spending a few words on Einstein's

solution to the problem of Brownian motion. In his idea, the motion of the pollen grain was caused by the exceedingly frequent impacts with the particles of the fluid in which it was suspended. Basing on a discrete-time assumption, he introduced a time interval τ, which could be considered very small compared to the observation time, but nevertheless sufficiently large that in two successive time intervals τ the motions executed by the particle could be considered independent events. Considering the x-coordinates of a particle, in a time interval τ he expected that the variation of the position could be described by an increment Δ, which he regarded as a random variable drawn from a symmetric *Probability Density Function* (PDF) $\phi(\sigma)$.

In this setting, let $p(x,t)$ be the density of particles in the interval $(x, x+\mathrm{d}x)$ at time t. The number of particles which at time $t+\tau$ are found in the interval $(x, x+\mathrm{d}x)$ equals the number of particles that at time t were found in the interval $(x-\sigma, x-\sigma+\mathrm{d}x)$ and jumped of an amount σ:

$$p(x,t+\tau)\mathrm{d}x = \mathrm{d}x \int_{-\infty}^{+\infty} p(x-\sigma,t)\phi(\sigma)\mathrm{d}\sigma. \tag{1.1}$$

Since τ is small, the left-hand side can be set to

$$p(x,t+\tau) = p(x,t) + \frac{\partial p(x,t)}{\partial t}\tau, \tag{1.2}$$

while on the right-hand side $p(x-\sigma,t)$ can be expanded in powers of σ up to second order. One obtains:

$$p + \frac{\partial p}{\partial t}\tau = p\int_{-\infty}^{+\infty}\phi(\sigma)\mathrm{d}\sigma + \frac{\partial p}{\partial x}\int_{-\infty}^{+\infty}\sigma\phi(\sigma)\mathrm{d}\sigma + \frac{1}{2}\frac{\partial^2 p}{\partial x^2}\int_{-\infty}^{+\infty}\sigma^2\phi(\sigma)\mathrm{d}\sigma. \tag{1.3}$$

By using the properties of normalization and symmetry of $\phi(\sigma)$, and setting

$$\frac{1}{\tau}\int_{-\infty}^{+\infty}\sigma^2\phi(\sigma) = D, \tag{1.4}$$

one arrives at the differential equation for the density of particles:

$$\frac{\partial p(x,t)}{\partial t} = \frac{1}{2}D\frac{\partial^2 p(x,t)}{\partial x^2}. \tag{1.5}$$

Eq. (1.5) is the diffusion equation, which at that time was already also known as heat equation, and D is called the diffusion coefficient. It is worth stressing one important feature of Einstein's approach: the evolution of a complex physical system was modelled with a simple mathematical object, namely a discrete-time random walk with independent and identically distributed increments; yet many of the important characteristics of the system could be captured in a satisfactory accuracy, and it was possible to assign a physical meaning to the parameters describing the motion by mapping them to those of the underlying mathematical model. For example, from Eq. (1.4) the diffusion coefficient can be defined as the mean square displacement of the particle per time interval, and this was the starting point for the second part of Einstein's work, where he finally related the diffusion coefficient to measurable physical quantities.

1.1 Characterization of the transport properties: normal and anomalous behaviour

This first example shows the relevance of the mathematical models of random walks in the description and analysis of complex systems. As for the case of Brownian motion, the most interesting quantity to derive is usually the *Mean Square Displacement* (MSD) of the process, which is used to characterize the transport properties of the quantity of interest.

Returning to the diffusion equation, Eq. (1.5), if we consider an initial condition where the particles are concentrated at the origin, the solution is the Gaussian PDF:

$$p(x,t) = \frac{1}{\sqrt{2\pi Dt}} e^{-\frac{x^2}{2Dt}}, \tag{1.6}$$

and the mean square displacement is defined as the second moment of the resulting distribution. It follows immediately that:

$$\langle x^2(t) \rangle = \int_{-\infty}^{\infty} x^2 p(x,t) \mathrm{d}x = Dt, \tag{1.7}$$

meaning that the MSD grows linearly with the observation time. Note that such a behaviour is determined entirely by the the solution of the diffusion equation, viz., by the PDF of the process. But there exists a well-known result, the *Central Limit Theorem* (CLT), stating that under proper rescaling the sum of independent and identically distributed random variables possessing finite mean and variance approaches, as the number of terms goes to infinity, the normal distribution. This means that a wide class of stochastic processes, whose random increments satisfy the hypotheses of the CLT, fall under the basin of attraction of the normal distribution, hence yielding a mean square displacement which grows linearly in time. The fact that such a behaviour is independent of the distribution of the increments makes it a *universal* result and for this reason these situations are referred to as *normal transport*.

Despite the huge range of systems for which transport can be classified as normal, there are still many cases where the MSD shows deviations from the linear behaviour. Today *anomalous transport* refers to an asymptotic power-law growth of the MSD of the kind:

$$\langle x(t) \rangle \sim t^{\nu}, \tag{1.8}$$

distinguishing between *subdiffusion* ($0 < \nu < 1$) and *superdiffusion* ($\nu > 1$). Subdiffusion has been observed in the diffusing motion of macromolecules and organelles in crowded environments of living cells [54], charge carriers transport in amorphous solids [105] and tracers dispersion in streamflows [106], to cite a few; superdiffusion describes for example the motion of microspheres in living eukaryotic cells [23], aphid movement [88] and even human mobility patterns [48]. Such situations reveal that the study of the mechanisms leading to anomalous diffusion is important from both a theoretical and practical point of view.

Recalling Einstein's derivation of Brownian motion, the result is based on three main assumptions: the independence of the individual particles; the existence of a small time scale beyond which individual displacement are statistically independent; and the existence of a common PDF $\phi(\sigma)$ describing all displacements, with zero mean and finite variance. Note that these assumptions respect the hypotheses of the CLT and hence the Gaussian form of the distribution is not surprising[1]. In general, one expects to observe anomalous diffusion when at least one of these assumptions is violated. The best-known case is probably the scenario of displacements' distributions not possessing finite first or second moment, e.g., fat-tailed distributions with a power-law decay:

$$\phi(\sigma) \sim \sigma^{-1-\alpha}, \quad 0 < \alpha < 2. \tag{1.9}$$

Exponents in such a range imply an infinite second moment, while in the restricted range $0 < \alpha \leq 1$ also the first moment is diverging. In such situations it holds a more general result, which is known under name of *Generalized Central Limit Theorem* (GCLT) [44]: the sum of independent and identically distributed random variables with symmetric distribution having a power-law tail as in Eq. (1.9) will fall in the basin of attraction of a Lévy stable law [63] rather than in that of the Gaussian distribution, which is the origin of the anomalous behaviour. Processes of this type are known in the literature as *Lévy flights*. We point out, however, that in these models yield a diverging second moment [2], therefore in many cases they provide an unphysical description of the phenomenon. For this reason, the related model of *Lévy walk* was introduced [108]: here the jumps length and the time duration of a jump are correlated, so that their ratio is always equal to a constant representing the fixed velocity of the walker. Thanks to to the fixed-velocity constraint, it is possible to compute the scaling of all moments, and in particular one finds that Lévy walks can describe correctly superdiffusion, with a second moment given by [24]:

$$\langle x^2(t) \rangle \sim \begin{cases} t^{3-\alpha} & 1 < \alpha < 2 \\ t^2 & \alpha \leq 1. \end{cases} \tag{1.10}$$

Conversely, a model used to describe subdiffusion is the *Continuous Time Random Walk* (CTRW). Rather than to the step length, the origin of the anomalies is due to random waiting times between successive steps, all drawn from a common distribution with density $\psi(t)$ not possessing a finite first moment. The paradigmatic case is that of waiting-time distribution with a power-law decay of the kind:

$$\psi(t) \sim t^{-1-\beta}, \quad 0 < \beta \leq 1. \tag{1.11}$$

The absence of the first moment is related to the absence of a time scale, i.e., a mean waiting time, characterizing the duration of the steps. The walker can wait for long times before performing a jump, hence the resulting motion is subdiffusive, with [63]:

$$\langle x^2(t) \rangle \sim t^{\beta}. \tag{1.12}$$

[1] The symmetry of the common distribution is not a necessary condition for the CLT to hold, but it is necessary to have a linear growth of the MSD.

Note that for exponents $\beta > 1$ the existence of the first moment assures the existence of a time scale τ for the jumps, which corresponds to one of Einstein's assumptions. Indeed in that case the process falls in the basin of attraction of the Normal distribution, and the MSD grows linearly with time[2].

It is important to observe that the models presented thus far have the important property of spatial homogeneity, meaning that the displacements are always identically distributed along the path. The validity of the two limit theorems we have mentioned is due to this fact, and also many of the other known results use this as a starting point. However, there are many examples where a correct modelling of the phenomenon requires position-dependent distributions of displacements. This may happen, e.g., in the presence of an external potential [16, 29, 50] or because of the disorder of the environment [58]. In general, the analysis of these kind of systems is often related to the solutions of highly non-trivial problems, which in most cases are very hard to find [57].

In the following we will focus on two major descriptions for space-dependent random systems: the first, which we will call *heterogeneous diffusion*, consists in processes where the distribution of the displacements has an explicit dependence on the position of the walker; the second, *diffusion in random environments*, is characterized by the fact that the jumps, although identically distributed, are performed only at random fixed positions, simulating the disorder of the environment in which the walker diffuses.

1.2 Heterogeneous diffusion

As we have seen, diffusion describes the dominant transport process on very small length scales. In homogeneous systems, the MSD is characterized by a linear time growth and a constant diffusion coefficient D. When diffusion happens in inhomogeneous systems, one or both of these features are not conserved. The sources of inhomogeneity may range from the presence of a temperature gradient [98] to locally varying viscosity of the solvent [72, 91], but these are just a couple of examples. To cite a specific case, Brownian motion with a space-dependent diffusion coefficient was used to model the dynamics of particles in a fluid confined between two nearly parallel walls [71], with the justification that the variation of the diffusivity D is due to the dependence of the particles hydrodynamic mobility on the gap width between the walls. Another example is the diffusion of particles in a medium with spatially dependent friction [103], where clearly the mobility is position-related: also in this case the dynamics is modelled by Brownian motion with a diffusion coefficient varying in space. A different case is the motion of atoms in a one-dimensional optical lattice formed by two counterpropagating laser beams with linear perpendicular polarization, which can be described, in momentum space and for large values of p, by Brownian motion in a logarithmic potential [81, 62].

[2]Note that this is true only as long as the dynamics is not influenced by any external field, otherwise we should expect a different behaviour depending on the nature of the bias.

Off course the examples are not limited to physics: in hydrology heterogeneous diffusion addresses the question of how to quantify contaminant transport in natural geological formations [30]. In biology for instance the diffusion of proteins in mammalian cell cytoplasm is modelled by Brownian motion with a space-dependent diffusion coefficient [67], and also the diffusion on DNA shows two-state kinetics with different diffusivities [117]. Many other examples can be encountered in finance [96], chemistry [41] and related fields.

The full representation of a heterogeneous diffusion process is made through the *Fokker-Planck equation*, which generalizes the heat equation, Eq. (1.5). It describes the time evolution of the probability density of a particle under the effect of drag forces and random forces. In one dimension it is expressed in the following way:

$$\frac{\partial p(x,t)}{\partial t} = -\frac{\partial}{\partial x}\left[\mu(x,t)p(x,t)\right] + \frac{1}{2}\frac{\partial^2}{\partial x^2}\left[D(x,t)p(x,t)\right], \tag{1.13}$$

where $\mu(x,t)$ is the *drift* and $D(x,t)$ is the *diffusion coefficient*. When both the drift and the diffusion coefficient are time-independent, we say that the process is time-homogeneous, and in the following we always consider time-homogeneous processes. Note that the Fokker-Planck equation is in the form of a continuity equation

$$\frac{\partial p(x,t)}{\partial t} = -\frac{\partial J(x,t)}{\partial x}, \tag{1.14}$$

where the probability current is given by

$$J(x,t) = \frac{\partial}{\partial x}\left\{\mu(x,t)p(x,t) - \frac{1}{2}\frac{\partial}{\partial x}\left[D(x,t)p(x,t)\right]\right\}. \tag{1.15}$$

Usually the Fokker-Planck equation in practical problems is associated with the initial condition

$$p(x,t_0) = \delta(x - x_0), \tag{1.16}$$

describing a packet of particles initially located at a point x_0, which spreads at later times according to Eq. (1.13). It is not possible to solve the equation in general, but only for few cases. However, we can still get a picture of the evolution process if we consider it for short times after t_0. Note that the solution will be still close to a delta function, and hence the derivatives of $\mu(x,t)$ and $D(x,t)$ will be negligible with respect to those of $p(x,t)$. Therefore the probability density will obey, approximately:

$$\frac{\partial p(x,t)}{\partial t} = -\mu(x_0,t_0)\frac{\partial p(x,t)}{\partial x} + \frac{1}{2}D(x_0,t_0)\frac{\partial^2 p(x,t)}{\partial x^2}, \tag{1.17}$$

where also the time dependence of μ and D has been neglected. The solution is a Gaussian, with mean $x_0 + \mu(x_0,t_0)t$ and variance $D(x_0,t_0)t$. Therefore the packet initially spreads under the effect of a Gaussian fluctuation with variance $D(x_0,t_0)t$

and a systematic drift with velocity $\mu(x_0, t_0)$ - hence the names drift and diffusion coefficient [41].

It is important to observe that the Fokker-Planck equation only describes processes whose sample paths are continuous. For more general processes, such as Lévy flights, where the possibility of instantaneous long jumps is not neglected and the corresponding paths are not continuous, other kinds of evolution equations must be considered [90]. This topic, however, is beyond the scope of this thesis.

1.3 Random walks in random environments

Up to this moment we have considered systems for which the nature of the disorder is temporal, resulting from random jumps performed by the evolving observable at fixed time steps. In many situation instead the disorder is frozen in space, resulting from the irregularity of the "medium" in which the motion occurs. In general, for such situations not much can be said, except when some degree of homogeneity can be assumed for the law of the environment. A *Random Walk in a Random Environment* (RWRE) can be seen as a random walk on the $\mathbb{Z}^d$ lattice, with nearest neighbour jumps, occurring in a random medium with a stationary law [122].

A motivation for the study of such systems is the modelling of light particle dynamics in dense gases [49], for which a simple model, the *Lorentz gas*, provides a basic description. In the Lorentz gas a particle initially moves with a fixed momentum and then scatters elastically off randomly located fixed scatterers. This model can also be studied in one dimension, introducing a transmission probability of the particle through the heavier molecules. In this sense, the Lorentz gas and, more generally, a RWRE, can be seen as a generalization of the *correlated random walk* on $\mathbb{Z}^d$, in which a moving particle hops between nearest-neighbouring sites choosing at each step, according to a certain probability $\mathfrak{t}$, whether to change or preserve the previous direction of motion [104]. Note that for $\mathfrak{t} \neq \frac{1}{2}$, this model is substantially different from that of the simple symmetric random walk, because the transition probabilities depend on the previous state of the walker. In a RWRE, the changes of direction can only be taken at fixed sites, whose position is randomly chosen when defining the environment.

To take into account both the randomness of the motion and the irregularity of the environment, there are two ways to study a RWRE. Roughly speaking, let us call Ω the set of all possible environments, P the law defined on it and ω the generic element of Ω, i.e., a possible environment; each ω has law P_ω, which defines the transition probabilities of the process defined on it. The law P_ω is called the *quenched* law and it is therefore specific to the individual environment. This corresponds to the study of the evolution of the process on a fixed environment and we will refer to this case as the quenched version of the RWRE. On the other hand, to consider the entire randomness of the system, one defines the *annealed* law, which measures each individual P_ω with respect to P. In other words, one studies the process on each environment and then considers an "averaged" process with respect to the law of Ω. We will refer to this case

as the annealed version. For more rigorous and mathematically precise definitions, see [122, 12].

Note that the study of RWRE's is not in general an easy task. Mathematically, and especially for dimensions higher than 1, the model leads to the analysis of irreversible, inhomogeneous Markov chains, to which standard tools of homogenization theory do not apply well. Furthermore, unusual phenomena such as super and sub-diffusive behaviour, polynomial decay of probabilities of large deviations and trapping effects, arise already in one dimension [122]. Therefore it is not surprising that such models have been extensively used for the study of anomalous transport in complex systems. For a detailed literature, see also [58].

1.4 The discrete approach: random walks and the continuum limit

In this thesis we will adopt a discrete approach to the analysis of random processes, which was already suggested by Smoluchovski and applied to the theory of Brownian motion. We will focus on the one-dimensional case and we will mainly consider random walks on the $\mathbb{Z}$ lattice with nearest-neighbour jumps. Beside being the natural model for the treatment of RWRE's, it is widely recognized that random walk models also provide us with a good approximation to the theory of diffusion. On the other hand, it is also known that theories based on the Fokker-Planck equation become valid only for time and length scales much larger than those at the microscopic level. This leads to seemingly paradoxical conclusions, e.g., the fact that the velocity of a Brownian particle is infinite, which result from stretching the theory beyond the bound of its applicability [59]. Instead, random walks often yield with good approximation a qualitative description of the process at very short scales. Indeed, random walks on ordered and disordered lattices have found a number of applications in chemistry and solid state physics [92, 51].

The connection between random walks and diffusion processes is made through the *continuum limit* [38, 57, 43]. This procedure can be seen as an analogy with Einstein's description of Brownian motion, according to which the observable effect is caused by the many molecular shocks experienced by the diffusing particle. Although each impact provides a negligible contribution, the superposition of a large number of them yields a macroscopic outcome. In the same way, the continuum limit consists in studying random walks where the individual steps, though extremely small, occur in such a rapid succession that in the limit the process produces an observable continuous motion. This is equivalent to studying the process over scales much greater compared to the fundamental stepping time and hopping length.

To consider the continuum limit for a random walk on $\mathbb{Z}$ with nearest-neighbour jumps, the starting point is the time evolution of the probability $P_n(k)$ of being at site

k after n steps, which can be expressed in terms of the following quantities:

$$\phi_R(k) = \text{Probability of jumping to the right when at site } k \tag{1.18}$$
$$\phi_L(k) = \text{Probability of jumping to the left when at site } k \tag{1.19}$$
$$\phi_S(k) = \text{Probability of not jumping when at site } k, \tag{1.20}$$

which obey the normalization condition $\phi_R(k) + \phi_L(k) + \phi_S(k) = 1$. Here we are considering the case in which the transition probabilities can depend on the position on the lattice and the walker is not constrained to jump at each step. We define

$$R_n(k) = P_n(k)\phi_R(k) \tag{1.21}$$
$$L_n(k) = P_n(k)\phi_L(k), \tag{1.22}$$

where $R_n(k)$ and $L_n(k)$ represent the probabilities of being at site k after n steps and then jumping to the right or left, respectively. Note that

$$P_n(k) = R_n(k) + L_n(k) + \phi_S(k)P_n(k). \tag{1.23}$$

The Chapman-Kolmogorov equation for the time evolution of the probability is:

$$P_{n+1}(k) = R_n(k-1) + L_n(k+1) + \phi_S(k)P_n(k). \tag{1.24}$$

Let δx the lattice spacing and δt the time between two consecutive steps. To perform the continuum limit, one seeks a function $p(x,t)$ of the continuous variables x and t such that when δx and δt become small, $p(x,t)$ becomes the probability density function for the position x of the walker at time t. We have to keep in mind, however, that for any finite n, the collection of the $P_n(k)$ is a set of delta functions rather than a continuous function. Therefore, the limit should be rather understood in terms of the sum of $P_n(k)$ over an interval approaching the integral of $p(x,t)$ over the same interval. In other words, we seek $p(x,t)$ such that

$$\lim \sum_{x_0 \le k\delta x \le x_1} P_n(k) = \int_{x_0}^{x_1} p(x,t)\mathrm{d}x. \tag{1.25}$$

In order to find $p(x,t)$, we call $x = k\delta x$ and $t = n\delta t$ and set

$$P_n(k) \approx p(k\delta x, n\delta t)\delta x \tag{1.26}$$
$$R_n(k) \approx r(k\delta x, n\delta t)\delta x \tag{1.27}$$
$$L_n(k) \approx l(k\delta x, n\delta t)\delta x \tag{1.28}$$

where $r(x,t)\delta x$ represents the fraction of particles that at time t are in a small interval of size δx centred around x, moving to the right, while $l(x,t)\delta x$ represents the fraction in the same interval that at the same instant t are moving to the left. Define:

$$\begin{aligned} a(k\delta x, n\delta t)\delta t &= r(k\delta x, n\delta t)\delta x - l(k\delta x, n\delta t)\delta x \\ &= p(k\delta x, n\delta t)\left[\phi_R(k) - \phi_L(k)\right]\delta x \end{aligned} \tag{1.29}$$

where $a(x,t)$ represents a probability drift in the positive direction - indeed, it is the difference between the density of particles that are in $(x-\frac{1}{2}\delta x, x+\frac{1}{2}\delta x)$ at time t and moving to the right, and the density of those in the same interval at the same time moving to the left, times their velocity. We assume that all functions are twice differentiable with respect to both x and t, and we seek the continuum limit of equation (1.24):

(i) on the l.h.s we expand up to first order in δt, obtaining:

$$\frac{P_{n+1}(k)}{\delta x} \approx p(x,t+\delta t) = p(x,t) + \frac{\partial p(x,t)}{\partial t}\delta t + o(\delta t);$$

(ii) on the r.h.s. we consider $R_n(k-1) + L_n(k+1)$ which is expressed in terms of continuous functions by

$$\frac{R_n(k-1)+L_n(k+1)}{\delta x} \approx r(x-\delta x,t) - l(x+\delta x,t).$$

By expanding up to second order in δx, we get

$$r(x-\delta x,t) - l(x+\delta x,t) = r(x,t) + l(x,t) - \frac{\partial r(x,t)}{\partial x}\delta x + \frac{\partial l(x,t)}{\partial x}\delta x + \frac{1}{2}\frac{\partial^2 r(x,t)}{\partial x^2}\delta x^2 + \frac{1}{2}\frac{\partial^2 l(x,t)}{\partial x^2}\delta x^2 + o(\delta x^2).$$

From the definitions (1.21), (1.22) and (1.29), we can finally substitute

$$r(x,t) + l(x,t) = [1-\phi_S(k)]\, p(x,t)\delta x$$
$$\left[\frac{\partial r(x,t)}{\partial x} - \frac{\partial l(x,t)}{\partial x}\right]\delta x = \frac{\partial a(x,t)}{\partial x}\delta t$$
$$\left[\frac{\partial^2 r}{\partial x^2} + \frac{\partial^2 l}{\partial x^2}\right]\delta x^2 = \frac{\partial^2}{\partial x^2}\left\{[1-\phi_S(k)]\, p(x,t)\right\}\delta x^2.$$

Plugging the two expansions in Eq. (1.24), we get the equation for $p(x,t)$:

$$\frac{\partial p(x,t)}{\partial t} = -\frac{\partial}{\partial x}\left\{a(x,t) - \frac{1}{2}\frac{\delta x^2}{\delta t}\frac{\partial}{\partial x}\left[(1-\phi_S(k))\, p(x,t)\right]\right\}, \tag{1.30}$$

which has the form of a Fokker-Planck equation, with the current $J(x,t)$ given by:

$$J(x,t) = a(x,t) - \frac{1}{2}\frac{\delta x^2}{\delta t}\frac{\partial}{\partial x}\left[(1-\phi_S(k))\, p(x,t)\right]. \tag{1.31}$$

Finally, in order to capture the continuum limit, we let δx and δt go to zero in such a way that the current $J(x,t)$ remains well-defined. However, note that here the probability $\phi_S(k)$ is still written in terms of the discrete variable $k = x/\delta x$, and the quantity $a(x,t)$, representing the probability drift, is defined through the difference

$\phi_R(k) - \phi_L(k)$ as well, see Eq. (1.29). Therefore, to obtain the correct Fokker-Planck equation we need to consider the expressions of the jump probabilities in terms of the continuum variable x and the lattice spacing δx, and take into account how they scale as the limit $\delta x, \delta t \to 0$ is approached. To give a better understanding of this statement, in the following we will consider some easy practical example for which the continuum limit can be captured correctly.

1.4.1 Bernoulli random walk

In a Bernoulli random walk a particle moves on $\mathbb{Z}$ making steps to the right with probability p or to the left with probability $q = 1 - p$:

$$\phi_R(k) = p$$
$$\phi_L(k) = q$$
$$\phi_S(k) = 0.$$

Therefore, in this case the probability drift is defined as

$$a(x,t) = \frac{\delta x}{\delta t}(p-q)p(x,t), \tag{1.32}$$

and hence the current is

$$J(x,t) = \frac{\delta x}{\delta t}(p-q)p(x,t) - \frac{1}{2}\frac{\delta x^2}{\delta t}\frac{\partial p(x,t)}{\partial x}. \tag{1.33}$$

As long as the difference $p - q$ remains finite, we see that to have a meaningful limit δx and δt must approach 0 in such a way that their ratio is kept constant. In this case, setting $c = \delta x/\delta t$, in the limit one obtains

$$\frac{\partial p(x,t)}{\partial t} = -v\frac{\partial p(x,t)}{\partial x}, \tag{1.34}$$

where $v = (p-q)c$. This corresponds to a Fokker-Planck equation with a vanishing diffusion coefficient, i.e., a deterministic motion. Indeed, in this case the solution corresponding to the initial condition $p(x,0) = \delta(x - x_0)$ is

$$p(x,t) = \delta(x - x_0 - vt), \tag{1.35}$$

i.e., a deterministic drift with velocity v. To obtain an equation describing both the deterministic drift and the random fluctuations, we need both terms on the r.h.s. of equation (1.33) to be non-vanishing in the limit. This can be achieved by imposing that the ratio $\delta x^2/\delta t$, rather than $\delta x/\delta t$, remains finite, and consequently that the difference $p - q$ be of order of δx. Therefore, by setting

$$p = \frac{1}{2} + \frac{v}{2D}\delta x$$
$$q = \frac{1}{2} - \frac{v}{2D}\delta x,$$

the current takes the form

$$J(x,t) = \frac{\delta x^2}{\delta t}\left[\frac{v}{D}p(x,t) - \frac{1}{2}\frac{\partial p(x,t)}{\partial x}\right], \tag{1.36}$$

and in the limit $\delta x, \delta t \to 0$, with $\delta x^2/\delta t = D$ kept constant, we get the following Fokker-Planck equation for the probability density function:

$$\frac{\partial p(x,t)}{\partial t} = -v\frac{\partial p(x,t)}{\partial x} + \frac{1}{2}D\frac{\partial^2 p(x,t)}{\partial x^2}. \tag{1.37}$$

Note that this equation can be simplified with the aid of the substitution[3]

$$y = \frac{x - vt}{\sqrt{Dt}}, \tag{1.38}$$

from which we obtain

$$-y\frac{\mathrm{d}p}{\mathrm{d}y} = \frac{\mathrm{d}^2 p}{\mathrm{d}y^2}. \tag{1.39}$$

It is easy to find the general solution and hence the solution of the original problem. For an initial condition of the kind $p(x,0) = \delta(x - x_0)$ we find:

$$p(x,t) = \frac{1}{\sqrt{2\pi Dt}}e^{-\frac{(x-x_0-vt)^2}{2Dt}}. \tag{1.40}$$

This solution is not surprising, since it is a consequence of the CLT. Indeed the Bernoulli walk is a sum of independent and identically distributed random variables with finite mean and variance and hence the probability distribution of the position expected to follow a Gaussian distribution, in the limit of large number of steps. In the continuum limit, as observed in [38], the theorem is still valid because the chosen scaling for the lattice spacing and the time step guarantees the finiteness of both the mean and the variance of the individual steps. Note that in the previous case we chose to keep constant the ratio $\delta x/\delta t$, which led to a vanishing variance in the limit, and indeed the solution in that case is a delta function. This shows that, as we already observed for the diffusion equation, the choice of the scaling strongly affects the limiting form of the probability distribution.

1.4.2 Kac random walk

The Kac random walk describes a particle subject to an elastic force directed towards the centre of coordinates and random fluctuations. The model was presented by Mark Kac in 1947 [59] to generalize Einstein's and Smoluchovski's discrete approaches to the theory of diffusion, in the presence of deterministic forces. It is defined on

[3] This substitution is suggested by the CLT.

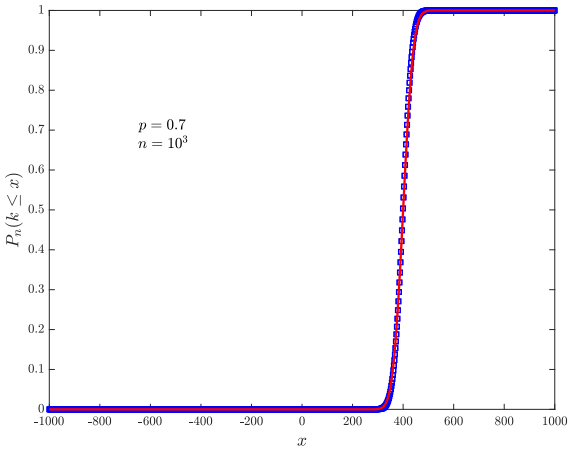

FIGURE 1.1: Cumulative distribution for the position k after $n = 10^3$ steps for the Bernoulli random walk, with $p = 0.7$. Data (blue squares) are compared to the result yielded by the continuum limit, Eq. (1.40)

a box $-M \leq k \leq M$ with reflecting boundaries condition, with the following jump probabilities depending on the walker's position:

$$\phi_R(k) = \frac{1}{2}\left(1 - \frac{k}{M}\right)$$
$$\phi_L(k) = \frac{1}{2}\left(1 + \frac{k}{M}\right)$$
$$\phi_S(k) = 0.$$

We want to derive in the continuum limit the evolution equation for the probability of the displacement of the walker. We can obtain the probability drift in terms of the continuous variables by substituting in the definition (1.29) the discrete indexes k and n with $x/\delta x$ and $t/\delta t$, respectively:

$$a(x,t) = -p(x,t)\frac{x}{M\delta x}\frac{\delta x}{\delta t} = -p(x,t)\frac{x}{M\delta t}. \tag{1.41}$$

Thus the current is

$$J(x,t) = -p(x,t)\frac{x}{M\delta t} - \frac{1}{2}\frac{\delta x^2}{\delta t}\frac{\partial p(x,t)}{\partial x}. \tag{1.42}$$

We see from this expression that when δx and δt approach zero, the second term on the r.h.s requires that the ratio $\delta x^2/\delta t$ is kept constant, while the first term suggests that M must diverge in such a way that the product $M\delta t$ remains finite. Hence by considering the limits $\delta x \to 0$, $\delta t \to 0$ and $M \to \infty$, with

$$\frac{\delta x^2}{\delta t} \to D \quad \text{and} \quad \frac{1}{M\delta t} \to \gamma,$$

the resulting diffusion equation is

$$\frac{\partial p(x,t)}{\partial t} = \gamma \frac{\partial}{\partial x}\left[x p(x,t)\right] + \frac{1}{2} D \frac{\partial^2 p(x,t)}{\partial x^2}, \tag{1.43}$$

which is the Fokker-Planck equation of the Ornstein-Uhlenbeck process. For the initial condition $p(x,0) = \delta(x - x_0)$, one finds the solution [41]:

$$p(x,t) = \sqrt{\frac{\gamma}{\pi D\left(1 - e^{-2\gamma t}\right)}} \exp\left[-\frac{\gamma}{D}\frac{\left(x - x_0 e^{-\gamma t}\right)^2}{1 - e^{-2\gamma t}}\right]. \tag{1.44}$$

The fact that the probability of the displacement of the walker converges - in the sense we have mentioned earlier, see Eq. (1.25) - to the solution of the Fokker-Planck equation of the Ornstein-Uhlenbeck process was proved rigorously by Kac.

Interestingly, the Kac random walk is analogous to the formulation of a problem proposed by P. and T. Ehrenfest to describe heat exchange between two isolated bodies [35]. Let us consider $2M$ balls distributed in two boxes, A and B. At random and with uniform probability, a ball is chosen and moved to the other box, and the process is repeated n times. If we denote with $2k$ the difference between the number of balls in box A and B, it is easy to see that at each step the probability of increasing the number of balls in A by one unit is

$$\phi_+(k) = \frac{M - k}{2M}, \tag{1.45}$$

which is the same probability of jumping to the right for the Kac random walk. In this model the number of balls in each box represents the temperatures of the two bodies, and the random process of moving the balls describes the heath exchange. Off course we expect that the process reaches an equilibrium state, since eventually the two bodies must acquire the same temperature. The validity of the continuum limit can be examined by observing that indeed, from the solution of the Fokker-Planck equation, the process reaches a stationary distribution, which is exponentially decaying for values outside the origin. Moreover, if we consider the average excess over M of the number of balls in the first box, it is easy to see that Eq. (1.44) yields:

$$\langle x(t) \rangle = x_0 e^{-\gamma t}, \tag{1.46}$$

which can be interpreted as Newton's law of cooling. The same result can be obtained from the discrete model, and then evaluating the limit for a large number of balls [59].

1.4.3 Kac random walk with bias

We can generalize the Kac random walk by including a constant force towards the positive direction, and find the corresponding Fokker-Planck equation in the continuum

limit. We define the walk on an asymmetric box $-M+m \leq k \leq M+m$, and

$$\phi_R(k) = \frac{1}{2}\left(1 - \frac{k-m}{M}\right)$$
$$\phi_L(k) = \frac{1}{2}\left(1 + \frac{k-m}{M}\right)$$
$$\phi_S(k) = 0.$$

From the definition of the probability drift (1.25) we have

$$a(x,t) = -p(x,t)\left[\frac{x}{M\delta x} - \frac{m}{M}\right]\frac{\delta x}{\delta t} = -p(x,t)\left[\frac{x}{M\delta t} - \frac{m\delta x}{M\delta t}\right], \tag{1.47}$$

and thus the current is

$$J(x,t) = -p(x,t)\left[\frac{x}{M\delta t} - \frac{m\delta x}{M\delta t}\right] - \frac{1}{2}\frac{\delta x^2}{\delta t}\frac{\partial p(x,t)}{\partial x}. \tag{1.48}$$

This means that with respect to the previous case we ought to add the condition $m \to \infty$ in such a way that the product $m\delta x$ remains finite[4]. Thus by considering the limits $\delta x, \delta t \to 0$ and $M, m \to \infty$, with

$$\frac{\delta x^2}{\delta t} \to D, \quad \frac{1}{M\delta t} \to \gamma \quad \text{and} \quad m\delta x \to \xi, \tag{1.49}$$

the resulting equation is

$$\frac{\partial p(x,t)}{\partial t} = -\gamma\frac{\partial}{\partial x}\left[(\xi - x)p(x,t)\right] + \frac{1}{2}D\frac{\partial^2 p(x,t)}{\partial x^2}, \tag{1.50}$$

which is a modification of the Ornstein-Uhlenbeck process, known in financial mathematics as the Vasicek model. In this case the solution corresponding to the initial condition $p(x,0) = \delta(x - x_0)$ is

$$p(x,t) = \sqrt{\frac{\gamma}{\pi D\left(1 - e^{-2\gamma t}\right)}}\exp\left\{-\frac{\gamma}{D}\frac{\left[x - x_0 e^{-\gamma t} - \xi\left(1 - e^{-\gamma t}\right)\right]^2}{1 - e^{-2\gamma t}}\right\}, \tag{1.51}$$

i.e., a Gaussian with mean

$$\langle x(t)\rangle = x_0 e^{-\gamma t} + \xi\left(1 - e^{-\gamma t}\right) \tag{1.52}$$

and variance

$$\langle x^2(t)\rangle - \langle x(t)\rangle^2 = \frac{D}{2\gamma}\left(1 - e^{-2\gamma t}\right). \tag{1.53}$$

[4]Note that this implies that we should take $M = O(m^2)$.

Note that in this case the MSD in the long-time limit converges to

$$\langle [x(t) - x_0]^2 \rangle \to \frac{D}{2\gamma} + (\xi - x_0)^2 , \tag{1.54}$$

indeed the process reaches a stationary distribution, as suggested by Eq. (1.51), yielding a finite second moment[5]:

$$p_s(x) = \sqrt{\frac{\gamma}{\pi D}} e^{-\frac{\gamma}{D}(x-\xi)^2} . \tag{1.55}$$

Note that in the limit $\xi \to 0$ we can recover the results obtained for the Ornstein-Uhlenbeck process.

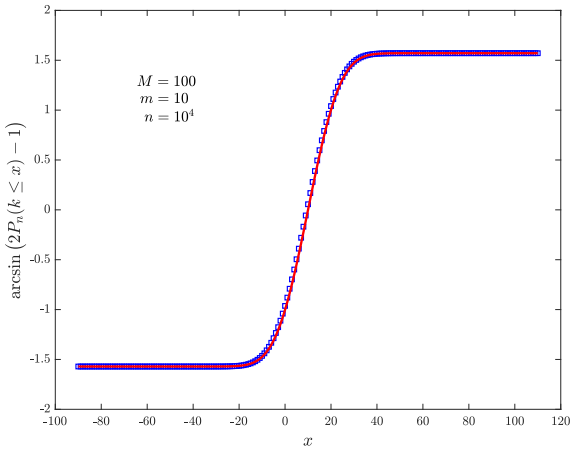

FIGURE 1.2: Cumulative distribution for the position k after $n = 10^4$ steps for the Kac random walk with bias, with $M = 100$ and $m = 10$. Data (blue squares) are compared to the result yielded by the continuum limit, Eq. (1.55)

1.4.4 Moran model

The Moran model is one of the most commonly used reproduction schemes in population genetics[14, 66, 93]. According to this scheme, an individual is characterized by a set of hereditary traits which are collectively referred to as its *type*. The most important trait governing the dynamics of each type is the *fitness* f, which quantifies the reproductive success of the individual. In the Moran model individuals reproduce asexually in a population consisting of a fixed number K of individuals. At each time step, an individual is chosen randomly for reproduction, with probability proportional to its fitness, creating an offspring of the same type. At the same time, to maintain the constraint of fixed population size, an individual is killed at random. All individuals are equally likely to be killed, except the newborn offspring.

[5] More generally, it can be shown that all moments are finite.

We consider the simple case of a population split in two types, A and B, with fitnesses denoted as f_A and f_B, respectively. The fitness of the A-type with respect to the B-type is expressed in terms of the *selection coefficient* s, which is positive if $f_A > f_B$, i.e., we can set

$$f_A = 1 + s$$
$$f_B = 1.$$

Since there are only two types, it is sufficient to consider the evolution of of the number of individuals of the A-type, which from now on we will denote with k. In the Moran model, discrete time steps are considered in such a way that at each iteration the population can increase or decrease by one unit, or not change. The transition probabilities are:

$$\phi_+(k) = (1+s)\frac{k}{K}\left(1 - \frac{k}{K}\right)$$
$$\phi_-(k) = \frac{k}{K}\left(1 - \frac{k}{K}\right)$$
$$\phi_0(k) = 1 - \phi_+(k) - \phi_-(k).$$

Note that the transitions are well defined as long as $-1 \leq s \leq 2$. The process corresponds to a random walk on $\{0, \ldots, K\}$ and we seek the evolution equation for the probability $P_n(k)$ of having k A-type individuals at time step t, in the limit where $K \to \infty$. We call δx the lattice spacing and δt the time between successive steps. In the continuous variables $x = k\delta x$ and $t = n\delta t$ the expression for the current is

$$J(x,t) = a(x,t) - \frac{1}{2}\frac{\delta x^2}{\delta t}\frac{\partial}{\partial x}\left[(2+s)\,\frac{x}{K\delta x}\left(1 - \frac{x}{K\delta x}\right)p(x,t)\right], \tag{1.56}$$

where

$$a(x,t) = s\frac{x}{K\delta x}\left(1 - \frac{x}{K\delta x}\right)\frac{\delta x}{\delta t}. \tag{1.57}$$

The product $K\delta x$ appearing in the denominator suggests that in the continuum limit we let the population size K increase with the same scale with which the lattice spacing goes to zero, so that $K\delta x \equiv X$ remains constant. Note that differently from the previous case, this implies that the variable x remains bounded. If we conveniently set $X = 1$, then $x \in [0,1]$ represents the population fraction of the A-type. At this point, the resulting diffusion equation depends on how the selection coefficient scales with the lattice spacing [14, 116]:

i) if $s = O(\delta x)$, say $s = \sigma\delta x$, then by keeping $\delta x^2/\delta t$ constant we get the *weak selection regime* [66]:

$$\frac{\partial p(x,t)}{\partial t} = -D\frac{\partial}{\partial x}\left\{\sigma x(1-x)p(x,t) - \frac{\partial}{\partial x}\left[x(1-x)p(x,t)\right]\right\}; \tag{1.58}$$

ii) if $s = o(\delta x)$, then only the diffusion term is relevant, and we get, by setting $\delta x^2/\delta t = D$:

$$\frac{\partial p(x,t)}{\partial t} = D\frac{\partial^2}{\partial x^2}\Big[x(1-x)p(x,t)\Big]; \tag{1.59}$$

iii) if s remains finite in the limit, the dominant term is the drift term. This time, by keeping $\delta x/\delta t$ constant and calling $v = s\delta x/\delta t$ the drift velocity, we have the so-called *strong selection regime* [66]:

$$\frac{\partial p(x,t)}{\partial t} = -v\frac{\partial}{\partial x}\Big[x(1-x)p(x,t)\Big]. \tag{1.60}$$

We stress once more that the chosen scaling implies a precise relation between the continuous coordinates x and t, and the population size. Indeed the definition of the x variable can be reformulated as $x = k/K$, while the t variable can be defined as $t = n/K^2$. See [14, 66] to have an insight regarding the physical implication and the interpretation of this fact.

1.4.5 Correlated random walk

The correlated random walk, or persistent random walk, is a non-trivial generalization of the simple symmetric random walk on $\mathbb{Z}$. In this model, a particle starts moving from x_0 with constant velocity in a random direction, and then at each step it can either reverse or preserve the direction of motion, according to the probabilities $\mathfrak{r}$ and $\mathfrak{t} = 1-\mathfrak{r}$, respectively. The model was presented in [104], along with some initial results. Note that the knowledge of the position of the particle at time n is not sufficient to determine the state of the process one step later, as it is also required information on the position at step $n-1$[6]. For this reason, the evolution equations ought to be put in a slightly different manner.

We call

$$R_n(k) = \text{Probability of being at site } k \text{ after } n \text{ steps, with velocity to the right} \tag{1.61}$$
$$L_n(k) = \text{Probability of being at site } k \text{ after } n \text{ steps, with velocity to the left,} \tag{1.62}$$

and

$$A_n(k) = R_n(k) - L_n(k) \tag{1.63}$$

the probability drift. In this case, it is easier to write first the equations for $R_n(k)$ and $L_n(k)$, which read:

$$\begin{cases} R_{n+1}(k) = \mathfrak{t}\cdot R_n(k-1) + \mathfrak{r}\cdot L_n(k+1) & (1.64)\\ L_{n+1}(k) = \mathfrak{t}\cdot L_n(k+1) + \mathfrak{r}\cdot R_n(k-1). & (1.65)\end{cases}$$

[6]Indeed, we say that the correlated random walk is a *Markov chain of order* 2, which is an example of Markov chain with memory.

By summing and subtracting these two equations, we get a pair of coupled equations for $P_n(k)$ and $A_n(k)$:

$$\begin{cases} P_{n+1}(k) = R_n(k-1) + L_n(k+1) & (1.66) \\ A_{n+1}(k) = (\mathfrak{t} - \mathfrak{r})\left[R_n(k-1) - L_n(k+1)\right]. & (1.67) \end{cases}$$

Now we want to obtain the continuum limit for the evolution of $P_n(k)$. Proceeding with the same prescriptions as before, keeping only terms of order δt and δx^2 and after rearranging, we get:

$$\begin{cases} \dfrac{\partial p}{\partial t}\delta t = -\dfrac{\partial a}{\partial x}\delta t + \dfrac{1}{2}\dfrac{\partial^2 p}{\partial x^2}\delta x^2 & (1.68) \\ 2\mathfrak{r}a\delta t = -(\mathfrak{t} - \mathfrak{r})\dfrac{\partial p}{\partial x}\delta x^2. & (1.69) \end{cases}$$

Now letting δx and δt go to zero, and keeping the ratio $\delta x^2/\delta t = \Delta$ constant, we recover for the first equation the form of the continuity equation, Eq. (1.24), with the probability drift given this time by

$$a(x,t) = -\frac{\mathfrak{t} - \mathfrak{r}}{2\mathfrak{r}}\Delta\frac{\partial p(x,t)}{\partial x}. \tag{1.70}$$

By plugging this expression into the continuity equation, we get a simple heat equation

$$\frac{\partial p(x,t)}{\partial t} = \frac{1}{2}D\frac{\partial^2 p(x,t)}{\partial x^2}, \tag{1.71}$$

where the diffusion coefficient is

$$D = \frac{\mathfrak{t}}{\mathfrak{r}}\Delta. \tag{1.72}$$

This result is consistent with what found in [104]. However, we point out that in the literature another way of performing the continuum limit for the correlated random walk is considered [119]. If we assume a scaling for the reflection coefficient of the type

$$\mathfrak{r} = \frac{\varrho}{T}\delta t, \tag{1.73}$$

we need to keep in Eq. (1.67) also terms of order δt^2, obtaining:

$$\frac{2\varrho}{T}a\delta t^2 + \frac{\partial a}{\partial t}\delta t^2 = -\frac{\partial p}{\partial x}\delta x^2, \tag{1.74}$$

which means that in this case we have to keep the ratio $\delta x/\delta t = v$ constant, when letting δx and δt go to zero. Consequently, we obtain a pair of coupled equations

$$\begin{cases} \dfrac{\partial p(x,t)}{\partial t} = -\dfrac{\partial a(x,t)}{\partial x} & (1.75) \\ v^2\dfrac{\partial p(x,t)}{\partial x} = -\dfrac{2\varrho}{T}a(x,t) - \dfrac{\partial a(x,t)}{\partial t}, & (1.76) \end{cases}$$

which can be transformed into a pair of uncoupled *telegrapher's equations*:

$$\begin{cases} \dfrac{\partial^2 p(x,t)}{\partial t^2} + \dfrac{2\varrho}{T}\dfrac{\partial p(x,t)}{\partial t} = v^2 \dfrac{\partial p(x,t)}{\partial x^2} & (1.77) \\ \dfrac{\partial^2 a(x,t)}{\partial t^2} + \dfrac{2\varrho}{T}\dfrac{\partial a(x,t)}{\partial t} = v^2 \dfrac{\partial a(x,t)}{\partial x^2}. & (1.78) \end{cases}$$

Hence, in this case we get a different limiting equation for the evolution of the probability of the walker's displacement. However, as it is often stressed when dealing with the telegrapher's equation [119], for times much longer than the value of the parameter T, i.e., in the limit $T \to 0$, a normal diffusion equation is recovered, with the diffusion coefficient given by

$$D = \frac{v^2 T}{\varrho}. \tag{1.79}$$

In other words, the asymptotic regime of a telegrapher's equation is normal diffusion, which means that the two procedures we have considered yield the same results in the long-time limit. Indeed, if we imagine that $T = \theta\delta t$, in the diffusion limit, i.e., $v \to \infty$[7], the previous expression for the diffusion coefficient would become

$$D = \frac{\theta}{\varrho}\Delta, \tag{1.80}$$

which, interpreting θ and ϱ as the microscopic transmission and reflection coefficients, is the same expression previously obtained. This is another example of how the continuum limit may change depending on the scaling of the parameters.

1.5 Summary

In this introductory chapter we have briefly discussed the relation between diffusion processes and random walk models: while the former provide a correct physical description for time and length scales much larger than those at the microscopic level, random walks offer a good approximation of the process at very short scales. The connection between the two is made through the procedure of the continuum limit, which consists in considering very small step lengths and hopping times. In practice, this is obtained by evolving the walk for a very large number of steps, in such a way that the time scale for a single step can be considered very small. If the evolution time is large enough, the asymptotic properties of the walk are expected to approach those of the related diffusion process.

We have also provided a general method to obtain the continuum limit for random walks with nearest neighbour jumps. This method is based on the structure of the

[7] In the diffusion limit $\delta x^2/\delta t = \Delta$ is kept constant, hence $v = \delta x/\delta t$ diverges. The choice $T = \theta\delta t$ is made so that the product $v^2 T$ remains finite.

supposed limiting Fokker-Planck equation, which takes the form of a continuity equation. We have discussed some examples of random walks and in some cases the continuum limit obtained with our method has been compared with the results already present in the literature. In the following, we will use the method presented in this chapter to discuss the continuum limit for two particular examples of random walks.

Gillis random walk 2

The *Gillis Random Walk* (GRW) was introduced in 1956 [42] to study the recurrence properties of a random process with transition probabilities not possessing translational invariance. It consists in a d-dimensional random walk with only nearest-neighbour jumps transitions defined as follows: let $\mathbf{k}$ be the general lattice point $(k_1, k_2, \ldots, k_d)$ and $\mathbf{e}_i$ the unit vector parallel to the i-th axis in the positive direction. The permitted transitions are those of the type $\mathbf{k} \to \mathbf{k} \pm \mathbf{e}_i$, so that in a single jump only the i-th coordinate of the position vector can change, increasing or decreasing by one unit. The respective probabilities ϕ^i_+ and ϕ^i_- depend on the i-th coordinate k_i itself and are given by

$$\phi^i_+(k_i) = \frac{1}{2d}\left(1 - \frac{\epsilon}{k_i}\right) \tag{2.1}$$

$$\phi^i_-(k_i) = \frac{1}{2d}\left(1 + \frac{\epsilon}{k_i}\right), \tag{2.2}$$

for $k_i \neq 0$, while for $k_i = 0$

$$\phi^i_+(0) = \phi^i_-(0) = \frac{1}{2d}, \tag{2.3}$$

where $\epsilon \in (-1, 1)$ and $i = 1, \ldots, d$. Thus the transition probabilities are characterized by a bias controlled by the parameter ϵ: for positive values the walker is biased to move towards the origin of coordinates, while for $\epsilon < 0$ there is a tendency to escape from it. For $\epsilon = 0$ there is no bias and one recovers the simple symmetric random walk in d dimensions.

The mathematical relevance of the model lies in the fact that it is one of the few examples of non-homogeneous random walk for which some analytical computations can be performed. For example in the original paper by Gillis [42] the author computes, in the one-dimensional case, the exact form of the generating function of the probability of being at the origin after n steps, through which it is possible to obtain other results such as the probability of eventual return to the starting site and the mean number of steps occurring between two consecutive visits at the origin [56]. However, the most considered result regards the recurrence of the starting site[1] depending both on the parameter ϵ and the dimensions d of the system. For these reasons the GRW was

[1] A point is defined recurrent if the walk visits it infinitely often with probability 1.

the starting point for many papers, see [69, 70, 94, 55], concerning recurrence and transience, extrema, returns and passage-time moments of stochastic processes.

In the physical literature, at least to our knowledge, the model has attracted little interest. Nevertheless, we want to show that the GRW can also be of physical relevance, as it provides a discrete approach to a widely studied problem, that of Brownian motion in a logarithmic potential. This problem has been deeply studied, see for instance [29, 53], since it has been recognized as a natural model for a large number of physical systems: examples can be found in vortex dynamics [16], interaction between probe particles in a driven fluid [76], time evolution of momenta of cold atoms trapped in optical lattices [86, 81, 33], and relaxation to equilibrium of long-range interacting systems [15, 22]. Moreover, diffusion in an effective logarithmic potential also appears outside the physical context, e.g., in the study of charged particles in the vicinity of a charged polymer [85], dynamics of DNA denaturation [5] and sleep-wake transitions during sleep [79].

In the following we will focus on the one-dimensional case. We will first discuss in detail a number of analytical results, beginning with the computation of the probability of being at the origin after n steps, having started the walk from a generic site k_0 (the computation can also be found in [57]), from which other related quantities can be derived; then we will show that in a certain range of ϵ the walk admits a normalizable stationary distribution, which we are able to compute; finally we will evaluate the continuum limit of the GRW, showing that it corresponds to the motion of a Brownian particle in a logarithmic potential $U(x) \sim \epsilon \log|x|$, and derive from this fact the transport properties of the system.

2.1 Generating function of the probability of being at the origin and related results

Let us consider a walk starting from k_0. In the one-dimensional case, the Gillis random walk is defined by the jump probabilities from k to k':

$$\phi(k'|k) = \frac{1}{2}\left(1 - \frac{\epsilon}{k}\right)\delta_{k',k+1} + \frac{1}{2}\left(1 + \frac{\epsilon}{k}\right)\delta_{k',k-1} \tag{2.4}$$

$$\phi(k'|0) = \frac{1}{2}\delta_{k',-1} + \frac{1}{2}\delta_{k',1}. \tag{2.5}$$

We want to evaluate the generating function of the transition probabilities from a site k_0 to the origin of coordinates, viz.,

$$P_z(0|k_0) = \sum_{n=0}^{\infty} P_n(0|k_0) z^n. \tag{2.6}$$

We begin by writing the evolution equation for $P_n(k|k_0)$ which, by the use of the Markov property, can be written as

$$P_{n+1}(k|k_0) = \phi_R(k-1)P_n(k-1|k_0) + \phi_L(k+1)P_n(k+1|k_0), \tag{2.7}$$

where $\phi_R(k')$ and $\phi_L(k')$ are the one-dimensional version of ϕ^i_+ and ϕ^i_-, respectively. By multiplying both sides for z^{n+1} and summing over n, $n = 0, 1, \ldots$, we obtain an equation involving generating functions which, by writing the explicit expressions of $\phi_L(k')$ and $\phi_R(k')$, reads

$$P_z(k|k_0) - \delta_{k,k_0} = \frac{z}{2}P_z(k+1|k_0) + \frac{z}{2}P_z(k-1|k_0) + \frac{\epsilon z}{2\,(k+1)}P_z(k+1|k_0) - \frac{\epsilon z}{2\,(k-1)}P_z(k-1|k_0). \quad (2.8)$$

We now consider the discrete Fourier transform of this equation, with

$$\hat{P}_z(q|k_0) = \sum_{k=-\infty}^{+\infty} e^{iqk} P_z(k|k_0), \quad (2.9)$$

obtaining

$$\frac{1 - z\cos q}{\sin q}\hat{P}_z(q|k_0) - \frac{e^{iqk_0}}{\sin q} = -i\epsilon z \sum_{k\neq 0} \frac{e^{iqk}}{k} P_z(k|k_0). \quad (2.10)$$

By taking the derivative with respect to q of both sides we get a linear first-order differential equation for $\hat{P}_z(q|k_0)$, which we put in the following form:

$$\hat{P}'_z(q|k_0) + f(q)\hat{P}_z(q|k_0) = \frac{\sin q}{1 - z\cos q}\frac{\mathrm{d}}{\mathrm{d}q}\left(\frac{e^{iqk_0}}{\sin q}\right) - \frac{\epsilon z \sin q}{1 - z\cos q}P_z(0|k_0), \quad (2.11)$$

where

$$f(q) = \frac{\sin q}{1 - z\cos q}\left[\frac{\mathrm{d}}{\mathrm{d}q}\left(\frac{1 - z\cos q}{\sin q}\right) - \epsilon z\right]. \quad (2.12)$$

This equation can be solved by means of the usual integrating factor method, yielding the general solution

$$\hat{P}_z(q|k_0) = \frac{\sin q}{(1 - z\cos q)^{1-\epsilon}} \int \frac{\mathrm{d}}{\mathrm{d}q'}\left(\frac{e^{iq'k_0}}{\sin q'}\right)\frac{\mathrm{d}q'}{(1 - z\cos q')^{\epsilon}} - \frac{\epsilon z \sin q}{(1 - z\cos q)^{1-\epsilon}} P_z(0|k_0) \int \frac{\mathrm{d}q'}{(1 - z\cos q')^{\epsilon}} + \frac{c\sin q}{(1 - z\cos q)^{1-\epsilon}}, \quad (2.13)$$

where we indicated by c the integration constant. We can now obtain $P_z(0|k_0)$ by using the inversion formula for the discrete Fourier transform. Integrating from 0 to 2π and dividing both sides by 2π we get, after integrating by parts and rearranging terms:

$$P_z(0|k_0) = \frac{\int_0^{2\pi} e^{iqk_0}\,(1 - z\cos q)^{-1-\epsilon}\,\mathrm{d}q}{\int_0^{2\pi}(1 - z\cos q)^{-\epsilon}\,\mathrm{d}q}. \quad (2.14)$$

The integrals can be evaluated in terms of hypergeometric functions, see Appendix A, yielding

$$P_z(0|k_0) = \frac{z^{|k_0|}}{|k_0|!}\frac{\Gamma(1+\epsilon+|k_0|)}{2^{|k_0|}\Gamma(1+\epsilon)}\frac{{}_2F_1\left(\frac{1+\epsilon+|k_0|}{2}, \frac{\epsilon+|k_0|}{2}+1; |k_0|+1; z^2\right)}{{}_2F_1\left(\frac{1}{2}\epsilon, \frac{1}{2}\epsilon+\frac{1}{2}; 1; z^2\right)}. \tag{2.15}$$

We point out that putting $k_0 = 0$ one recovers the original result by Gillis [42] regarding the generating function of the return probability at the origin:

$$P_z(0|0) = \frac{{}_2F_1\left(\frac{1}{2}\epsilon+\frac{1}{2}, \frac{1}{2}\epsilon+1; 1; z^2\right)}{{}_2F_1\left(\frac{1}{2}\epsilon, \frac{1}{2}\epsilon+\frac{1}{2}; 1; z^2\right)}. \tag{2.16}$$

A number of results can now be derived. For example, we can compute the generating function of the first return time at the origin. Indeed the first hitting time of a point k, starting the walk from k_0, are related to the transition probability from k_0 to k by the following equation [56, 63, 102]:

$$P_n(k|k_0) = \delta_{k,k_0}\delta_{n,0} + \sum_{m=1}^{n} F_m(k|k_0)P_{n-m}(k|k), \tag{2.17}$$

where $F_m(k|k_0)$ is the probability of reaching k for the first time at the m-th step, having started from k_0. By multiplying each side for z^n, summing over n and introducing the generating function

$$F_z(k|k_0) = \sum_{n=1}^{\infty} F_n(k|k_0)z^n, \tag{2.18}$$

we get

$$P_z(k|k_0) = \delta_{k,k_0} + F_z(k|k_0)P_z(k|k), \tag{2.19}$$

which for $k \neq k_0$ reduces to

$$F_z(k|k_0) = \frac{P_z(k|k_0)}{P_z(k|k)}. \tag{2.20}$$

Therefore for $k = 0$ and $k_0 \neq 0$ we have, by using Eq. (2.15):

$$F_z(0|k_0) = \frac{z^{|k_0|}}{|k_0|!}\frac{\Gamma(1+\epsilon+|k_0|)}{2^{|k_0|}\Gamma(1+\epsilon)}\frac{{}_2F_1\left(\frac{1+\epsilon+|k_0|}{2}, \frac{\epsilon+|k_0|}{2}+1; |k_0|+1; z^2\right)}{{}_2F_1\left(\frac{1+\epsilon}{2}, \frac{1}{2}\epsilon+1; 1; z^2\right)}. \tag{2.21}$$

In order to compute the generating function of the first return time at the origin, it is not sufficient to evaluate the previous expression for $k_0 = 0$, because when $k = k_0 = 0$, F_z is no more related to P_z by Eq. (2.20); indeed, from Eq. (2.19) we obtain

$$F_z(0|0) = 1 - \frac{1}{P_z(0|0)}, \tag{2.22}$$

and thus, by using Eq. (2.16), we get the correct result:

$$F_z(0|0) = 1 - \frac{{}_2F_1\left(\frac{1}{2}\epsilon, \frac{1}{2}\epsilon + \frac{1}{2}; 1; z^2\right)}{{}_2F_1\left(\frac{1}{2}\epsilon + \frac{1}{2}, \frac{1}{2}\epsilon + 1; 1; z^2\right)}. \tag{2.23}$$

For the purposes of this thesis we are interested in evaluating the asymptotic decay of the probabilities of being at the origin and the first return probabilities at the initial point, starting the walk from $k_0 = 0$. The former can be obtained from Eq. (2.16), by using Tauberian theorems for power series, see Appendix B. We get

$$P_{2n}(0|0) \sim \begin{cases} a_\epsilon \cdot n^{-(1/2-\epsilon)} & -1 < \epsilon < \frac{1}{2} \\ \frac{4}{\log n} & \epsilon = \frac{1}{2}, \end{cases} \tag{2.24}$$

where the coefficient a_ϵ is

$$a_\epsilon = \frac{4^\epsilon}{\Gamma\left(1/2 - \epsilon\right)} \frac{\Gamma(1-\epsilon)}{\Gamma(1+\epsilon)}, \tag{2.25}$$

while in the case $\epsilon > \frac{1}{2}$ the probability converges to a constant value:

$$P_{2n}(0|0) \to \frac{2\epsilon - 1}{\epsilon}. \tag{2.26}$$

We point out that the same asymptotic results, including the coefficients, are obtained when computing the probability of reaching $k = 0$ starting from $k_0 \neq 0$. However, note that a walker can reach the origin only in a number of steps whose parity is that of k_0, hence the $2n$ index must be replaced by $2n + |k_0|$. In particular, one has that for $\epsilon > \frac{1}{2}$ and any k_0:

$$P_{2n+|k_0|}\left(0|k_0\right) \to \frac{2\epsilon - 1}{\epsilon}. \tag{2.27}$$

This fact will be used in the following section.

Regarding the first return probabilities, an application of Tauberian theorems to the generating function of Eq. (2.23) yields:

$$F_{2n}(0|0) \sim \begin{cases} b_\epsilon \cdot n^{-(1/2-\epsilon)} & -1 < \epsilon < -\frac{1}{2} \\ \frac{4}{n \log^2 n} & \epsilon = -\frac{1}{2} \\ c_\epsilon \cdot n^{-(3/2+\epsilon)} & -\frac{1}{2} < \epsilon < 1, \end{cases} \tag{2.28}$$

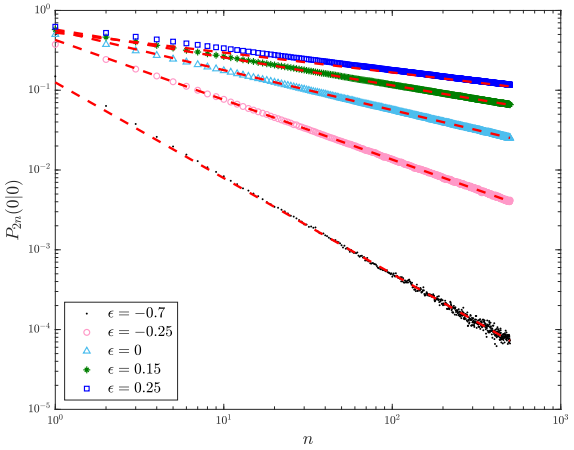

FIGURE 2.1: Probability of finding the particle at the origin after $2n$ steps for the Gillis random walk, for various values of ϵ. The asymptotic behaviours (dashed red lines) in the large-n limit are given by $a_\epsilon \cdot n^{-(1/2-\epsilon)}$, as predicted by Eq. (2.24). Data are obtained simulating 10^6 walks of 10^3 steps.

where

$$b_\epsilon = \left(\frac{2\epsilon - 1}{\epsilon}\right)^2 \frac{4^\epsilon}{\Gamma(1/2 - \epsilon)} \frac{\Gamma(1-\epsilon)}{\Gamma(1+\epsilon)} \tag{2.29}$$

$$c_\epsilon = \left(\frac{2\epsilon - 1}{2}\right) \frac{4^{-\epsilon}}{\Gamma(1/2 + \epsilon)} \frac{\Gamma(1+\epsilon)}{\Gamma(1-\epsilon)}. \tag{2.30}$$

For the sake of completeness, we point out that the same exponents are obtained for the first hitting time of the origin starting from $k_0 = 0$, but with different coefficients, which depend on the starting point.

Let us comment briefly on the last result: the first return probabilities show different behaviours in the ranges $\epsilon \in \left(-1, -\frac{1}{2}\right)$ and $\epsilon \in \left(-\frac{1}{2}, 1\right)$, with the $\epsilon = -\frac{1}{2}$ representing a "phase transition point". This is related to the recurrence properties of the process: we recall that a random walk can be classified as recurrent if

$$\sum_{n=0}^{\infty} F_n(k_0|k_0) = 1. \tag{2.31}$$

For the GRW every point is recurrent if and only if $k_0 = 0$ is recurrent [42], hence it is sufficient to evaluate $F_n(0|0)$ to show [56, 57] that the Gillis random walk is recurrent only for $\epsilon \in \left[-\frac{1}{2}, 1\right)$, meaning that in this range the first return probabilities sum to 1, or rather, their generating function approaches 1, in the limit $z \to 1^-$. Note that for $\epsilon \in \left(-1, -\frac{1}{2}\right)$ the sum of the first return probabilities is still finite, but it converges to a

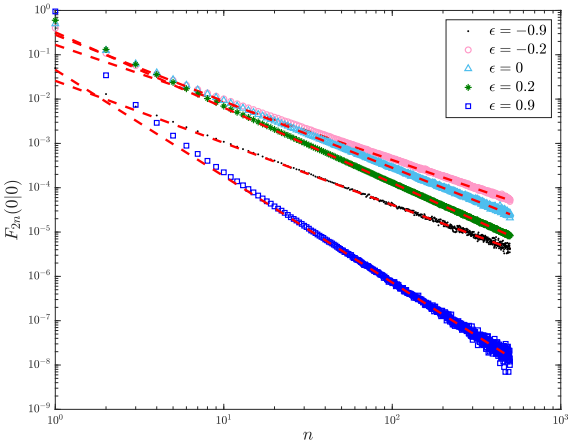

FIGURE 2.2: First return probability at the origin after $2n$ steps for the Gillis random walk, for various values of ϵ. The asymptotic behaviours (dashed red lines) in the large-n limit are those predicted by Eq. (2.28). Data are obtained simulating 10^7 walks of 10^3 steps, except for the case $\epsilon = 0.9$, where a larger number of walks $\left(10^9\right)$ is needed for sufficiently precise results.

value less than 1 - see [56]:

$$\sum_{n=0}^{\infty} F_n(0|0) = |\epsilon|^{-1} - 1, \quad -1 < \epsilon < -\frac{1}{2}. \tag{2.32}$$

Recurrence can be more easily probed by evaluating the occupation probability of the starting site, since from Eq. (2.19) we have

$$F_z(0|0) = 1 - \frac{1}{P_z(0|0)}, \tag{2.33}$$

hence the process is recurrent if and only if $P_z(0|0)$ diverges as z approaches 1. The asymptotic decays of the probabilities of occupying the origin for the Gillis random walk as given by Eq. (2.24) reveal in fact that their sum diverges for $\epsilon \geq -\frac{1}{2}$, and converges for $\epsilon < -\frac{1}{2}$.

We also observe that $P_n(0|0)$ shows different asymptotic behaviours in the ranges $\epsilon \in \left(-1, \frac{1}{2}\right)$ and $\epsilon \in \left(\frac{1}{2}, 1\right)$, with $\epsilon = \frac{1}{2}$ acting as a "phase transition point". Indeed, in the following we will show that this corresponds to a transition between a non-ergodic phase and an ergodic phase, which is reached for $\epsilon > \frac{1}{2}$. Observe that the occurrence of the ergodic phase in this range is suggested by the convergence of $P_n(0|0)$ to a constant value, see Eq. (2.26).

2.2 Stationary distribution

We now show that for $\epsilon > \frac{1}{2}$ the Gillis random walk admits a stationary distribution. For a random walk defined on a state space S with transition probabilities from state i to state j given by $\phi(j|i)$, a stationary distribution is a set of non-negative numbers $\{\pi_k : k \in S\}$ such that:

$$\sum_{k \in S} \pi_k = 1 \tag{2.34}$$

$$\sum_i \phi(j|i)\pi_i = \pi_j, \tag{2.35}$$

i.e., π_k are the components of an eigenvector of the transition matrix $\phi_{ji} = \phi(j|i)$ with eigenvalue 1. In the case of the one-dimensional GRW, the state space is the set of integers and the transition probabilities are given by Eqs. (2.4) and (2.5). Due to the symmetry of walk, the π_k must satisfy the symmetry condition $\pi_k = \pi_{-k}$, hence we are left to solve the infinite set of linear equations:

$$\begin{cases} \pi_0 = 2\phi(0|1)\pi_1 \\ \pi_1 = \phi(1|0)\pi_0 + \phi(1|2)\pi_2 \\ \quad \vdots \\ \pi_k = \phi(k|k-1)\pi_{k-1} + \phi(k|k+1)\pi_{k+1} \\ \quad \vdots \end{cases}$$

By solving this system by iteration, one easily finds the solution

$$\pi_k = \frac{k\,(1-\epsilon)_{k-1}}{(1+\epsilon)_k} \cdot \pi_0, \quad k > 1, \tag{2.36}$$

where $(x)_n$ is the Pochhammer symbol, see Appendix A, and π_0 can be determined by the normalization condition. If the sum of the π_i can not be normalized, then they do not represent a proper distribution and we say that the walk does not admit a stationary distribution. For large values of k, by using the definition of the Pochhammer symbol in terms of the Gamma function we may deduce that

$$\pi_k \sim \pi_0 \cdot \frac{\Gamma(1+\epsilon)}{\Gamma(1-\epsilon)} k^{-2\epsilon}, \tag{2.37}$$

hence the GRW admits a stationary distribution only for $\epsilon > \frac{1}{2}$, and we can say that the process is ergodic in this range.

To find π_0, let us consider a large ensemble of $2M$ particles and suppose that each one starts the walk from a different site, so that M start from even positions and M from odd positions. We previously showed that for $\epsilon > \frac{1}{2}$ the probability of finding a particle at the origin converges to a constant value, which is independent of the starting

point k_0. However, for any number of steps $n \geq |k_0|$, a particle can be at the origin only if n has the same parity of k_0, meaning that only M particles are eligible to be found at $k = 0$. Therefore we expect that π_0 be equal to one half the limiting value of the occupation probability of the origin:

$$\pi_0 = \frac{2\epsilon - 1}{2\epsilon}. \tag{2.38}$$

Moreover, note that for $\epsilon > \frac{1}{2}$, from the generating function of Eq. (2.23) it is possible to compute the mean return time at the origin starting from $k_0 = 0$, which reads:

$$\mathscr{T} = \frac{2\epsilon}{2\epsilon - 1}, \tag{2.39}$$

see also [56]. It turns out that the value of $\mathscr{T}$ is strictly connected to π_0: indeed, let us call x_n the position of the random walk starting from $k_0 = 0$ after n steps and R_n the number of returns at the origin:

$$R_n = \sum_{i=1}^{n} \delta_{0,x_i}. \tag{2.40}$$

From Birkhoff's ergodic theorem, we have that the time average of R_n converges, in the long-time limit, to the ensemble average of $\delta_{0,k}$, i.e., to the stationary probability π_0:

$$\lim_{n\to\infty} \frac{R_n}{n} = \pi_0. \tag{2.41}$$

On the other hand, the mean return time can be evaluated as the ratio of the total time to the number of returns, hence in the limit:

$$\lim_{n\to\infty} \frac{R_n}{n} = \frac{1}{\mathscr{T}}, \tag{2.42}$$

from which one obtains $\pi_0 = 1/\mathscr{T}$, confirming the validity of Eq. (2.38). This may be double-checked by evaluating numerically the sum

$$\sum_{i=-n}^{n} \pi_i = \pi_0 + 2\pi_0 \sum_{i=1}^{n} \pi_i \equiv \pi_0 \cdot \mathscr{S}_n \tag{2.43}$$

for large values of n, and showing that $\mathscr{S}_n$ converges to

$$\mathscr{S}_n \to \mathscr{S} = \frac{2\epsilon}{2\epsilon - 1}. \tag{2.44}$$

In Fig. 2.3 we show the behaviour of $\mathscr{S}_n$ as a function of n, for various values of ϵ and a number of iterations up to 10^5. Note that the convergence becomes slower as $\epsilon \to \frac{1}{2}$. We also present in the following table the values of $\mathscr{S}_n$ computed for a larger number of iterations $\left(n = 10^7\right)$, compared to $\mathscr{S}$. We see that for $n \to \infty$ the partial sum converges to $2\epsilon/(2\epsilon - 1)$.

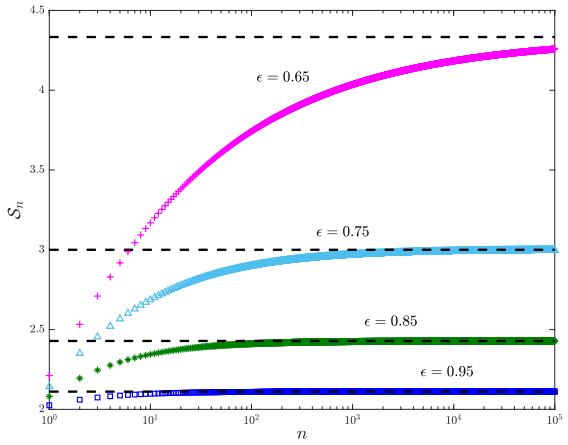

FIGURE 2.3: $\mathcal{S}_n$ versus n for various values of ϵ. The theoretical sums of the corresponding series are represented by the dashed black lines.

ϵ	$\mathcal{S}_n,\ n = 10^7$	$\mathcal{S} = 2\epsilon/(2\epsilon - 1)$
0.95	2.111	$2.\overline{1}$
0.85	2.4285	2.4286
0.75	2.9995	3
0.65	4.3137	$4.\overline{3}$

Finally, in Fig. 2.4 we show that for $\epsilon > \frac{1}{2}$ the probability of finding a particle at site k is correctly given by π_k, normalized according to Eq. (2.38). However, note that the agreement is good up to a certain threshold, which moves toward higher values of k for higher number of steps. Therefore, for any finite time, π_k does not reproduce correctly the high-k range of the distribution. We will see in the following section how this regime can be instead effectively described.

2.3 The continuum limit

To obtain the continuum limit for the GRW, we proceed as explained in Chapter 1. We recall that the probabilities of jumping right and left when being at site k are given by:

$$\phi_R(k) = \frac{1}{2}\left(1 - \frac{\epsilon}{k}\right) \tag{2.45}$$

$$\phi_L(k) = \frac{1}{2}\left(1 + \frac{\epsilon}{k}\right), \tag{2.46}$$

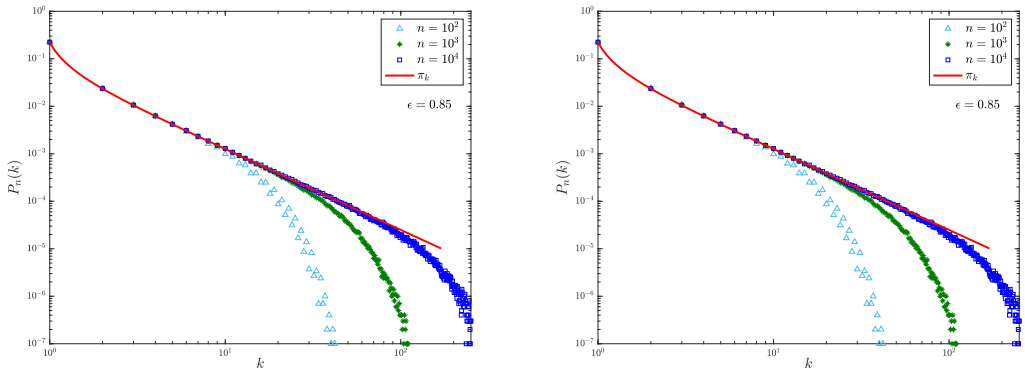

FIGURE 2.4: Distributions of the position k for positive values of k and stationary distributions. Data are obtained simulating 10^7 walks for different times. The red lines correspond to a continuous interpolation of the stationary distribution π_k. The power-law profile is clear, except for the first values of k.

and hence the probability drift function has the expression:

$$a(x,t)\delta t = \left[\phi_R\left(\frac{x}{\delta x}\right) - \phi_L\left(\frac{x}{\delta x}\right)\right] p(x,t)\delta x \tag{2.47}$$

$$= -\frac{\epsilon}{x} p(x,t)\delta x^2. \tag{2.48}$$

Consequently, the resulting current is

$$J(x,t) = -\frac{\delta x^2}{\delta t}\left[\frac{\epsilon}{x} + \frac{1}{2}\frac{\partial}{\partial x}\right] p(x,t), \tag{2.49}$$

and therefore, in the limit $\delta x, \delta t \to 0$, by keeping the ratio $\delta x^2/\delta t = D$ constant, we get the following Fokker-Planck equation for the evolution of $p(x,t)$:

$$\frac{\partial p(x,t)}{\partial t} = \epsilon \frac{\partial}{\partial x}\left[\frac{p(x,t)}{x}\right] + \frac{1}{2}\frac{\partial^2 p(x,t)}{\partial x^2}, \tag{2.50}$$

where for the sake of simplicity we set $D = 1$. This equation corresponds to the diffusion of a Brownian particle in the presence of a logarithmic potential tuned by the parameter ϵ: $U(x) \sim 2\epsilon \log|x|$, and it is related to the Bessel process, representing the stochastic evolution of the radial displacement of the d-dimensional Brownian motion [16, 74, 87, 96]. However, the validity of Eq. (2.50) in describing the long-time properties of the GRW must be considered along with a small caveat: the definitions of the probabilities (2.45) and (2.46) are correct as long as $k \neq 0$, while at $k = 0$ the particle has equal probability of jumping right or left. Thus we expect that in a neighbourhood of the origin the particle experiences no force and diffuses freely. In other words, the potential must be regularized in such a way that it assumes a constant value in a neighbourhood $(-a, a)$ of the origin. Hence we are led to consider

a logarithmic potential of the kind:

$$U(x) = \theta\left(|x| - a\right) \cdot 2\epsilon \log\left(\frac{|x|}{a}\right), \tag{2.51}$$

where

$$\theta(y) = \begin{cases} 0 & \text{if } y \leq 0 \\ 1 & \text{if } y > 0. \end{cases} \tag{2.52}$$

The solution of the Fokker-Planck equation with a logarithmic potential as in Eq. (2.51) has been computed in [29]. Here we only state the results to test the validity of the continuum limit. First of all, Eq. (2.50) admits a stationary solution for $\epsilon > \frac{1}{2}$ which, considering the regularized potential, can be written as [29]:

$$p_s(x) = \frac{e^{-U(x)}}{Z} = \begin{cases} \dfrac{2\epsilon - 1}{4a\epsilon} & \text{if } |x| \leq a \\ \dfrac{2\epsilon - 1}{4a\epsilon} \left|\dfrac{x}{a}\right|^{-2\epsilon} & \text{if } |x| > a. \end{cases} \tag{2.53}$$

This solution is valid in the limit $t \to \infty$, representing the equilibrium state of the process. Therefore in this range of ϵ the process is ergodic, as anticipated in the previous sections. Note that $p_s(x)$ features the same power-law profile of the stationary distribution of the GRW. It is also possible to evaluate the probability distribution in a pre-asymptotic regime, with t large but finite. Considering at $t_0 = 0$ the particle located at $x_0 = 0$, one has that for large t, outside the central region [29]:

$$p(x,t) \sim \frac{a^{2\epsilon-1}}{2\epsilon\Gamma\left(\epsilon - 1/2\right)} \Gamma\left(\frac{1}{2} + \epsilon, \frac{z^2}{2}\right) |z|^{-2\epsilon} t^{-\epsilon} \tag{2.54}$$

where z is the scaling variable

$$z = \frac{x}{\sqrt{t}}, \tag{2.55}$$

and $\Gamma(\alpha, y)$ denotes the incomplete gamma function:

$$\Gamma(\alpha, y) = \int_y^\infty e^{-u} u^{\alpha-1} \mathrm{d}u. \tag{2.56}$$

Note that for large values of y, $\Gamma\left(\alpha, y\right) \sim y^{\alpha-1} e^{-y}$, hence all moments of $p(x,t)$ are finite. Moreover, we observe that for small z, $p(x,t)$ reproduces the equilibrium solution Eq. (2.53) in $|x| > a$.

For $\epsilon < \frac{1}{2}$, there is no normalizable stationary solution. For a process starting at $x_0 = 0$ at time $t_0 = 0$ the non-equilibrium solution is given by [29]:

$$p(x,t) \sim \begin{cases} \dfrac{2^{\epsilon-1/2}}{a\Gamma\left(1/2 - \epsilon\right)} \left(\dfrac{a^2}{t}\right)^{1/2-\epsilon} & \text{if } |x| \leq a \\ \dfrac{2^{\epsilon-1/2}}{\Gamma\left(1/2 - \epsilon\right)} |z|^{-2\epsilon} e^{-z^2/2} t^{-1/2} & \text{if } |x| > a, \end{cases} \tag{2.57}$$

valid for large t. We point out that the central part decays with time as $t^{-(1/2-\epsilon)}$, in agreement with the decay of the probability of being at the origin for the GRW, Eq. (2.24).

To test the continuum limit, rather than evaluating the distribution of the position k of the random walk after n steps, we consider the distribution of the variable $z = k/\sqrt{n}$. In the case $\epsilon > \frac{1}{2}$, from Eq. (2.54) one has that for large values of t and $|x| > a$

$$p(x,t) \sim \mathscr{Q}(z) t^{-\epsilon}, \tag{2.58}$$

hence the distribution of z is given by:

$$p(z,t) \sim \mathscr{Q}(z) t^{\frac{1}{2}-\epsilon}, \tag{2.59}$$

where

$$\mathscr{Q}(z) = \frac{a^{2\epsilon-1}}{2\epsilon\Gamma(\epsilon - 1/2)} \Gamma\left(\frac{1}{2} + \epsilon, \frac{z^2}{2}\right) |z|^{-2\epsilon}. \tag{2.60}$$

The function $\mathscr{Q}(z)$ is called *Infinite Covariant Density* [29, 62], since it describes the distribution of z presenting a non-integrable singularity at $z = 0$. This is connected to the fact that the scaling $z = x/\sqrt{t}$ is not valid in the central region for any finite time. However, the Infinite Covariant Density correctly reproduces the distribution of z, outside a small region around $z = 0$. We point out that in order to match the result of the continuum limit to that of the GRW, the parameter a must be tuned in such a way that $p(x,t)$ in Eq. (2.54) correctly reproduces, as $z \to 0$, the asymptotic decay of the stationary distribution given in Eq. (2.37). In other words, we need to take a satisfying:

$$\frac{a^{2\epsilon-1}}{2} = \frac{\Gamma(1+\epsilon)}{\Gamma(1-\epsilon)}. \tag{2.61}$$

This means that in the ergodic case the validity of the continuum limit is sensitive to the size of the central region, where the scaling does not hold. In Ref. [29] it has been suggested that the scaling breaks down for $x \approx 1$. We observe that according to the definition given in Eq. (2.61), the size a always assumes values smaller than 1 in the range $\frac{1}{2} < \epsilon < 1$, hence we expect that for the GRW the Infinite Covariant Density only fails in describing the occupation probability of the origin. This is confirmed by the simulations presented in Fig. 2.5 regarding the distribution of the scaling variable z: only the data corresponding to the origin do not agree with Eq. (2.60).

We now turn to $\epsilon < \frac{1}{2}$. We see from Eq. (2.57) that the distribution of $z = x/\sqrt{t}$ is

$$p(z,t) \sim \begin{cases} \dfrac{2^{\epsilon-1/2}}{\Gamma(1/2-\epsilon)} \left(\dfrac{a^2}{t}\right)^{-\epsilon} & \text{if } |z| \leq \dfrac{a}{\sqrt{t}} \\ \mathscr{P}(z) & \text{if } |z| > \dfrac{a}{\sqrt{t}}, \end{cases} \tag{2.62}$$

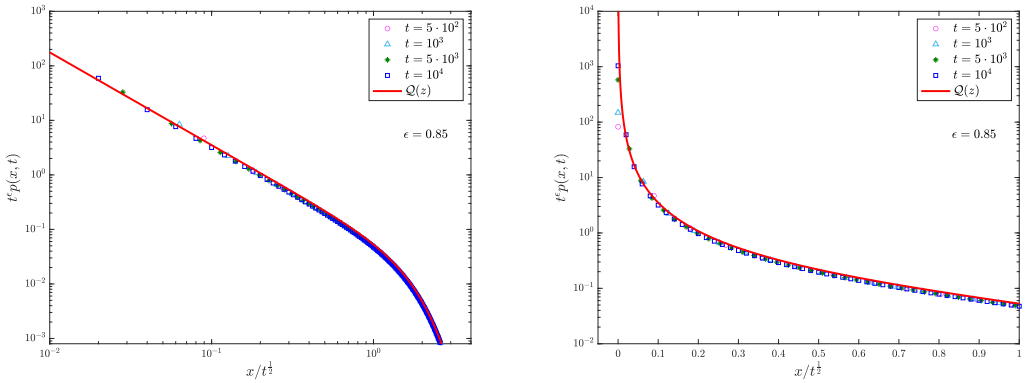

FIGURE 2.5: Plot of $t^{\epsilon} p(x,t)$ versus $z = x/\sqrt{t}$ for positive values of x and theoretical predictions, with $\epsilon = 0.85$. The red line corresponds to $\mathcal{Q}(z)$, given in Eq. (2.60). Data are obtained by evolving the Chapman-Kolmogorov equation, Eq. (2.7), up to different times. The left panel shows that the agreement is good for t large enough. The right panel focuses on the small-z region: only data corresponding to the occupation probability of the origin disagree with $\mathcal{Q}(z)$.

where

$$\mathcal{P}(z) = \frac{2^{\epsilon-1/2}}{\Gamma(1/2-\epsilon)} |z|^{-2\epsilon} e^{-z^2/2}, \tag{2.63}$$

thus outside the central region $\left(-\frac{a}{\sqrt{t}}, \frac{a}{\sqrt{t}}\right)$, the distribution is a function of z only. Note that for positive values of ϵ, $\mathcal{P}(z)$ presents a singularity close to $z = 0$, but this time the singularity is integrable. Moreover, $\mathcal{P}(z)$ does not depend on the parameter a, defining the size of the central region. These two facts mark a huge difference with the ergodic case, which we will discuss later. Nevertheless, as in the ergodic case, $\mathcal{P}(z)$ can not describe the occupation probability of the origin, which is instead represented by the other branch of Eq. (2.62). In Fig. 2.6 we present the results of our simulations regarding the distribution of $z = k/\sqrt{n}$, showing indeed good agreement with the theoretical predictions given by Eq. (2.62), for all values of z but those corresponding to the origin.

We can naively try to tune the parameter a in such a way that the branch of Eq. (2.62) referring to the central region correctly reproduces the asymptotic decay of the probability of being at the origin of the GRW. In other words, we can define

$$a^{2\epsilon} = \frac{\Gamma(1+\epsilon)}{\Gamma(1-\epsilon)}, \tag{2.64}$$

having taken into account the correcting factor $\frac{1}{2}$ needed to compare the result of the discrete-time model to that of the continuous-time model[2]. However, for any

[2]The factor comes from the fact that in a nearest-neighbour random walk, for n even(old) only even(odd) positions can be occupied. This does not happen in the corresponding continuous-time model, where at any given time all positions are accessible.

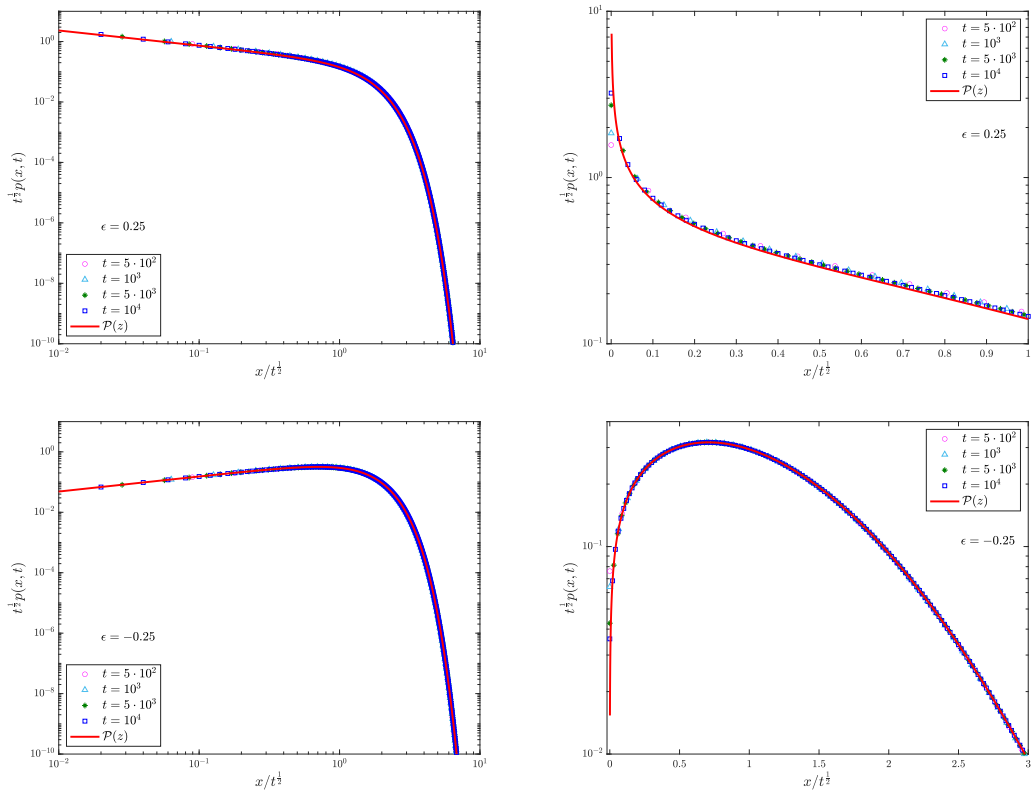

FIGURE 2.6: Distributions of the random variable $z = x/\sqrt{t}$ for positive values of x and theoretical predictions (red lines), as given in Eq. (2.62). Data are obtained by evolving the Chapman-Kolmogorov equation, Eq. (2.7), up to different times. The plots on the left and right panels on the same row refer to the same ϵ and are represented in different scales, to show the agreement for both large and small values of z, except for the data corresponding to the origin.

choice of a we can not use Eq. (2.62) to define a continuous function which correctly reproduces the distribution of z for all possible positions, including the origin, due to the discontinuity at $x = a$. Furthermore, this choice is not consistent with the one of the ergodic case. Therefore, in both the ergodic and non-ergodic regimes the solutions provided by the continuum approximation have some limitations in describing the distribution of the central region, which for the GRW corresponds to the site $k = 0$, and the central part of the distribution can only be correctly described by the discrete model. In the following section we will show how to solve this issue by defining an uniform solution reproducing both the result of the discrete model, valid for small $|x|$, and those of the continuum model, valid for large $|x|$.

2.3.1 Uniform approximation of the probability distribution

In order to find a uniform solution able to describe well both the small and large $|x|$ regimes for sufficiently large t, we can use the stationary distribution π_k of the GRW. This is defined on the integers, but we can extend its definition on the real line, by expressing the Pochhammer symbol in terms of the Gamma function [1]:

$$(x)_n \equiv \frac{\Gamma(x+n)}{\Gamma(x)}. \tag{2.65}$$

Hence, for $x \neq 0$, we can define

$$\pi(x) = \frac{2\epsilon-1}{2\epsilon}\frac{\Gamma(1+\epsilon)}{\Gamma(1-\epsilon)}\frac{\Gamma(|x|-\epsilon)}{\Gamma(|x|+\epsilon+1)}|x|, \tag{2.66}$$

which is the continuum equivalent of π_k for $k \neq 0$. Ideally, for $x = 0$ we want $\pi(0) = (2\epsilon-1)/2\epsilon$, but the previous expression converges instead to 0. Therefore we need to introduce a regularizing region around the origin, of size a, in such a way that $\pi(x)$ is continuous and:

$$\pi(x) = \begin{cases} \dfrac{2\epsilon-1}{2\epsilon} & \text{if } |x| < a \\ \dfrac{2\epsilon-1}{2\epsilon}\dfrac{\Gamma(1+\epsilon)}{\Gamma(1-\epsilon)}\dfrac{\Gamma(|x|-\epsilon)}{\Gamma(|x|+\epsilon+1)}|x| & \text{if } |x| > a. \end{cases} \tag{2.67}$$

A proper choice for a would be to take it as the solution of

$$\frac{\Gamma(1+\epsilon)}{\Gamma(1-\epsilon)}\frac{\Gamma(|x|-\epsilon)}{\Gamma(|x|+\epsilon+1)}|x| = 1. \tag{2.68}$$

Note that this equation can be solved numerically not only for $\epsilon > \frac{1}{2}$, i.e., in the ergodic regime, but also for $\epsilon < \frac{1}{2}$, see Fig. 2.7. Hence this particular choice, differently from those suggested previously, is valid for both regimes.

Now, the potential is related to the stationary distribution by

$$\pi(x) = \frac{e^{-U(x)}}{Z}, \tag{2.69}$$

hence for the Gillis model we can introduce the potential

$$U(x) = \begin{cases} 0 & \text{for } |x| < a \\ \log\left[\dfrac{\Gamma(1-\epsilon)}{\Gamma(1+\epsilon)}\dfrac{\Gamma(|x|+1+\epsilon)}{|x|\Gamma(|x|-\epsilon+1)}\right] & \text{for } |x| > a, \end{cases} \tag{2.70}$$

while $1/Z = (2\epsilon-1)/2\epsilon$ is the normalization constant. The potential is indeed of the form $U(x) \sim 2\epsilon \log|x|$ for large $|x|$, due to the asymptotic decay of $\pi(x)$, see also Eq.

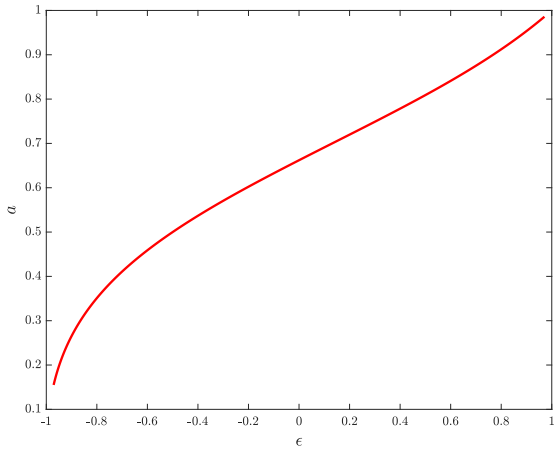

FIGURE 2.7: Plot of the size a versus ϵ, defined as a solution of Eq. (2.68).

(2.37), but it is of different form for smaller values of $|x|$. The uniform solution we are looking for can be written in terms of the potential or the stationary distribution as

$$p_u(x,t) = \frac{e^{-U(x)}}{Z} \frac{\Gamma(\epsilon + 1/2, x^2/2t)}{\Gamma(\epsilon + 1/2)}, \tag{2.71}$$

as already showed in [29, 62]. This corresponds to the stationary distribution multiplied by a factor which for large $|x|$ guarantees the matching to the result of the continuum limit. Indeed the stationary distribution decays as in Eq. (2.37), hence

$$p_u(x,t) \sim \frac{\Gamma(1+\epsilon)\Gamma(\epsilon + 1/2, x^2/2t)}{\epsilon\Gamma(1-\epsilon)\Gamma(\epsilon - 1/2)} |x|^{-2\epsilon}, \tag{2.72}$$

which is precisely the solution obtained in the continuum limit with a given by Eq. (2.61), see Eq. (2.54). On the other hand, for small $|x|$ and t sufficiently large, the factor $\Gamma(\epsilon + 1/2, x^2/2t)/\Gamma(\epsilon + 1/2)$ approaches 1, hence $p_u(x,t)$ approaches $\pi(x)$. Thus $p_u(x,t)$ correctly describes both the central and the outer part of the distribution. Indeed, Fig. 2.8 shows the agreement for any value of x between the data obtained by the evolution of the Chapman-Kolmogorov equations and the respective uniform solutions, for different times. Data also agree with the stationary distribution $\pi(x)$, as long as $x^2/2t \approx 0$.

In the case $\epsilon < \frac{1}{2}$ there is not a normalizable steady state, but the uniform solution can be written instead in terms of the *Infinite Invariant Density*. The Infinite Invariant Density is the non-normalizable zero-current solution of the Fokker-Planck equation [74] and is proportional to the steady state, $\mathscr{I}(x) \propto e^{-U(x)}$. It is related to the long-time properties of the time-dependent solution by

$$\lim_{t\to\infty} t^{\beta} p(x,t) = \mathscr{I}(x), \tag{2.73}$$

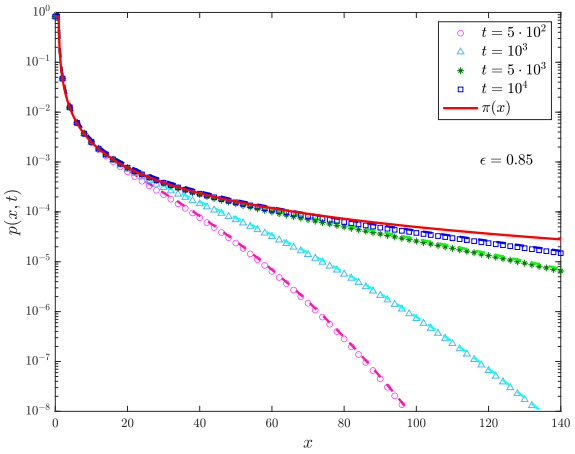

FIGURE 2.8: Distribution of the position for the Gillis random walk, with $\epsilon = 0.85$. Data (symbols) are obtained by evolving the Chapman-Kolmogorov equation, Eq. (2.7), up to different times. Each data set is interpolated with good agreement by the corresponding uniform approximations $p_u(x,t)$ (dashed lines). As the evolution time increases, data approach the values predicted by the stationary distribution $\pi(x)$ (solid red line).

where β is a proper exponent. The exponent and the proportionality constant can be thus determined from the knowledge of the probability distribution at a single point, e.g, the origin. For the Gillis model we know that the probability of being at the origin is given by Eq. (2.24), which, as we have already observed, must be corrected by the factor $1/2$ to make a comparison with the continuum limit. We hence have

$$\lim_{n\to\infty} n^{1/2-\epsilon} P_n(0|0) = \frac{2^{\epsilon-1/2}}{\Gamma(1/2-\epsilon)} \frac{\Gamma(1-\epsilon)}{\Gamma(1+\epsilon)} \equiv \mathscr{N}, \tag{2.74}$$

thus $\beta = \frac{1}{2} - \epsilon$ and since $e^{-U(0)} = 1$, we can interpret $\mathscr{N}$ as the proportionality constant. The Infinite Invariant Density of the Gillis model is therefore:

$$\mathscr{I}(x) = \frac{2^{\epsilon-1/2}}{\Gamma(1/2-\epsilon)} \frac{\Gamma(1-\epsilon)}{\Gamma(1+\epsilon)} e^{-U(x)}. \tag{2.75}$$

The Infinite Invariant Density is indeed non-integrable. It describes the central part of the distribution, but it fails in describing the outer part, due to its large $|x|$ behaviour. The uniform solution can be obtained by applying a Gaussian cutoff to $\mathscr{I}(x)$ in order to match the behaviour of the solution given by the continuum limit, namely

$$p_u(x,t) = \mathscr{I}(x) t^{\epsilon-\frac{1}{2}} e^{-\frac{x^2}{2t}}, \tag{2.76}$$

see [29]. Indeed for large $|x|$ we obtain

$$p_u(x,t) \sim \frac{2^{\epsilon-1/2}}{\Gamma(1/2-\epsilon)} |x|^{-2\epsilon} e^{-\frac{x^2}{2t}} t^{\epsilon-\frac{1}{2}}, \tag{2.77}$$

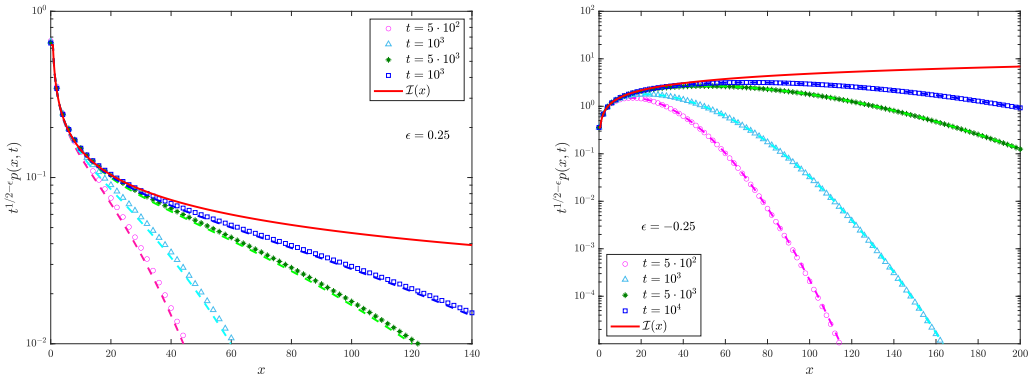

FIGURE 2.9: Plot of $t^{1/2-\epsilon} p(x,t)$ versus x, with $\epsilon = 0.25$ and $\epsilon = -0.25$. Data (symbols) are obtained by evolving the Chapman-Kolmogorov equation, Eq. (2.7), up to different times. Each data set is interpolated with good agreement by the corresponding uniform approximations $p_u(x,t)$ (dashed lines). As the evolution time increases, data approach the values predicted by the infinite invariant density $\mathscr{I}(x)$ (solid red line).

which reproduces Eq. (2.57); on the other hand, for small $|x|$ and t sufficiently large, the Gaussian factor approaches 1 and the distribution is effectively described by $\mathscr{I}(x)$. Fig. 2.9 shows the agreement for any value of x between the data obtained by the evolution of the Chapman-Kolmogorov equations and the respective uniform solutions, for different times. Data also agree with the Infinite Invariant Density $\mathscr{I}(x)$ as long as the Gaussian factor can be approximated by 1. For large values of x, the Gaussian factor cuts off the divergence of $\mathscr{I}(x)$.

2.3.2 Transport properties

Given the close relation of the GRW to the diffusion of a Brownian particle in a logarithmic potential, illustrated by the continuum limit, we expect that the transport properties of the two systems should be related as well. Indeed, at least where the scaling $z = k/\sqrt{t}$ is valid, if the distribution of z for the random walk is correctly described by the probability density functions of the corresponding diffusion process, also the moments of the distribution should behave, at least asymptotically, as those of the corresponding PDF.

For $\epsilon < \frac{1}{2}$ we have seen that $\mathscr{P}(z)$ describes correctly the distribution of z outside the central region. Close to $z = 0$, where the scaling is not valid, this function presents a singularity, which however is integrable, and one has that $|z|^q$ is measurable with respect to $\mathscr{P}(z)$ for all q. In other words, all the moments of $\mathscr{P}(z)$ are constant and this implies that all the moments of $p(x,t)$ scale like normal diffusion [29]:

$$\langle |x(t)|^q \rangle \sim t^{\frac{q}{2}}. \tag{2.78}$$

The situation is marked differently for $\epsilon > \frac{1}{2}$. Here the process reaches eventually an equilibrium state characterized by the stationary distribution. However, due to its

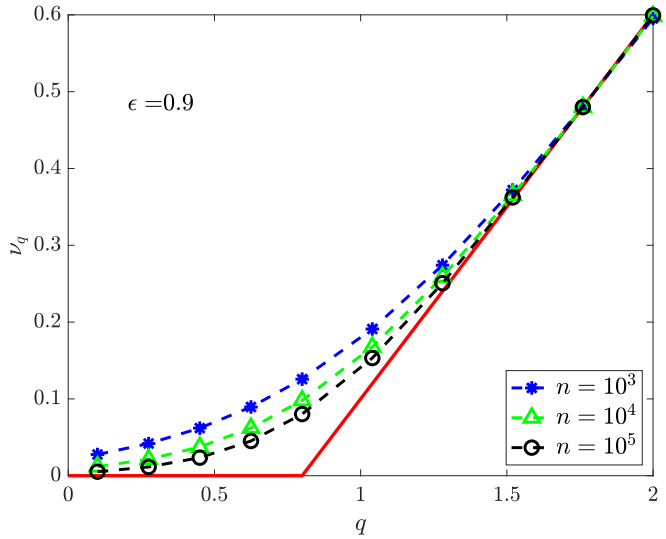

FIGURE 2.10: Exponents of the asymptotic power-law growth of the q-th moment for the Gillis random walk, as a function of q, with $\epsilon = 0.9$. Data are obtained by directly evolving the Chapman-Kolmogorov equation for $P_n(k|0)$, Eq. (2.7), up to $n = 10^5$. The red line depicts the theoretical exponents of Eq. (2.79). Note that the convergence to the theoretical values are slower close to the transition point between the two scales.

power-law decay $|x|^{-2\epsilon}$, only the low-order moments of the stationary distribution are measurable, while the high-order moments diverge. The time growth of the corresponding expectation values are given correctly by the Infinite Covariant Density $\mathscr{Q}(z)$ [29], which however presents a non-integrable singularity around $z = 0$, where the scaling breaks down. Hence the Infinite Covariant Density and the stationary distribution yield correctly the expectation values of $|x|^q$ in different ranges of q. Note that $|x|^q$ is measurable with respect to the stationary distribution as long as $q < 2\epsilon - 1$, thus in this range the moments are constant. For higher values of q, the expectation values are given by $p(z,t)$; the moments of $\mathscr{Q}(z)$ are measurable, hence one has:

$$\langle |x(t)|^q \rangle \sim t^{\frac{1}{2}(1+q)-\epsilon} \cdot 2 \int_0^\infty |z|^q \mathscr{Q}(z) \mathrm{d}z, \quad q > 2\epsilon - 1. \tag{2.79}$$

Such a scaling implies that the system exhibits strong anomalous diffusion [24] for $\epsilon > \frac{1}{2}$. Indeed, the exponent ν_q featured by the asymptotic power-law growth of the q-th moment is not characterized by a single scale, as we show in Fig. 2.10. There are in fact two different scales, acting in $0 \leq q < 2\epsilon - 1$ and $2\epsilon - 1 < q$ respectively.

It is interesting to focus on the exponent of the second moment, which specify the transport properties of the system. It should be clear by now that these depend on the value of ϵ: up to $\epsilon < \frac{1}{2}$, the system displays a normal behaviour and the second moment grows linearly in time, i.e., $\langle x^2(t) \rangle \sim t$. When the systems enters into the ergodic regime, the moments spectrum becomes anomalous and in particular the second

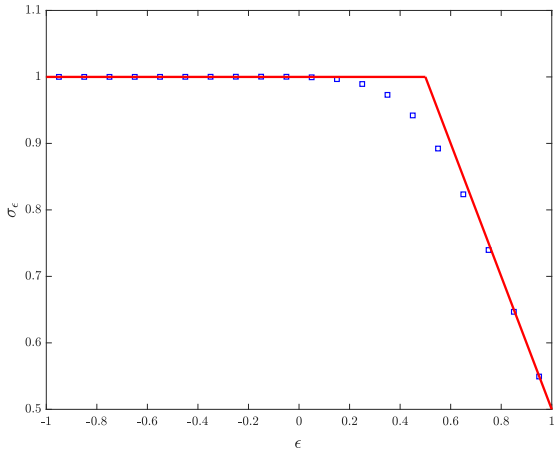

FIGURE 2.11: Exponents of the asymptotic power-law growth of the second moment for the Gillis random walk, as a function of ϵ. Data are obtained by directly evolving the Chapman-Kolmogorov equation for $P_n(k|0)$, Eq. (2.7), up to $n = 2^{15}$. The red line depicts the theoretical exponents of Eq. (2.81).

moment is given by:

$$\langle x^2(t)\rangle \sim t^{\frac{3}{2}-\epsilon}, \quad \epsilon > \frac{1}{2} \tag{2.80}$$

displaying a subdiffusive exponent. Summarizing, the exponent σ_ϵ characterizing the asymptotic growth of the second moment is

$$\sigma_\epsilon = \begin{cases} 1 & \text{for } \epsilon < \frac{1}{2} \\ \frac{3}{2} - \epsilon & \text{for } \epsilon > \frac{1}{2}. \end{cases} \tag{2.81}$$

This behaviour may be better understood by looking at the problem from a physical point of view. Let us imagine that the GRW describes the microscopic fluctuations of a particle in contact with a thermal bath at temperature T and subject to a logarithmic potential energy $V(x) \sim V_0 \log|x|$. The parameter ϵ controls the relative strength of the potential with respect to the thermal energy $k_B T$. Indeed, the steady state is given by $p_s(x) \propto \exp[-V(x)/k_B T]$, which in this case yields the power-law profile $|x|^{-V_0/k_B T}$. Comparing this to Eq. (2.37), we may identify

$$\epsilon = \frac{V_0}{2k_B T}, \tag{2.82}$$

hence $\epsilon > \frac{1}{2}$ means $V_0 > k_B T$. Then, as long as the thermal energy is stronger than V_0, pure diffusion is in control, while for lower temperatures the dominant contribution to the dynamics of the particle is that of the deterministic force towards the origin, resulting in subdiffusion.

In Fig. 2.11 we show the results of our simulations, which confirm the prediction of Eq. (2.81). Note that close to the transition point, the convergence to the expected results is slower: we can not exclude that this may be due to logarithmic corrections arising at the critical point $\epsilon = \frac{1}{2}$, of which, however, we are not presently able to prove the existence (or non-existence).

2.4 Summary

In this chapter we have presented the Gillis Random Walk, which can be seen as a non-trivial generalization of the simple symmetric random walk on the integer lattice. Focusing on the one-dimensional model and starting from the classical analytical results regarding the generating function $P_z(0|k_0)$ [42, 58], we were able to derive other related results, such as the generating functions of the first hitting time of the origin $F_z\,(0|k_0)$ and the first return time $F_z(0|0)$. From the knowledge of such generating functions, we could derive the asymptotic decay, for large n, of the respective probabilities.

We have also shown, by performing the continuum limit, that the Gillis random walk is the discrete analogous of a diffusion process in a logarithmic potential $U(x) \sim 2\epsilon \log|x|$. For a thermal system, ϵ is proportional to the ratio of the strength of the potential energy, $V(x) = V_0 \log|x|$, to the thermal energy $k_B T$, viz., $\epsilon = V_0/2k_B T$. Indeed, we have shown that for $\epsilon > \frac{1}{2}$ the Gillis random walk admits a stationary distribution π_k, which we have computed, representing the steady state of the thermal system. Furthermore, we have shown that the results regarding the solution of the Fokker-Planck equation of a Brownian particle in a logarithmic potential [29] also apply to the Gillis random walk, provided that the evolution equation are evolved for sufficiently long times. These results include the distribution of the position in both the ergodic and non-ergodic regimes and the asymptotic growth of the moments, showing that the random walk and the diffusion process share the same major dynamical properties in the long-time regime. We point out that part of the content of this chapter constitutes the basis of Ref. [97].

The Lévy-Lorentz gas 3

The Lorentz gas was introduced in 1905 [80] to model transport properties of electrons in metals. In this model the interactions between electrons are neglected and the positions of the ions are fixed, so that in its standard form it consists in a point particle moving in a periodic array of scatterers, with which it collides elastically. Translational symmetry allows to infer many properties of this extended system from the reduced dynamics in an elementary cell - see for instance [27]. In particular dynamical and transport properties are deeply influenced by the shape of scatterers and the geometry of the lattice: circular obstacles lead to a Sinai billiard for the reduced dynamics, and the chaotic properties of such a system - see [25] - are crucial in dealing with the extended case. The geometry of the lattice, and eventually the size of the scatterers, determine whether particles may travel for arbitrarily long times without experiencing any collision: the so called infinite horizon case, which leads, in two dimensions, to a logarithmic correction to the variance of the particle position. For a recent review of (transport) properties of different types of Lorentz gases see [31].

Much less is known about dynamical and transport properties when the scatterers are placed randomly, breaking translational symmetry [75]. This motivates the introduction of simplified models, which however still present, as we will see, considerable complexity: a major role is played by persistent random walks in one dimension. Persistency consists in assigning to each site a transmission and a reflection coefficient in such a way that each step the walker undertakes at time n not only depends on the position at the same time, but also on where the walker was one time step earlier. It is interesting to observe that (homogeneous) persistent random walks have been introduced nearly a century ago, as a model of diffusion by discontinuous movements [40, 113]: many of the relevant results have been obtained (for different time regimes) by introducing appropriate continuum limits [47, 60, 104, 119]. Inhomogeneous persistency arises naturally when we distribute randomly scatterers in the lattice (empty sites being given a null reflection coefficient): models of this kind have been introduced in [112] as a variant of Sinai diffusion (see [58]).

In recent years a great interest emerged for the case of a diluted distribution of scatterers, whose mutual distance is characterized by a heavy tailed distribution [7, 20, 12, 13]. This model, known in the literature as *Lévy-Lorentz* (LL) gas, is made particularly interesting by the fact that the long ballistic flights performed by the walker are due to the nature of the medium, not to a special law governing the walker's decision, which is the case, e.g., of an homogeneous Lévy walk [121, 26]. This

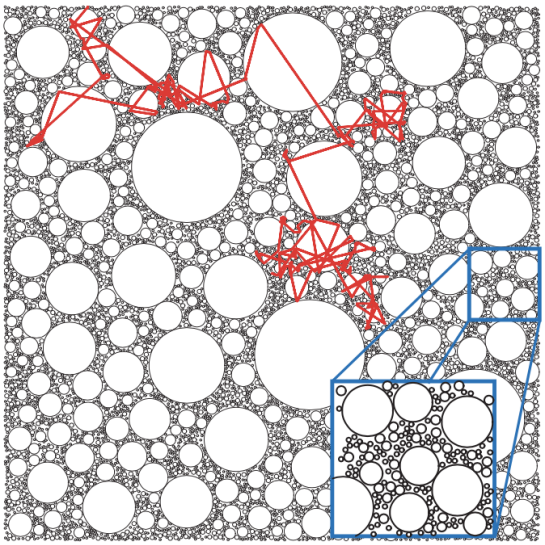

FIGURE 3.1: The trajectory of a light particle in a Lévy glass (red). Note the long ballistic flights, which are possible for the presence of large non-scattering glass spheres (from P. Barthelemy, J. Bertolotti and D.S. Wiersma, *Nature*, 453: 495, 2008).

produces a significant difference in the diffusion properties: for example, a LL gas in an environment where the distance between obstacles is Lévy-distributed with parameter $\alpha \in (1, 2)$ is diffusive [12], but the Lévy walk whose flights have the same distribution is not [26, 82]. Besides theoretical interest the LL gas model is tightly connected to experimentally fabricated Lévy glasses [8], consisting of high-refractive-index scattering particles of titanium dioxide placed in a glass host. The local density of scattering particles is modified by including non-scattering glass microspheres of a highly non-trivial distribution of diameters characterized by a particular power-law decay. A light particle in a Lévy glass is expected to move alternating between a rapid succession of scattering events and long ballistic flights, thus resembling the trajectory of a Lévy walk, see Fig. 3.1.

The LL gas is an interesting example of RWRE and in fact in recent years it has been considered as the object of study for many works. The system can be studied from a double prospective: the *quenched*, where one asks how the properties of the dynamics are related to each fixed realization of disorder, and the *annealed*, where one is interested in the effects of averaging over different processes evolved on different environments. In order to study a mean field evolution over a fast changing environment, in [3] we proposed a third viewpoint, that of the *averaged* process, where the dynamics is considered on a single, particular environment, which can be seen as the outcome of an average over all possible realizations of disorder. This construction leads to a non-homogeneous persistent random walk where the reflection probability depends non-trivially on the distance from the origin. In the following we will first discuss the most important results obtained for both the quenched and the annealed versions of the LL gas and then we will present the averaged model, its relation with other two and

some basic results regarding its transport properties.

3.1 Lévy-Lorentz gas: quenched, annealed and averaged

We start with a general setting: a one-dimensional persistent random walk on $\mathbb{Z}$ with position-dependent transmission and reflection coefficients. In the canonical (homogeneous) persistent random walk scheme a particle starts moving with fixed velocity v from position $x_0 = 0$ in a random direction and then at each site it is reflected or transmitted according to a certain (constant) probability. In the LL gas scheme instead reflection may only occur at certain positions, where the scatterers are present. Scattering sites are placed at random positions in such a way that the relative distances are distributed according to a Lévy-like PDF, i.e., a distribution that decays with a heavy polynomial tail for large values of the argument:

$$\mu(\xi) \sim \xi^{-(1+\alpha)}, \quad 0 < \alpha < 2. \tag{3.1}$$

Notice that in this range the variance of the distance diverges, and in the restricted range $0 < \alpha \leq 1$ also the average distance is infinite.

The set of the positions of the scatterers through which transmittance and reflection are assigned among the lattice is called the *environment*, namely

$$\omega = \big\{k \in \mathbb{Z} \,|\, k\text{-th site is a scatterer}\big\}.$$

When defining the environment, one can set the origin in two different ways: in the *nonequilibrium* case the process is always conditioned to start with a scattering event, therefore the starting point is always occupied by a scatterer - note that this situation is the closest to experimental realizations [20]; in the *equilibrium* case instead - see [7] - the starting point is not considered a special point, thus it can be placed at any site of the lattice, independently of the presence of a scatterer.

Given a realization of the environment, transmittance and reflection among the lattice are assigned according to

$$\mathfrak{r}_k^\omega = r \cdot \delta_k^\omega$$
$$\mathfrak{t}_k^\omega = 1 - \mathfrak{r}_k^\omega$$

where

$$\delta_k^\omega = \begin{cases} 1 & \text{if } k \in \omega \\ 0 & \text{if } k \notin \omega \end{cases}$$

and $0 < r < 1$, which in the literature is commonly taken equal to $\frac{1}{2}$. Notice that in the nonequilibrium case we always have $\delta_0^\omega = 1$. Time evolution is written in its simplest form once we introduce the quantities $R_k^\omega(n)$ and $L_k^\omega(n)$, representing the probabilities

of being at site k after n steps with right and left momentum, respectively. These probabilities evolve according to the Chapman-Kolmogorov equations:

$$\begin{cases} R^{\omega}_{n+1}(k) = \mathfrak{t}^{\omega}_{k} \cdot R^{\omega}_{n}(k-1) + \mathfrak{r}^{\omega}_{k} \cdot L^{\omega}_{n}(k+1) & (3.2) \\ L^{\omega}_{n+1}(k) = \mathfrak{t}^{\omega}_{k} \cdot L^{\omega}_{n}(k+1) + \mathfrak{r}^{\omega}_{k} \cdot R^{\omega}_{n}(k-1) & (3.3) \end{cases}$$

with initial conditions

$$\begin{cases} R^{\omega}_{0}(0) = L^{\omega}_{0}(0) = \dfrac{1}{2} & (3.4) \\ R^{\omega}_{0}(k) = L^{\omega}_{0}(k) = 0 \quad \forall k \neq 0. & (3.5) \end{cases}$$

From (3.2)-(3.3) and (3.4)-(3.5) one can derive the equations and the initial conditions for the probability of the displacement of the walker $P^{\omega}_{n}(k) = R^{\omega}_{n}(k) + L^{\omega}_{n}(k)$ and the probability drift $A^{\omega}_{n}(k) = R^{\omega}_{n}(k) - L^{\omega}_{n}(k)$:

$$\begin{cases} P^{\omega}_{n+1}(k) = R^{\omega}_{n}(k-1) + L^{\omega}_{n}(k+1) & (3.6) \\ A^{\omega}_{n+1}(k) = (\mathfrak{t}^{\omega}_{k} - \mathfrak{r}^{\omega}_{k}) \cdot \left[R^{\omega}_{n}(k-1) - L^{\omega}_{n}(k+1)\right] & (3.7) \end{cases}$$

with

$$\begin{cases} P^{\omega}_{0}(0) = 1 & (3.8) \\ A^{\omega}_{0}(0) = 0. & (3.9) \end{cases}$$

These are the basic equations describing the dynamics of a particle in the LL gas. We will now discuss, without going too deep into mathematical details, the main known results for each version of the model.

3.1.1 Quenched model

In general, in the quenched version of a RWRE one is interested in the dynamics on a single, typical environment. More precisely, let us denote with Ω the set of all possible environments ω, and P the law defined on it - for instance, in the case of the LL gas, P is a Lévy-like law as in Eq. (3.1), describing the distribution of the distances between nearest-neighbour scatterers. The object of study in this case is P_{ω}, the law of the process defined on a fixed environment, and one aims at finding properties of the process which hold for P-a.e. environment, i.e., valid except for a subset $\Omega_0 \in \Omega$ of measure zero.

For the quenched LL gas, few results have been established hitherto. Remarkably, in the case $1 < \alpha < 2$, when considering nonequilibrium initial conditions, it can be proven that for almost every environment, the process $x_{\omega}(t)$ verifies the CLT. Let $\langle \xi \rangle$ denote the mean of the distribution of the distances between scatterers. Then it holds the following [12]:

Theorem 1. *For P-a.e.* $\omega \in \Omega$,

$$\lim_{t\to\infty} P_\omega \left\{ \frac{x_\omega(t)}{\sqrt{t}} < z \right\} = \frac{1}{\sqrt{2\pi}} \int_{-\infty}^{z/\langle\xi\rangle} e^{-\frac{1}{2}u^2} \mathrm{d}u. \tag{3.10}$$

It is important to stress that this result does not imply a diffusive scaling for the moments, whose behaviour, indeed, still remains an open question. To our knowledge, no relevant results are known for the infinite-mean case, neither regarding the transport properties nor regarding the law of the process.

3.1.2 Annealed model

The objective of the annealed model is to investigate the effects of averaging over all realizations of disorder. Roughly speaking, the annealed law $\langle P_\omega \rangle$ is the average over all possible environments of the respective P_ω. For $1 < \alpha < 2$ and nonequilibrium initial conditions, it can be proved that the quenched result of Theorem 1 implies the validity of the CLT for the annealed process as well [12]. Regarding the infinite-mean case, it has been recently proved for $0 < \alpha < 1$ and nonequilibrium initial conditions the validity of a generalized CLT - see [13] for a more precise statement. In this case, the convergence to the limiting process is obtained thanks to a superdiffusive scaling, with exponent $1/(1+\alpha)$. It is worth observing that these mathematically rigorous results agree with those previously obtained in the physical literature [20], whose starting point is a scaling hypothesis for the probability distribution of the walker, which is decomposed into a central part and a subleading term describing the behaviour at large distances:

$$\langle p_\omega(x,t) \rangle = \frac{1}{\ell(t)} \mathscr{F}\left(\frac{x}{\ell(t)}\right) + \mathscr{G}(x,t). \tag{3.11}$$

The correlation length $\ell(t)$ is determined by using estimates according to the related resistance model treated in [9], which give

$$\ell(t) \sim \begin{cases} t^{\frac{1}{1+\alpha}} & 0 < \alpha < 1 \\ t^{\frac{1}{2}} & \alpha \geq 1. \end{cases} \tag{3.12}$$

The tail function $\mathscr{G}(x,t)$ has been recently investigated using the single-big-jump principle [118]. This term describes the behaviour of the PDF at large distances and provides important contributions to the higher moments of the distribution. It can be shown that it exhibits the following scaling [118]:

$$\mathscr{G}(x,t) \sim \begin{cases} t^{-\frac{1+\alpha+\alpha^2}{1+\alpha}} \mathscr{I}_\alpha\left(\frac{|x|}{vt}\right) & 0 < \alpha < 1 \\ t^{-\frac{1}{2}-\alpha} \mathscr{I}_\alpha\left(\frac{|x|}{vt}\right) & \alpha \geq 1, \end{cases} \tag{3.13}$$

where v is the velocity of the particle and $\mathscr{I}_\alpha(z)$ is a scaling function that can be evaluated analytically using the big-jump principle. It can be shown that this function

is an infinite covariant density that can be used to estimate the moments of the process [118]. The whole moments spectrum is in fact provided by the competition of the time scales in (3.12) and (3.13), yielding a strongly anomalous behaviour [20, 118]:

$$\langle |x(t)|^q \rangle \sim \begin{cases} t^{\frac{q}{1+\alpha}} & \text{if } \alpha < 1,\ q < \alpha \\ t^{\frac{q(1+\alpha)-\alpha^2}{1+\alpha}} & \text{if } \alpha < 1,\ q > \alpha \\ t^{\frac{q}{2}} & \text{if } \alpha > 1,\ q < 2\alpha - 1 \\ t^{\frac{1}{2}+q-\alpha} & \text{if } \alpha < 1,\ q > 2\alpha - 1. \end{cases} \tag{3.14}$$

In particular, the second moment grows as

$$\langle |x(t)|^2 \rangle \sim \begin{cases} t^{2-\frac{\alpha^2}{1+\alpha}} & \alpha < 1 \\ t^{\frac{5}{2}-\alpha} & 1 < \alpha < \frac{3}{2} \\ t & \alpha > \frac{3}{2}. \end{cases} \tag{3.15}$$

Note that, although the validity of the CLT has been proved for $\alpha > 1$, only low-order moments present a diffusive scaling. As a consequence, the second moment grows linearly in time only in the restricted range $\alpha > \frac{3}{2}$, while for $1 < \alpha < \frac{3}{2}$ the system is characterized by superdiffusion.

We remark that these results are valid for nonequilibrium initial conditions. Things are different when considering equilibrium initial conditions: if the origin of the motion can be placed at any point of the structure, then a major role is played by the random variable d_f describing the distance between the initial position and the first scatterer in $x > 0$. For $\alpha < 1$ the motion is always ballistic [20], while for $1 < \alpha < 2$ it can be shown that the distribution $q\left(d_f\right)$ of the random variable d_f decays as $d_f^{-\alpha}$, i.e., much more slowly than the distance between nearest-neighbour scatterers [7]. The first jump provides a dominant contribution to the MSD, which grows in this case as $t^{3-\alpha}$ [7, 20].

Finally, it is interesting to observe that despite the huge difference in the behaviours of the moments spectra, equilibrium and nonequilibrium initial conditions share a common feature in the range $1 < \alpha < 2$, viz., the temporal decay of the probability of being at the origin, which in both cases is characterized by the power-law behaviour $t^{-1/2}$, as in standard Gaussian diffusion, see [7, 20].

3.2 Averaged model

Both the quenched and the annealed model present analytical and technical difficulties. For example, the numerical study of the quenched model is made hard by the large fluctuations experienced in the construction of different environments, especially in the infinite mean case, $\alpha < 1$. Also, very few analytical results are known. For the annealed model instead we have a larger number of results, which, however, can be difficult to verify numerically, due to the need of averaging over a huge number of different environments.

In [3] we presented the averaged version of the LL gas. In this case, the random disorder of the environment is replaced by a non-trivial behaviour of the reflection probability along the lattice. In other words, the averaged LL gas consists in a non-homogeneous persistent random walk on $\mathbb{Z}$ where at each step the particle can be reflected according to a position-dependent probability $\mathfrak{r}_k$. The relation with the original LL gas is thus given by the definition of $\mathfrak{r}_k$. The aim is to study a mean field evolution over a fast-changing landscape, by connecting the reflection probability at site k to the probability of finding a scatterer at the same position, for a quenched environment of the LL gas.

Let us introduce the averaged environment. For the quenched model of the LL gas, we call ϖ_k the probability of having a scatterer at position k, given the distribution of distances $\mu(\xi)$. We recall that we are considering the motion on the integer lattice, hence ξ is integer and strictly positive, and we can consider for simplicity the following analytical form, in agreement with (3.1):

$$\mu(\xi) = \frac{\xi^{-1-\alpha}}{\zeta(1+\alpha)}, \quad \xi = 1, 2, \dots, \tag{3.16}$$

where $\zeta(z)$ is the Riemann zeta function. We consider only nonequilibrium initial condition, therefore $\varpi_0 = 1$ and this implies the symmetry $\varpi_k = \varpi_{-k}$. We can therefore write the probability ϖ_k in terms of $\mu(\xi)$, which reads:

$$\begin{aligned}\varpi_k &= \sum_{m=1}^{|k|} \left[\sum_{\sum_{i=1}^m \xi_i = |k|} \prod_{i=1}^{m} \mu\left(\xi_i\right) \right] \\ &= \mu\left(|k|\right) + \sum_{\xi_1+\xi_2=|k|} \mu(\xi_1)\mu(\xi_2) + \dots + \mu(1)^{|k|}.\end{aligned} \tag{3.17}$$

In Appendix C we analytically evaluate the asymptotic value of the probability of having a scatter at position k, for $|k| \gg 1$, which is:

$$\varpi_k \sim \pi_k = \begin{cases} \dfrac{\alpha \sin(\pi\alpha)}{\pi} \dfrac{\zeta(1+\alpha)}{|k|^{1-\alpha}} & 0 < \alpha < 1 \\ \dfrac{\zeta(1+\alpha)}{\zeta(\alpha)} & \alpha > 1. \end{cases} \tag{3.18}$$

The expression of π_k is the starting point in the definition of the reflection probability along the lattice for the averaged environment. We recall that in the quenched LL gas the reversal probability is given by $\mathfrak{r}_k^\omega = \frac{1}{2}\delta_k^\omega$, where δ_k^ω is equal to one if site k is occupied by a scatterer and zero otherwise. In the averaged LL gas we replace δ_k^ω with π_k. Hence we finally define the averaged LL gas as a persistent random walk on $\mathbb{Z}$ with nearest-neighbour jumps and a site-dependent reversal probability $\mathfrak{r}_k$ given by:

$$\mathfrak{r}_k = \frac{1}{2} \cdot \begin{cases} \pi_k & k \neq 0 \\ 1 & k = 0. \end{cases} \tag{3.19}$$

We remark, however, that such a choice is arbitrary and different models could be defined starting from (C.9). For instance, in [100] we studied a related model where the same expression on the right-hand side of Eq. (3.19) is used to determine the transmission coefficient:

$$\mathfrak{t}_k = \frac{1}{2} \cdot \begin{cases} \pi_k & k \neq 0 \\ 1 & k = 0. \end{cases} \tag{3.20}$$

In the following we will discuss some basic properties of both models that can be obtained thanks to suitable continuum limits, highlight the differences between the two and explain which features of the original LL gas are recovered in the averaged model.

3.3 Continuum limits

To obtain the limiting equation governing the dynamics of a particle in the averaged LL gas, we first consider the continuum limit of a persistent random walk characterized by a reflection probability with a generic spatial dependence. We can proceed as done in Chapter 1 for the standard persistent random walk scheme. We call δx the lattice spacing, δt the time step and set $x = k\delta x$ and $t = n\delta t$. We denote with $r(x,t)$ and $l(x,t)$ the probability densities of being at position x at time t and leaving to the right or left respectively, and set

$$\begin{cases} R_n(k) = \delta x \cdot r(x,t) & (3.21) \\ L_n(k) = \delta x \cdot l(x,t), & (3.22) \end{cases}$$

while for the quantities $P_n(k) = R_n(k) + L_n(k)$ and $A_n(k) = R_n(k) - L_n(k)$ we set

$$\begin{cases} P_n(k) = \delta x \cdot p(x,t) & (3.23) \\ A_n(k) = \delta t \cdot a(x,t), & (3.24) \end{cases}$$

where $p(x,t)$ and $a(x,t)$ are defined in terms of $r(x,t)$ and $l(x,t)$ as:

$$\begin{cases} p(x,t) = r(x,t) + l(x,t) & (3.25) \\ a(x,t) = \dfrac{\delta x}{\delta t} \cdot \left[r(x,t) - l(x,t) \right]. & (3.26) \end{cases}$$

Inserting (3.21)-(3.21) and (3.23)-(3.24) into the Chapman-Kolmogorov equations (3.6)-(3.7) and expanding the functions r, l, p, a up to second order in both δx and δt, one gets the following pair of coupled equations:

$$\begin{cases} \dot{p}\delta t + \dfrac{1}{2}\ddot{p}\delta t^2 = -a'\delta t + \dfrac{1}{2}p''\delta x^2 & (3.27) \\ a\delta t + \dot{a}\delta t^2 + \dfrac{1}{2}\ddot{a}\delta t^3 = (\mathfrak{t} - \mathfrak{r}) \cdot \left(a\delta t - p'\delta x^2 + \dfrac{1}{2}a''\delta x^2\delta t \right) & (3.28) \end{cases}$$

We get a closed equation for p by employing the diffusion approximation: we consider the limit $\delta x, \delta t \to 0$ with $\delta x^2/\delta t = \Delta$ kept constant. By dropping higher order terms we obtain the following set of equations:

$$\begin{cases} \dfrac{\partial p}{\partial t} = -\dfrac{\partial a}{\partial x} + \dfrac{\Delta}{2}\dfrac{\partial^2 p}{\partial x^2} & (3.29) \\ a = -\dfrac{\Delta}{2}\dfrac{\mathfrak{t}-\mathfrak{r}}{\mathfrak{r}}\dfrac{\partial p}{\partial x}. & (3.30) \end{cases}$$

Inserting the second one into the first, we finally get

$$\frac{\partial p}{\partial t} = \frac{\partial}{\partial x}\left[D_\alpha(x)\frac{\partial p}{\partial x}\right] \tag{3.31}$$

where $D_\alpha(x)$ is

$$D_\alpha(x) = \frac{\Delta}{2}\frac{\mathfrak{t}(x)}{\mathfrak{r}(x)} \tag{3.32}$$

and we set $\Delta = 1$. Such an expression for the diffusion coefficient is remarkable, since in Chapter 1 we showed that in the long-time limit the evolution of the homogeneous persistent random walk can be described by the heat equation, and the numerical value of the diffusion coefficient is given by the ratio between the transmission and reflection probabilities. Now we have obtained that when reflectance and transmittance possess and explicit spatial dependence, we recover the same structure for the diffusion coefficient, as expressed by Eqs. (3.31) and (3.32). We also observe that Eq. (3.31) may characterize diffusion in an inhomogeneous medium with position-dependent friction coefficient [103], studies of chemical reactions [41] or the stock market in finances [96] and measurements of proteins' diffusivity in mammalian cells [67].

For the averaged LL gas, we define the diffusion coefficient by taking as $\mathfrak{r}(x)$ and $\mathfrak{t}(x)$ the continuous-space limit of π_k , Eq. (C.9):

$$\pi_k \to \pi(x) = \begin{cases} \dfrac{\alpha \sin(\pi\alpha)}{\pi}\dfrac{\zeta(1+\alpha)}{|x|^{1-\alpha}} & 0 < \alpha < 1 \\ \dfrac{\zeta(1+\alpha)}{\zeta(\alpha)} & \alpha > 1. \end{cases} \tag{3.33}$$

Hence we have an explicit expression for $D_\alpha(x)$, which may be used to solve the diffusion equation and obtain the main statistical properties of the system.

3.3.1 Superdiffusive Lévy-Lorentz gas

In the first version of the averaged LL gas presented in [3], the reflection coefficient is proportional to $\pi(x)$ and defined as in Eq. (3.19). This means that for $\alpha < 1$ the reversal events are less probable as the particle reaches greater distances from the origin, and we shall see that this implies superdiffusion.

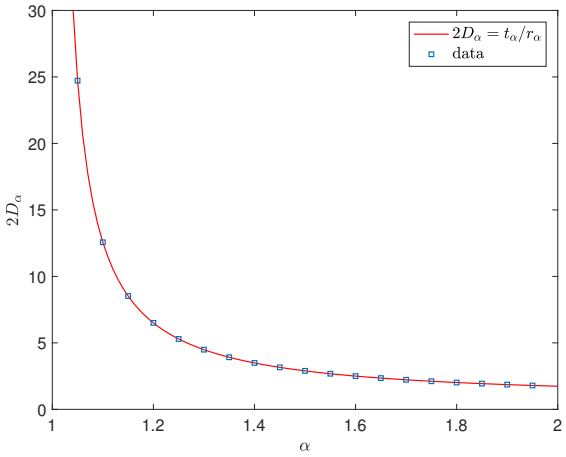

FIGURE 3.2: Slope of linear growth of the second moment as obtained by numerically evolving the forward Kolmogorov equation (3.6)-(3.7) (squares) and the analytic prediction in terms of the diffusion constant (3.34). Each numerical slope has been obtained by evolving the system up to time 2^{15}.

From Eq. (3.32) we obtain the diffusion coefficient:

$$D_\alpha(x) \simeq \frac{1}{\pi(x)} - \frac{1}{2} = \begin{cases} \Lambda|x|^{1-\alpha} - \dfrac{1}{2} & 0 < \alpha < 1 \\ \dfrac{\zeta(\alpha)}{\zeta(1+\alpha)} - \dfrac{1}{2} & \alpha > 1, \end{cases} \tag{3.34}$$

where

$$\Lambda = \frac{\pi}{\alpha \sin(\pi\alpha)\,\zeta(1+\alpha)}. \tag{3.35}$$

Note that for $0 < \alpha < 1$, Eq. (3.34) leads to negative values of $D_\alpha(x)$ in a neighbourhood of the origin, thus the expression must be considered valid only outside that region. This issue will be discussed in more detail later.

For $\alpha > 1$ the diffusion coefficient is constant, hence equation (3.31) becomes a simple heat equation. This agrees with the fact that for both the quenched and the annealed models, in the same range of α, the validity of the CLT has been proved. Our system therefore displays normal diffusion, with the second moment asymptotics given by

$$\langle x^2(t)\rangle \sim 2D_\alpha \cdot t. \tag{3.36}$$

This is confirmed by numerical simulations, see Fig. 3.2, where for each α we supposed a linear growth of the second moment for the data and obtained the corresponding slope by a linear fit.

We can also recover other important properties of Gaussian diffusion, such as the $n^{-1/2}$ decay of the autocorrelation function $P_{2n}(0|0)$. Note that this feature is in

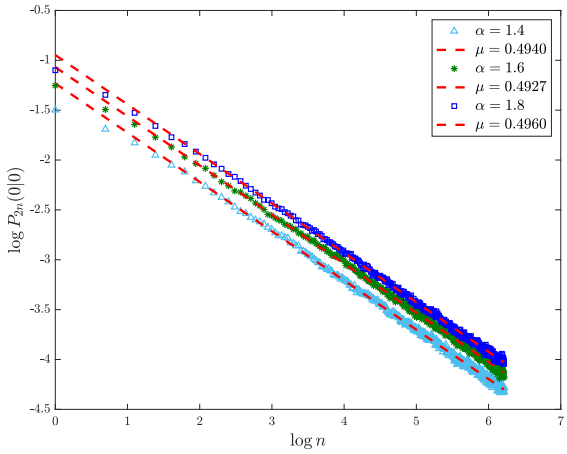

FIGURE 3.3: Probability of being at the origin after $2n$ steps, for different values of α. For each value of the parameter, data are obtained evolving 10^5 walks up to 10^4 number of steps. The exponent μ of the asymptotic power law decay is estimated by the slope of the linear fit: each value is close to the theoretic result $\mu = 0.5$.

agreement with the results obtained for the annealed model, where for $\alpha > 1$ the scaling $x/\sqrt{t}$ is assumed for the bulk part of the PDF, see Eqs. (3.11) and (3.12). Fig. 3.3 displays the asymptotic power law decay of $P_{2n}(0|0)$ for different values of α in the range $\alpha > 1$, and we note that the decay is independent of the value of the parameter. Indeed, the linear fit of the data in the logarithmic plot results in a set of parallel straight lines.

Finally we observe that the heat equation is also useful to describe the distribution of the position of the particle. By considering the scaling variable $z = x/\sqrt{4D_\alpha t}$, we expect that in the $t \to \infty$ regime:

$$p(z) = \frac{1}{\sqrt{\pi}} e^{-z^2}, \tag{3.37}$$

which is confirmed by the simulations in Fig. 3.4. Note that although the scaling depends on α through the diffusion coefficient, the limiting distribution is independent of it, thus we have Gaussian diffusion for each $\alpha > 1$.

The interesting regime is of course $\alpha < 1$, where $D_\alpha(x)$ displays a true spatial dependence, see Eq. (3.34). We note that for large enough values of the distance from the origin, the diffusion coefficient can be approximated by $D_\alpha(x) \sim \Lambda|x|^{1-\alpha}$. The problem of heterogeneous diffusion with diffusion coefficient displaying a power-law dependence on space and the system evolving according to Eq. (3.31) has been treated, for example, in [103], where also the solution of the diffusion equation is provided. Assuming $D_\alpha(x) = \Lambda|x|^{1-\alpha}$, in our case the PDF reads:

$$p(x,t) = \frac{(K_\alpha t)^{-\frac{1}{1+\alpha}}}{2\Gamma\left(1+\frac{1}{1+\alpha}\right)} \exp\left[-\frac{|x|^{1+\alpha}}{K_\alpha t}\right], \tag{3.38}$$

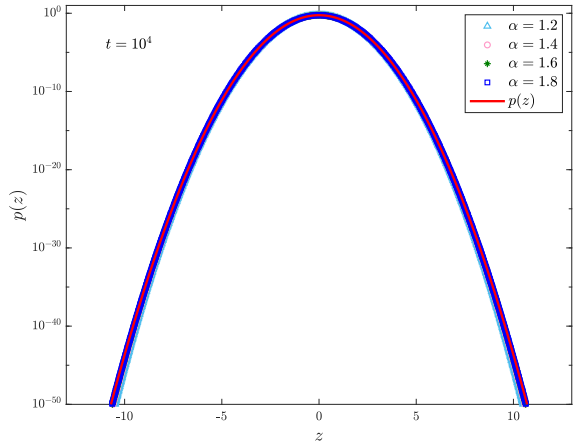

FIGURE 3.4: Distribution of the random variable $z = x/\sqrt{4D_\alpha t}$ for positive values of x, compared to the Gaussian probability density function (red line). Data are obtained by considering different α and evolving the Chapman-Kolmogorov equations (3.2)-(3.3) up to $t = 10^4$ number of steps.

where

$$K_\alpha = (1+\alpha)^2 \Lambda. \tag{3.39}$$

We point out that this solution is just an approximation, since the structure of the diffusion coefficient characterizing our system is more complicated than a pure power-law. Nevertheless, we see from Fig. 3.5 that in the long-time regime data show a good agreement with Eq. (3.38). In this case we considered the distribution of the scaled variable

$$z = \frac{x}{(K_\alpha t)^{\frac{1}{1+\alpha}}}, \tag{3.40}$$

which is distributed according to

$$p_\alpha(z) = \frac{e^{-|z|^{1+\alpha}}}{2\Gamma\left(1+\frac{1}{1+\alpha}\right)}. \tag{3.41}$$

We note that, differently from the case $\alpha > 1$, the limiting distribution is not universal and the distribution of z this time depends explicitly on α. Moreover, the scaling of Eq. (3.40) is the same scaling involved in the proof of a generalized CLT for the annealed model [13].

The result regarding the solution of the diffusion equation let us obtain the behaviour of the moments spectrum. Indeed, the q-th moment of $p_\alpha(z)$ is constant for any q, hence the average value of $|x|^q$ grows in time as

$$\langle |x(t)|^q \rangle \sim t^{\frac{q}{1+\alpha}}. \tag{3.42}$$

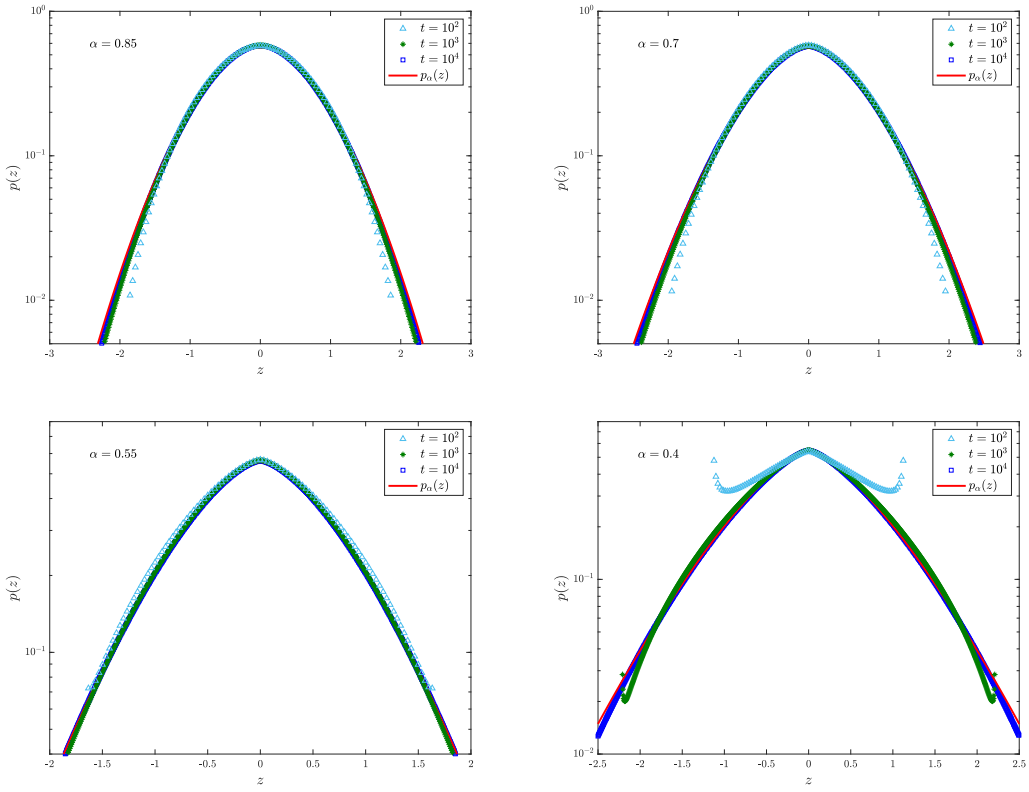

FIGURE 3.5: Distributions of the random variable $z = x/(K_\alpha t)^{1/(1+\alpha)}$ and theoretical predictions (red lines), as given in Eq. (3.41). Data are obtained for different values of α, evolving the Chapman-Kolmogorov (3.2)-(3.3) equations up to $t = 10^4$ number of steps. Note the ballistic peaks for low values of α, which however vanish for higher numbers of steps.

Therefore we can classify the system as weakly anomalous, meaning that there is a single scale $\beta(\alpha)$ ruling the whole moments' spectrum [24], with the exponent of the q-th moment given by:

$$\gamma_q(\alpha) = q \cdot \beta(\alpha) = \frac{q}{1+\alpha}. \tag{3.43}$$

This implies, in particular, that the second moment $q = 2$ is superdiffusive.

Fig. 3.6 shows the exponents of the q-th moment, for different values of q, computed by numerical simulations. These are compared to the theoretically predicted exponent $\gamma_q(\alpha)$. We see that the agreement is good for α far enough from zero, while for small values of the parameter data show discrepancies with respect to the theoretical prediction. In particular, the computed exponents are always higher than the theoretical ones. We may explain this feature by recalling the discussion on the continuum limit for the homogeneous persistent random walk we made in Chapter 1. Although in the long-time regime the heat equation approximates well the evolution equation of the system, there is an intermediate regime where the dynamics can be described by the

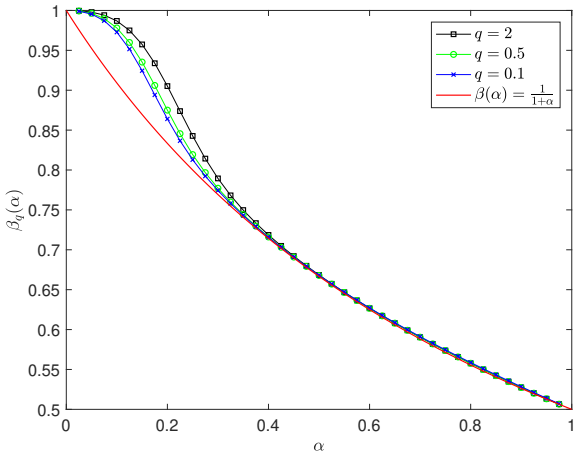

Figure 3.6: Asymptotic growth exponent of q-th moment, $\langle |x(t)|^q \rangle \sim t^{\gamma_q(\alpha)}$, for different q. The y-axis displays the renormalized exponent $\beta_q(\alpha) = \gamma_q(\alpha)/q$, which agrees with the theoretical scale $\beta(\alpha)$. Each numerical exponent has been obtained by directly evolving the evolution equations (3.6)-(3.7) up to time 2^{18}.

telegrapher's equation. We recall that in order to obtain the telegrapher's equation, one supposes that the lattice spacing and the time step go to zero with the same "speed", i.e., their ratio remains constant. In other words, the velocity of the particle remains well-defined (and fixed), even in the procedure of going to the continuum. Indeed, a well-known property of the telegrapher's equation is that for very short times it provides the same description to the dynamics as a wave equation [119]. This means that in such a regime the process is governed by ballistic flights, where the particle experiences a very low number of reversal events. The presence of such ballistic flights yields ballistic contributions to the MSD, $\langle x^2(t) \rangle \sim t^2$, which vanish as time increases and the number of reflections becomes non-negligible, allowing the system to eventually reach the diffusion regime. Hence, the discrepancies in the moments spectrum we have in Fig. 3.6 can be explained by assuming that the system has not been evolved for times long enough to reach the diffusion regime. Indeed, such discrepancies are observed only for small values of α, for which the reflection coefficient attains lower values. This guess is partially confirmed by Fig. 3.7, showing the distribution of the scaled random variable z for $\alpha = 0.3$. The system is evolved up to different times: we observe that for each time the data sets are peaked close to $z \approx 1$, which means that in each case the particle is most-likely found at

$$|x| \approx (K_\alpha t)^{\frac{1}{1+\alpha}} . \tag{3.44}$$

For $\alpha = 0.3$ and up to the times of our simulations $\left(10^2 - 10^4\right)$, such a distance is of the same order of the total evolution time, meaning that the contribution of ballistic flights is still dominant. We also observe that the ballistic peaks decay as time increases and data slowly converge to the theoretical diffusion prediction.

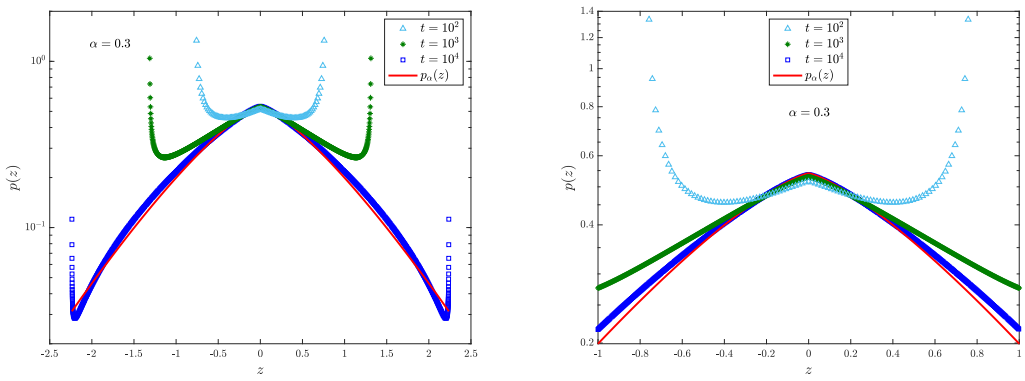

FIGURE 3.7: Distribution of the random variable $z = x/(K_\alpha t)^{1/(1+\alpha)}$ compared to the theoretical predictions (red lines), as given in Eq. (3.41). Data are obtained by considering $\alpha = 0.3$ and evolving the Chapman-Kolmogorov equations (3.2)-(3.3) up to $t = 10^4$ number of steps. We note that in this case the agreement is not good, due to the presence of the ballistic peaks, which tend to vanish as the total time is increased. We also observe, accordingly, that the theoretical prediction overestimates the central part of the distribution (right panel).

A final remark should be made regarding the diffusion coefficient we defined in Eq. (3.34). For $\alpha < 1$, as we have already anticipated, $D_\alpha(x)$ can attain negative values in a neighbourhood of the origin up to a distance

$$|x_c| = (2\Lambda)^{-\frac{1}{1-\alpha}} . \tag{3.45}$$

This is due to the fact that in the same region the continuous-space version of the reflection coefficient attains values higher than one, which is unphysical. Hence the diffusion equation Eq. (3.31) is meaningful only outside of this region and a regularization procedure should be considered in order to describe the evolution of the system in the whole space. A similar case in treated in [74]. However, we observe that this does not affect the prediction of the long-time properties of the system, such as the asymptotic growth exponent of the moments, as we have already shown with numerical simulations. Moreover, this does not even affect the asymptotic decay exponent of the autocorrelation function $P_{2n}(0|0)$, i.e., the probability of being at the origin, which decays as predicted by Eq. (3.38):

$$P_{2n}(0|0) \sim n^{-\frac{1}{1+\alpha}}. \tag{3.46}$$

This is confirmed by the simulations presented in Fig. 3.8, where the exponents for different α have been computed as the result of a linear fit, with a good agreement with theoretical predictions.

This final result let us conclude that the averaged LL gas, in its superdiffusive version, and the annealed LL gas share the asymptotic power-law exponent of the probability of being at the origin, in the whole range $0 < \alpha < 2$. The same exponent

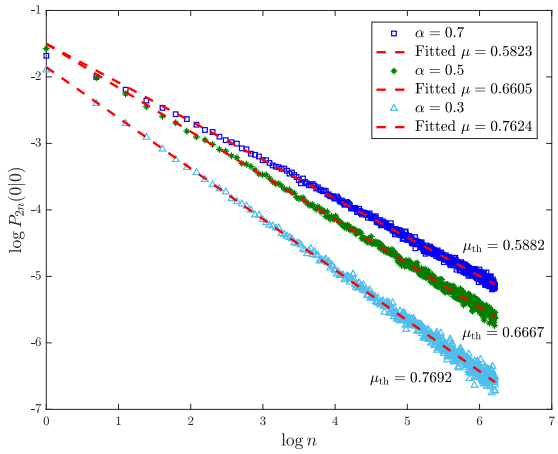

FIGURE 3.8: Probability of being at the origin after $2n$ steps, for different values of α. For each value of the parameter, data are obtained evolving 10^5 walks up to 10^4 number of steps. The exponent μ of the asymptotic power law decay is estimated by the slope of the linear fit: each value is close to its corresponding theoretical value $\mu_{\text{th}} = \frac{1}{1+\alpha}$.

also gives the scaling of the limiting distribution, for the averaged model, and the scaling of the bulk part of the PDF, for the annealed model. However, we remark that this is not sufficient to obtain a correspondence between the moments' spectra. Indeed, from Eq. (3.14) we see that only the exponents of low-order moments agree between the two systems. This is due to the fact that for the averaged model a single scale is sufficient to determine the exponent of each moment, while for the annealed model the presence of the tail function provides important contributions, leading to a more complicated moments' spectrum. We also observe that in the restricted range $1 < \alpha < 2$ the averaged model behaves as Gaussian diffusion, in agreement with the validity of the CLT proved for both the quenched and the annealed versions of the LL gas.

3.3.2 Subdiffusive Lévy-Lorentz gas

As we have already said, the second version of the averaged LL gas [100] is obtained by switching the definitions of the reflection and transmission coefficients of the previous model, meaning that

$$\mathfrak{r}_k = 1 - \frac{1}{2}\pi_k. \tag{3.47}$$

Hence in this case for $\alpha < 1$ the transmission events become less probable as the distance from the origin increases, yielding subdiffusion.

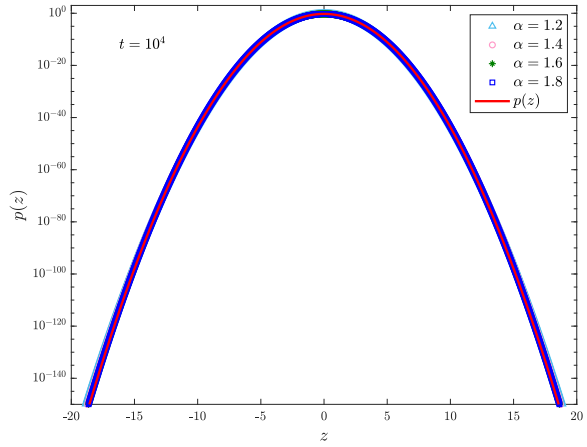

FIGURE 3.9: Distribution of the random variable $z = x/\sqrt{4D_\alpha t}$ for positive values of x, compared to the Gaussian probability density function (red line). Data are obtained by considering different α and evolving the Chapman-Kolmogorov (3.2)-(3.3) equations up to $t = 10^4$ number of steps.

From Eq. (3.32) we get the diffusion coefficient for the system:

$$D_\alpha(x) \simeq \frac{1}{2} \cdot \frac{\pi(x)}{2 - \pi(x)} = \frac{1}{2} \cdot \begin{cases} \dfrac{1}{2\Lambda|x|^{1-\alpha} - 1} & 0 < \alpha < 1 \\ \dfrac{1}{2\zeta(\alpha)/\zeta(1+\alpha) - 1} & \alpha > 1, \end{cases} \tag{3.48}$$

where Λ is the same constant formerly defined, see Eq. (3.35). For $\alpha > 1$ the situation is not different from the previous case: $D_\alpha(x)$ shows no dependence on space and thus we still have standard Gaussian diffusion. The distribution of $z = x/\sqrt{4D_\alpha t}$ is given for $t \to \infty$ by the standard normal distribution:

$$p(z) = \frac{1}{\sqrt{\pi}} e^{-z^2}, \tag{3.49}$$

see Fig. 3.9.

Moreover, we can also recover the $n^{-1/2}$ decay of the autocorrelation function and the linear growth of the MSD, with the slope correctly given by the diffusion coefficient, Eq. (3.48), see Fig. 3.10.

Once again, the peculiar regime occurs for $\alpha < 1$. In this case the diffusion coefficient for high values of the distance from the origin can be approximated by $D_\alpha(x) \sim \Sigma|x|^{\alpha-1}$, where

$$\Sigma = \frac{1}{4\Lambda}. \tag{3.50}$$

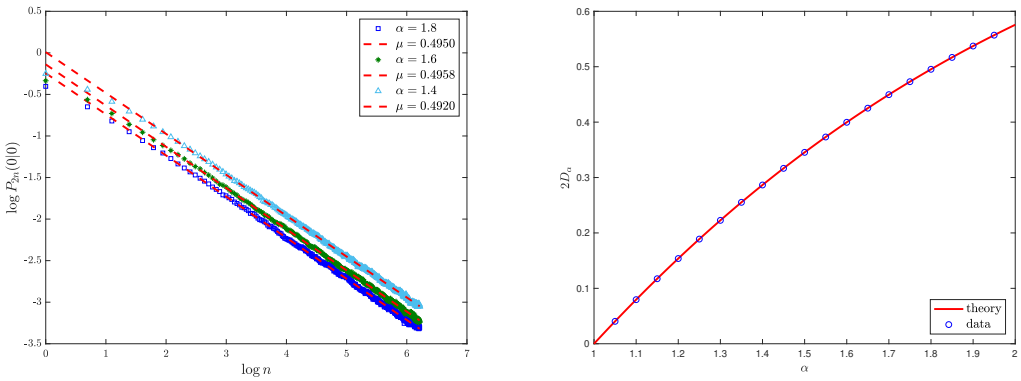

FIGURE 3.10: Probability of being at the origin after $2n$ steps and slope of linear growth of the second moment, for the subdiffusive Lévy-Lorentz gas. In both cases, the parameters of interest are obtained by linear fits of the data.

Hence, if we assume $D_\alpha(x) = \Sigma|x|^{\alpha-1}$, the solution of the diffusion equation reads [103]:

$$p(x,t) = \frac{(M_\alpha t)^{-\frac{1}{3-\alpha}}}{2\Gamma\left(1+\frac{1}{3-\alpha}\right)} \exp\left[-\frac{|x|^{3-\alpha}}{M_\alpha t}\right], \tag{3.51}$$

with

$$M_\alpha = (3-\alpha)^2\,\Sigma. \tag{3.52}$$

Such a solution must be considered along with the same caveats of the previous case. Note that the diffusion coefficient is well-defined in the same region of definition we identified for the superdiffusive version. By defining the scaled variable

$$z = \frac{x}{(M_\alpha t)^{\frac{1}{3-\alpha}}}, \tag{3.53}$$

we find the α-dependent distribution of z, which reads

$$p_\alpha(z) = \frac{e^{-|z|^{3-\alpha}}}{2\Gamma\left(1+\frac{1}{3-\alpha}\right)}, \tag{3.54}$$

see Figure 3.11.

Once again this result predicts a weakly anomalous behaviour for the system, with the moments' spectrum given by:

$$\langle|x(t)|^q\rangle \sim t^{\frac{q}{3-\alpha}}, \tag{3.55}$$

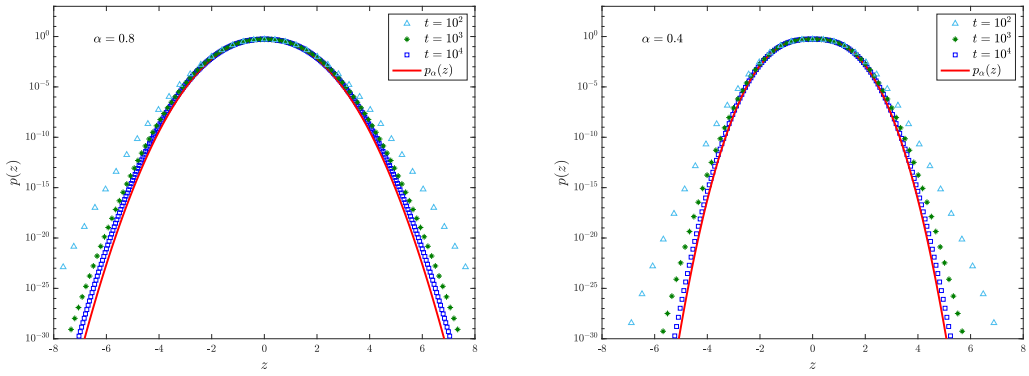

FIGURE 3.11: Distributions of the random variable $z = x/(M_\alpha t)^{1/(3-\alpha)}$ for positive values of x and theoretical predictions (red lines), as given in Eq. (3.54). Data are obtained by evolving the Chapman-Kolmogorov equations (3.2)-(3.3) up to $t = 10^4$ number of steps.

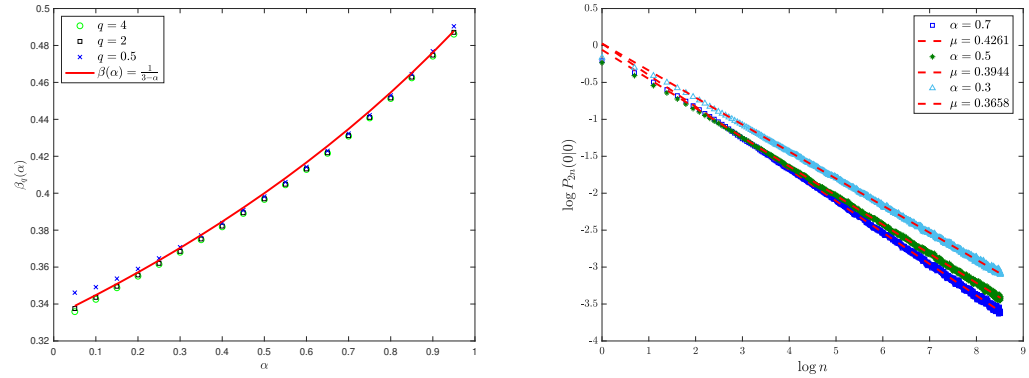

FIGURE 3.12: Asymptotic growth exponent of q-th moment and probability of being at the origin after $2n$ steps. In the latter case, the theoretic exponents are: $\mu_{\text{th}} = 0.4348$ ($\alpha = 0.7$, blue squares), $\mu_{\text{th}} = 0.4$, ($\alpha = 0.5$, green asterisks) and $\mu_{\text{th}} = 0.3704$ ($\alpha = 0.3$, light blue triangles).

hence displaying in this case a subdiffusive MSD, with exponent $\gamma_2(\alpha) = 2/(3-\alpha)$. Moreover, we can obtain the asymptotic power-law decay of the autocorrelation function $P_{2n}(0|0)$, which in this case is

$$P_{2n}(0|0) \sim n^{-\frac{1}{3-\alpha}}. \tag{3.56}$$

Fig. 3.12 shows both the behaviour of the moments' spectrum and the asymptotic decay of the autocorrelation function. We note that regarding the moments' spectrum the discrepancies we observed for the superdiffusive case are not present, due to the fact that the ballistic peaks in this case decay much faster and thus their contributions becomes negligible in much shorter times.

Let us conclude with an observation regarding the physical meaning of the averaged model. As we have already said, the superdiffusive version corresponds to a definition of a reflection probability along the lattice which is the result of a particular averaging procedure: indeed, if in the original model the probability of being reflected is $\frac{1}{2}$ in the presence of a scatterer, and 0 otherwise, then the expected reflection probability at site k is

$$\mathfrak{r}_k = \frac{1}{2} \cdot \varpi_k + 0 \cdot (1 - \varpi_k) \,, \tag{3.57}$$

where ϖ_k is the probability of having a scatterer at position k. By substituting ϖ_k with its corresponding asymptotic expression π_k, we obtain the definition of the reflection coefficient in the superdiffusive averaged LL gas. In the subdiffusive version of the model, instead, we consider the following expression for the expected reflection probability:

$$\mathfrak{r}_k = \frac{1}{2} \cdot \varpi_k + 1 \cdot (1 - \varpi_k) \,. \tag{3.58}$$

This means that the related quenched model corresponds to a system similar to the LL gas, but with empty sites substituted by perfectly reflecting barriers. Such a system is trivial, since the particle will be confined between two barriers and there will be no diffusion at all. The averaged version instead keeps track of all the possible configurations of disorder and shows highly non-trivial features. Therefore, despite the set of results regarding the LL gas we recovered in the superdiffusive version, we conclude that in general the averaged model can yield results which can sometimes be very far from those of the related quenched model.

3.4 Summary

In this chapter we have presented the averaged Lévy-Lorentz gas in both the superdiffusive and subdiffusive versions, which we introduced in [3] and [100]. This model consists in a one-dimensional non-homogeneous persistent random walk, with space-dependent reflection probability, which can be seen as a mean-field version of the original Lévy-Lorentz gas, namely a random walk in a random environment characterized by a fat polynomial tail of the distribution of scatterers' distance. By applying the continuum limit, we have been able to determine the asymptotic properties of the averaged model, including the distribution of the position, the long-time decay of the autocorrelation function $P_{2n}(0|0)$ and the growth of the moments. Depending on the value of the exponent α, the system displays a normal regime ($\alpha > 1$), where the major features of Gaussian diffusion are in control, and an anomalous one ($\alpha < 1$), where instead the observables of interest are characterized by non-trivial power-laws.

By comparing our results to those previously obtained in the literature [12, 13, 20], we have been able to point out the similarities and the differences between the superdiffusive version of the averaged model, and the quenched and annealed models,

depending on the value of α. Remarkably, when the mean distance between scatterers is finite ($\alpha > 1$), the Central Limit Theorem holds for both the quenched and the annealed Lévy-Lorentz gas [12], and indeed in the averaged model we recover the major features of normal diffusion. Instead, when the mean distance is infinite ($\alpha < 1$), all models become highly non-trivial, and show rather different behaviours. However, in this case for the annealed Lévy-Lorentz gas a generalized Central Limit Theorem holds [13, 20], which dictates a particular scaling that we recover in the superdiffusive version of the averaged model. Furthermore, the annealed model [20] and the averaged one share the same power-law decay of the autocorrelation function $p(0, t|0, 0)$. This fact is not trivial and we will discuss in the next chapter how from the exponent of the probability of being at the origin one can deduce important properties of the stochastic process. Finally, we point out that this chapter is mainly based on Refs. [3] and [100].

Statistics of occupation times 4

Until now we have analysed stochastic processes mainly from the point of view of the transport properties, focusing on the role of heterogeneity and/or disorder. However, there are many applications where one asks how much a process *survives*, or *persists* in a given state, before a certain condition is verified. This kind of problems are often considered in the study of critical phenomena in equilibrium and nonequilibrium systems, for instance spin systems in one or higher dimensions [111], phase-ordering kinetics [17, 65, 84] and twisted nematic liquid crystals exhibiting planar Ising model dynamics [120]. Such problems are characterized by the *persistence exponent* [16, 18], which gives the scaling of the probability that the order parameter $x(t)$ - for example, the magnetization of a ferromagnet - of a system quenched from the disordered phase to its critical point has not changed sign in a time interval t following the quench [83, 95]. In this context the time evolution of the order parameter is treated as a stochastic process and a number of questions regarding the statistics of $x(t)$ naturally arise: for instance, one can ask what is the fraction $u = t^+/t$ of time in which the process has assumed positive values [10, 45, 64], which is associated, e.g., with the mean magnetization.

In this regard, a well-known result valid for both Brownian motion [77] and its discrete counterpart, the simple and symmetric random walk [38], states that in the long-time limit, u is distributed according to the arcsine law:

$$\lim_{t\to\infty} P\{u < z\} = \frac{1}{\pi}\int_0^z \frac{\mathrm{d}x}{\sqrt{x(1-x)}} = \frac{2}{\pi}\arcsin\left(\sqrt{z}\right). \tag{4.1}$$

The density in Eq. (4.1) is represented by a U-shaped curve diverging at the outer values 0 and 1, a behaviour which is indeed recovered for the mean magnetization of many physical systems [32, 34, 115]. This shows in a surprising fashion that, contrarily to what one would expect from intuition, the order parameter most likely preserves its sign during the entire observation time.

It is worthy of note that the exponent of the singularities at the outer values of the U-shaped curve is closely related to the persistent exponent. This connection can be proved [45] by considering $x(t)$ as generated by a renewal process: starting from the initial state $x(t_0)$, during the time evolution the process resets itself to the initial condition at random times t_i, $i = 1, 2, \ldots$, such that the intervals $\Delta t_i = t_i - t_{i-1}$ are independent and identically distributed random variables. In this setting it is also worth asking what is the number of renewals observed up to time t, as it provides an interpretation to the arcsine law. Indeed, the arcsine law can be qualitatively explained by the fact

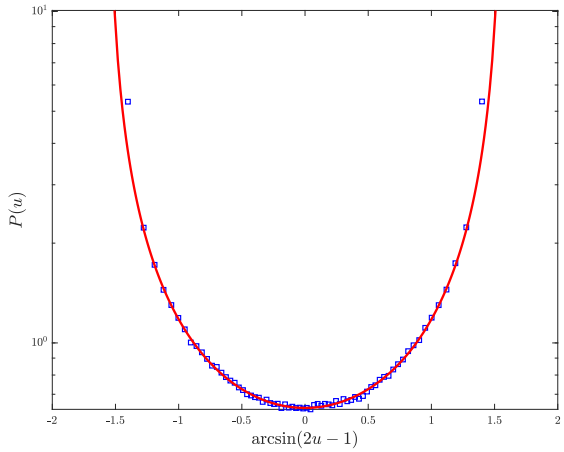

FIGURE 4.1: Distribution of the fraction of steps spent on the positive side for the simple symmetric random walk compared to the arcsine law. Data are obtained considering 10^6 walks of 10^4 steps. To enhance readability of the outer values, the x-axis represents the variable $\arcsin(2u-1)$ rather than u.

that enormously many trials are required before the stochastic process returns to the origin [38]. The number of renewals is found to follow a Mittag-Leffler distribution of an adequate parameter determining the shape of the distribution. The value of such a parameter depends on the scaling exponent of the probability density function of waiting times between renewals: for a distribution which decays asymptotically as $F(\Delta t) \sim \Delta t^{-1-\theta}$, with $0 \leq \theta < 1$, one obtains a Mittag-Leffler of parameter θ [52, 74, 89, 107].

The advantage of renewal theory is that it applies to a broad range of stochastic processes, including, for example, random walks with spatially inhomogeneous transition probabilities and correlations between steps. However, the major difficulty in applying renewal theory to general diffusion processes is that one has to determine the waiting-time distribution, which is often a difficult task to perform, especially when translational symmetry is broken or for walks of non-Markovian nature. In the language of random walks, for example, this corresponds to computing the probabilities of first return to the starting position, which can be analytically done only in few cases. In [101] we showed that it is possible to obtain the fraction of time spent in the positive axis, the number of renewals and the persistence exponent just by considering the autocorrelation function $p(x_0, t|x_0, t_0)$, i.e., the probability that at time t the process is at the initial state:

$$p(x_0, t|x_0, t_0) = \Pr\{x(t) = x(t_0)\}\,. \tag{4.2}$$

The first part of this chapter is devoted to the discussion of the aforementioned result, with the following outline: in the next section we introduce the class of processes to which our results apply; then we present the known results regarding the occupation time of the positive axis (Sec. 4.2), the number of returns at the origin (Sec. 4.3) and

the survival probability (Sec. 4.4), and discuss how to establish a connection between the three, starting from the probability of occupying the initial state; finally in Sec. 4.5 we describe the stochastic processes we have considered in our simulations and show the numerical results. In the second part of the chapter we show how to generalize the results of the first part to the case of continuous time random walks, by connecting the statistics of occupation times to both the exponent of the waiting time distribution between steps and the properties of the underlying random walk. Even though the theory in this case has already been well developed in the literature [6, 10, 11, 45, 64], we revise some of the known result by including our findings, and test our results by introducing a slight modification of the classical CTRW model [63] (Sec. 4.6). Finally, in Sec. 4.7 we draw our conclusions.

4.1 The Lamperti class

The class of stochastic processes for which the results of this chapter apply is similar to that considered in a classic paper by Lamperti [68], and we will call it here the *Lamperti class*. This class regroups processes (not necessarily Markovian), whose time evolution is described by a discrete parameter n, with the property that the states are divided into two sets, say A and B, which communicate through the occurrence of a recurrent state x_0, assumed as the initial state. More precisely, denoting with x_n the state at time n of the stochastic process, starting from x_0, we consider processes such that if $x_{n-1} \in A$ and $x_{n+1} \in B$ or vice versa, then $x_n = x_0$; moreover, the occupation of x_0 is a *persistent recurrent event* [37], by which we mean that, calling F_n the probability that the process returns to x_0 for the first time after n steps, having started from x_0, then

$$\sum_{n=1}^{\infty} F_n = 1, \tag{4.3}$$

i.e., the return to x_0 is certain. We will furthermore assume that the return to x_0 defines a renewal event, so that x_n can be treated as a renewal process, with F_n describing the waiting-time distribution between renewals.

In practice, in this chapter we will consider one-dimensional random walks on the integer lattice, starting from $x_0 = 0$, with nearest-neighbour jumps (without specifying the rules followed by the jumps). We will call $A(B)$ the set of positive(negative) integers, and will assume that the occupation of state x_0, i.e., the return to the origin, is a persistent recurrent event.

4.2 Occupation time of the positive axis

For stochastic processes belonging to the Lamperti class, the result stated in [68] provides the distribution, as the number of steps tends to infinity, of the fraction of time spent in the positive(negative) axis, which we call the *Lamperti distribution* $\mathcal{G}_{\eta,\rho}(\xi)$.

Such a distribution is defined through two parameters. The first parameter is

$$\eta = \lim_{n\to\infty} \mathbb{E}\left(\frac{N_n}{n}\right), \tag{4.4}$$

where N_n denotes the occupation time of set $A(B)$ up to step n, using the convention that the occupation of the origin is counted or not according to whether the last other state occupied was in $A(B)$ [1]. Clearly η is equal to $1/2$ if the process is symmetric with respect to A and B. The second parameter is defined as the limit

$$\rho = \lim_{z\to 1^-} \frac{(1-z)F'(z)}{1-F(z)}, \tag{4.5}$$

where $F(z)$ denotes the generating function of the recurrence times of x_0, i.e., the first return probabilities F_n:

$$F(z) = \sum_{n=1}^{\infty} F_n z^n. \tag{4.6}$$

We have the following [68]:

Theorem 2 (Lamperti)**.** *Let x_n be a Lamperti-class process. Then*

$$\lim_{n\to\infty} \Pr\{N_n/n \le u\} \equiv \mathscr{G}_{\eta,\rho}(u) \tag{4.7}$$

exists if and only if both limits $0 \le \eta \le 1$, Eq. (4.4), and $0 \le \rho \le 1$, Eq. (4.5), exist. In this case $\mathscr{G}_{\eta,\rho}(u)$ is the distribution on $[0,1]$ which, provided both η and $\rho \neq 0, 1$, has the density:

$$\mathscr{G}'_{\eta,\rho}(u) = \mathscr{N}\frac{u^\rho(1-u)^{\rho-1} + u^{\rho-1}(1-u)^\rho}{a^2u^{2\rho} + 2au^\rho(1-u)^\rho\cos(\pi\rho) + (1-u)^{2\rho}}, \tag{4.8}$$

where

$$a = \frac{1-\eta}{\eta} \tag{4.9}$$

$$\mathscr{N} = \frac{a\sin(\pi\rho)}{\pi}. \tag{4.10}$$

In the particular cases $\eta = 0, 1$ the distribution is:

$$\mathscr{G}_{\eta,\rho}(u) = \begin{cases} 1 & \text{for } \eta = 0 \\ 0 & \text{for } \eta = 1 \end{cases} \tag{4.11}$$

[1] This is the same convention used in [68]

for $0 < u < 1$*; when* $\rho = 1$ *we have:*

$$\mathscr{G}_{\eta,1}(u) = \begin{cases} 0 & \text{for } u < \eta \\ 1 & \text{for } u \geq \eta, \end{cases} \tag{4.12}$$

while for $\rho = 0$*,* $0 \leq u < 1$*:*

$$\mathscr{G}_{\eta,0}(u) = 1 - \eta. \tag{4.13}$$

An important observation is that the existence of the limit (4.5) is equivalent to a condition on the form the generating function $F(z)$ must assume, namely - see [68]:

$$F(z) = 1 - (1-z)^{\rho} L\left(\frac{1}{1-z}\right), \tag{4.14}$$

where $L(x)$ is a *slowly-varying* function, see Appendix B.

Eq. (4.14) suggests that the distribution of the occupation time can be determined by evaluating the analytical expression of $F(z)$. As we have already observed, however, in general the computation of the first return probabilities is hard to perform. Nevertheless, since we are taking as x_0 the site $k = 0$, one can use a well-known formula, valid for any renewal process, relating $F(z)$ to the generating function $P(z)$ of the probabilities of occupying the origin at time n, P_n, which reads [56, 63]

$$F(z) = 1 - \frac{1}{P(z)}, \tag{4.15}$$

to recast condition (4.14) as:

$$P(z) = \frac{1}{(1-z)^{\rho}} H\left(\frac{1}{1-z}\right), \tag{4.16}$$

where $H(x) = 1/L(x)$ is a slowly-varying function. In particular, Eq. (4.16) shows that the parameter ρ of the Lamperti distribution appears as an exponent in the generating function $P(z)$.

A first consequence is that ρ can be computed by evaluating P_n. In order to show this, we make use of the Tauberian theorem of Appendix B, which we report here for the sake of ease:

Theorem 3. *Let* $g_n \geq 0$ *and suppose that*

$$\sum_{n=0}^{\infty} g_n z^n = G(z) \tag{4.17}$$

converges for $0 \leq z < 1$*. Then*

$$G(z) \sim \frac{1}{(1-z)^{\gamma}} \mathscr{H}\left(\frac{1}{1-z}\right), \; z \to 1^- \iff$$
$$g_0 + \cdots + g_n \sim \frac{1}{\Gamma(\gamma+1)} n^{\gamma} \mathscr{H}(n), \; n \to \infty \tag{4.18}$$

where $\mathscr{H}(x)$ is a slowly-varying function and $\gamma \geq 0$.
Furthermore, if the sequence $\{g_n\}$ is ultimately monotonic and $\gamma > 0$, it also holds

$$G(z) \sim \frac{1}{(1-z)^{\gamma}} \mathscr{H}\left(\frac{1}{1-z}\right),\ z \to 1^{-} \iff g_n \sim \frac{1}{\Gamma(\gamma)} n^{\gamma-1} \mathscr{H}(n),\ n \to \infty. \quad (4.19)$$

By using Eq. (4.16) and applying the theorem, one has that, for $0 < \rho \leq 1$, P_n decays as

$$P_n \sim \frac{1}{\Gamma(\rho)} \frac{H(n)}{n^{1-\rho}}, \quad (4.20)$$

meaning that ρ is related to the exponent appearing in the long-time limit of the occupation probability of the origin.

We remark that this result connects the behaviour of the process regarding the occupation time of the sets A and B, which is a non-local property, to a local property. For instance, for a simple symmetric random walk it is known that P_n decays with the power-law $P_n \sim n^{-1/2}$, which corresponds to $\rho = \frac{1}{2}$. In this case the distribution of the occupation time follows the first arcsine law [38], which is indeed recovered by Theorem 2 in the case $\rho = \eta = \frac{1}{2}$. In general, for $0 < \rho < 1$ the probability of being at the origin has the asymptotic decay $P_n \sim n^{-(1-\rho)}$, up to a factor given by the slowly-varying function, and the distribution of the occupation time is represented by U-shaped or W-shaped curves. From formula (4.8) we see that the divergence of these curves at $u = 0$ and $u = 1$ is given exactly by the exponent $1 - \rho$. The situation is different for $\rho = 1$: we have $P_n \sim H(n)$, hence P_n does not decay as a power law. Instead it must behave for large n as a (ultimately) decreasing slowly-varying function, converging to a constant (indeed, for each n, P_n is a non-negative number). In this case the occupation time is split among the two sets, in such a way that the process spends a fraction η of time in A and the remaining in B. The distribution of the fraction of time in A is therefore a Dirac delta function centred around $u = \eta$ and we will refer to this as the *ergodic* case [68]. In the opposite case, $\rho = 0$, regarding P_n we can only conclude that

$$\sum_{m=0}^{n} P_m \sim H(n), \quad (4.21)$$

where this time $H(n)$ must be (ultimately) increasing. Since by using Eqs. (4.3) and (4.15), one can show that a necessary and sufficient condition for recurrence is the divergence of $P(z)$ [56], we can say that $H(n)$ must diverge, but we expect the divergence to be slow. In this sense, the case $\rho = 0$ corresponds to a crossover for the occupation of x_0 between being or not a persistent recurrent event. This can be better understood by observing that the distribution of the occupation time has masses $m_A = \eta$ on $u = 1$ and $m_B = 1 - \eta$ on $u = 0$, meaning that the process spends all the time either in A, with probability η, or in B, with probability $1 - \eta$.

4.3 Number of visits at the origin

The number of renewals for a random walk is closely related to the number of visits at the origin. Indeed, if the return defines a renewal event, N visits at the starting site for a walker correspond to $N-1$ renewals. The distribution of the occupation time of the origin can be obtained from a classic result by Darling and Kac [28], where they showed that the limiting distribution of the occupation time of a set of finite measure for a Markov process is the Mittag-Leffler distribution:

$$\mathscr{M}_\nu(\xi) = \frac{1}{\nu \xi^{1+\frac{1}{\nu}}} L_\nu\left(\frac{1}{\xi^{\frac{1}{\nu}}}\right), \tag{4.22}$$

where $L_\nu(x)$ denotes the Lévy one-sided density of parameter ν, defined through the inverse Laplace transform from p to x: $L_\nu(x) = \mathscr{L}^{-1}\left[\exp\left(-p^\nu\right)\right]$; the parameter ν depends on the process itself. For the sake of clarity, here we briefly state the result, limiting ourselves to the case of random walks on a lattice - we point out, however, that the result holds in a more general setting.

Let x_n be a random walk on the integer lattice. Consider the generating function of the probabilities $P_n(k|k_0)$ of arriving at site k in n steps, starting from k_0:

$$P_z(k|k_0) = \sum_{n=0}^{\infty} P_n(k|k_0) z^n. \tag{4.23}$$

Let $V(k)$ be an integrable, non-negative function and suppose there exists a function $\pi(z)$, $\pi(z) \to \infty$ as $z \to 1^-$, and a positive constant c, such that

$$\lim_{z\to 1^-} \frac{1}{\pi(z)} \sum_k P_z(k|k_0) V(k) = c, \tag{4.24}$$

the convergence being uniform in $E = \{k_0 | V(k_0) > 0\}$. Then the following result holds [28]:

Theorem 4. *For some normalizing sequence $\{u_n\}$ the limiting distribution of*

$$\frac{1}{u_n} \sum_{m=0}^{n} V(x_m) \tag{4.25}$$

exists and it is non-singular if and only if, for some $0 \leq \nu < 1$,

$$\pi(z) = \frac{1}{(1-z)^\nu} \mathscr{H}\left(\frac{1}{1-z}\right), \tag{4.26}$$

where $\mathscr{H}(x)$ is a slowly-varying function. Moreover, if (4.26) *is satisfied, u_n can be taken to be $c\pi\left(1-\frac{1}{n}\right)$ and the limiting distribution is the Mittag-Leffler distribution $\mathscr{M}_\nu(\xi)$.*

We will use this result to find the distribution of the occupation time of the origin. In order to do so, we take $V(k) = \delta_{k,0}$ so that

$$\sum_k P_z(k|k_0)V(k) = \sum_k P_z(k|k_0)\delta_{k,0} = P_z(0|k_0), \tag{4.27}$$

is the generating function of the probabilities of reaching the origin starting from k_0. Now, since $\delta_{k_0,0} > 0$ only for $k_0 = 0$, we have to prove the existence of $\pi(z)$ of the desired form, Eq. (4.26), such that

$$\lim_{z\to 1^-} \frac{P_z(0|0)}{\pi(z)} = c. \tag{4.28}$$

Now, by definition,

$$P_z(0|0) \equiv P(z) \tag{4.29}$$

and we know from the discussion made in section 4.2, see Eq. (4.16), that

$$P(z) = \frac{1}{(1-z)^\rho} H\left(\frac{1}{1-z}\right), \tag{4.30}$$

where $H(x)$ is slowly-varying. Then, for any positive constant c, we can take

$$\pi(z) = \frac{1}{c\,(1-z)^\rho} H\left(\frac{1}{1-z}\right) \tag{4.31}$$

and have

$$\lim_{z\to 1^-} \frac{P(z)}{\pi(z)} = c. \tag{4.32}$$

Hence, for the theorem stated above, the limiting distribution of the random variable

$$T_n \equiv \frac{1}{H(n)n^\rho} \sum_{m=0}^{n} \delta_{x_m,0}, \tag{4.33}$$

describing the occupation time of the origin, is the Mittag-Leffler distribution of parameter ρ, for $0 \le \rho < 1$.

We point out that when $\rho = 0$ the Mittag-Leffler distribution becomes the exponential distribution, while for $\rho = \frac{1}{2}$ we have an half-Gaussian:

$$\mathscr{M}_{1/2}(\xi) = \pi^{-1/2} \exp\left(-\xi^2/4\right), \tag{4.34}$$

which is the limiting distribution of the number of returns for the simple symmetric random walk [38]. For $\rho = 1$ one has a degenerate case, with the convergence:

$$\frac{1}{H(n)n} \sum_{m=0}^{n} \delta_{x_m,0} \to 1 \tag{4.35}$$

in probability, which is a kind of weak ergodic theorem [28], as the long-time limit of $H(n)$ gives in this case the probability of occupying the origin, which decays to a constant (see discussion in Sec. 4.2). This means that the process possesses a stationary distribution and the value of such a distribution at $k = 0$ corresponds to the ensemble average of $V(k)$. Therefore we have the convergence of the time average of $V(k)$ over a single trajectory to its ensemble average, so that the density of T_n converges to a Dirac delta function centred around $\xi_0 = 1$.

In Appendix D we show that in the long-time limit T_n is proportional to the number of visits at the origin up to step n, which we denote as M_n, rescaled for its mean value:

$$T_n \sim \frac{1}{\Gamma(1+\rho)} \frac{M_n}{\langle M_n \rangle}. \tag{4.36}$$

We may therefore conclude that the result states that the random variable

$$\xi = \lim_{n\to\infty} \frac{1}{\Gamma(1+\rho)} \frac{M_n}{\langle M_n \rangle} \tag{4.37}$$

follows a Mittag-Leffler distribution of parameter ρ, for $0 \leq \rho < 1$, and a degenerate Mittag-Leffler distribution for $\rho = 1$, whose density is

$$P(\xi) = \delta(\xi - 1). \tag{4.38}$$

We remark that the result also holds if x_n is not a Markov process, provided that the return to x_0 defines a renewal event, so that the transition can be characterized by a waiting-time distribution between renewals, i.e., by the distribution of the first returns times. This happens, for example, if x_n is symmetric with respect to the starting point, or more generally whenever Eq. (4.15) holds. Indeed, we could obtain the same from renewal theory, see [52, 74, 89, 107] and references therein. It is worth observing that in these cases the parameter characterizing the distribution of the occupation time of the origin is the same of the Lamperti distribution, which in our setting describes the occupation time of the positive(negative) axis for a symmetric process. We point out that a similar connection was proved in [45] by using scaling arguments, and also in the context of infinite ergodic theory for deterministic systems [114].

4.4 Decay of the survival probability

As we have seen, the Lamperti and the Mittag-Leffler distribution are closely related, all due to the particular form that the generating functions $P(z)$ and $F(z)$ must assume. We will show that this is also related to the asymptotic decay of the survival probability in the set $A(B)$. We define the survival probability in a set for a random walk on the integers with nearest-neighbour jumps as the probability Q_n of never leaving the set up to step n. If A is the set of positive integers, then, following the convention in [68] on how to count the occupation time, we have

$$Q_n = \Pr\{x_1 \geq 0, x_2 \geq 0, \ldots, x_n \geq 0 | x_0 = 0\}, \tag{4.39}$$

with $Q_0 = 1$. Such a quantity can be computed exactly for random walks with i.i.d. jumps drawn from a continuous distribution, by using a well-known combinatorial identity known as the Sparre-Andersen theorem [110]:

$$Q(z) = \sum_{n=0}^{\infty} Q_n z^n = \exp\left[\sum_{n=1}^{\infty} \frac{z^n}{n} \Pr\{x_n \geq 0\}\right]. \tag{4.40}$$

For any symmetric jump distribution, one obtains the behaviour $Q_n \sim n^{-1/2}$ for large n, independently of the distribution itself. It can be shown that such a decay also holds for walks with nearest-neighbour jumps, i.e., a particular case of non-continuous jump distribution, provided that the jumps are symmetric, independent and identically distributed [46]. Therefore, in the paradigmatic case of the simple symmetric random walk on the integers, one finds that the value $\frac{1}{2}$ describes the power-law decay of the survival probability and gives the correct parameter describing both the Lamperti and the Mittag-Leffler distributions. However, no results for the survival probability are available if jumps are correlated or not identically distributed.

In our setting, we can obtain a relation between the survival probability Q_n and the *persistence* probability [45], namely the probability U_n of not observing any return up to time n, which can be computed as

$$U_n = 1 - \sum_{m=0}^{n} F_m. \tag{4.41}$$

In Appendix E we show that the generating functions $Q(z)$ and $U(z)$ satisfy the relation:

$$Q(z) = \frac{1 + U(z)}{1 + (1 - z)\, U(z)} \tag{4.42}$$

and that this implies $Q(z) \sim U(z)$ as $z \to 1$, for $0 \leq \rho < 1$. This means that the survival and the persistence probabilities have the same behaviour for large n.

By using Eq. (4.41) and the condition $U_0 = 1$, we can compute the generating function

$$U(z) = \frac{1 - F(z)}{1 - z} \tag{4.43}$$

and hence, by using equation (4.14), we find that $U(z)$ must be of the form

$$U(z) = \frac{1}{(1 - z)^{1-\rho}} L\left(\frac{1}{1 - z}\right), \tag{4.44}$$

where $L(x) = 1/H(x)$ is a slowly-varying function, and $H(x)$ is the same appearing in equation (4.16). Since, as we already stated, for $z \to 1$ we have $Q(z) \sim U(z)$, the use of the Tauberian theorem implies that the survival probability Q_n decays as

$$Q_n \sim \frac{1}{\Gamma(1 - \rho)} \frac{n^{-\rho}}{H(n)}. \tag{4.45}$$

Once again, the quantity of interest is characterized by the Lamperti parameter. We remark that this result holds for the class of processes we are considering, therefore not only for walks with i.i.d. jumps. For $\rho = 1$ the Tauberian theorem only assures that as $n \to \infty$

$$\sum_{m=0}^{n} Q_m \sim \frac{1}{H(n)} \tag{4.46}$$

where $H(n)$ is a (ultimately) decreasing slowly-varying function, hence the asymptotic relation (4.45) is not valid in this regime. We recall that in this case P_n does not decay as a power law, see Sec. 4.2.

4.5 Numerical results

In this section we present numerical results for the two different classes of walks we introduced in the previous chapters. In order to obtain the analytical predictions to compare with the simulations results, all we need to do is to evaluate the Lamperti parameter ρ.

For the Gillis random walk we use the analytical result regarding the generating function of the probabilities of being at the origin:

$$P(z) = \frac{{}_2F_1\left(\frac{1}{2}\epsilon + 1, \frac{1}{2}\epsilon + \frac{1}{2}; 1; z^2\right)}{{}_2F_1\left(\frac{1}{2}\epsilon, \frac{1}{2}\epsilon + \frac{1}{2}; 1; z^2\right)}. \tag{4.47}$$

We recall that the walk is recurrent only for $\epsilon \geq -\frac{1}{2}$, see [42, 56], hence we will consider this range only. By using the properties of the hypergeometric function [1], we can rewrite $P(z)$ in the form given in Eq. (4.16), obtaining (see Appendix F):

$$\rho = \begin{cases} 0 & \text{for } \epsilon = -\frac{1}{2} \\ \frac{1}{2} + \epsilon & \text{for } -\frac{1}{2} < \epsilon < \frac{1}{2} \\ 1 & \text{for } \frac{1}{2} \leq \epsilon < 1. \end{cases} \tag{4.48}$$

For the averaged Lévy-Lorentz gas we evaluate ρ by using the long-time asymptotics of the probability of occupying the origin, which can be computed performing a continuum limit. We recall that the probability P_n decays as [3, 100]

$$P_n \sim \begin{cases} n^{-1/(1+\alpha)} & \text{superdiffusive} \\ n^{-1/(3-\alpha)} & \text{subdiffusive,} \end{cases} \tag{4.49}$$

where $0 < \alpha < 1$. Since the exponent is connected to ρ by Eq. (4.20), we immediately get:

$$\rho = \begin{cases} 1 - \frac{1}{1+\alpha} & \text{superdiffusive} \\ 1 - \frac{1}{3-\alpha} & \text{subdiffusive.} \end{cases} \tag{4.50}$$

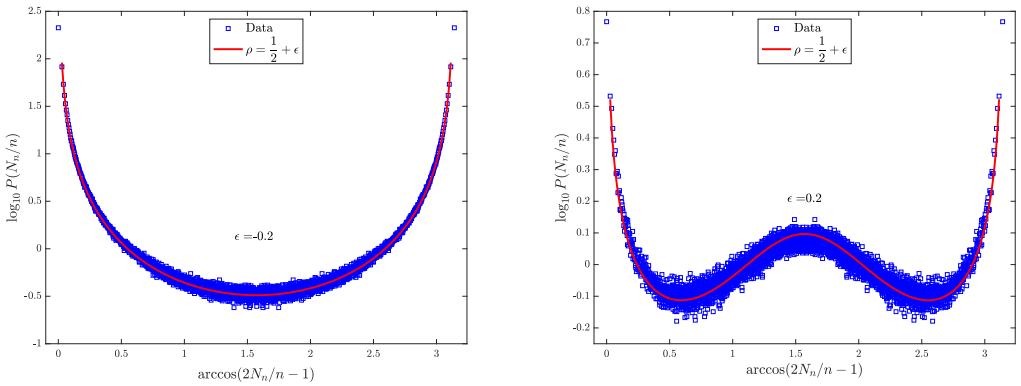

FIGURE 4.2: Distribution of the fraction of time spent in the positive axis for the Gillis random walk, in semi-logarithmic scale. To enhance readability of the outer values, it has been performed the transformation $x \longrightarrow \arccos(2x - 1)$ on the x-axis. The left panel displays the case $\epsilon = -0.2$, the right panel $\epsilon = 0.2$. In both cases the results are obtained simulating 10^6 walks of 10^4 steps.

4.5.1 Occupation time of the positive axis

Here we provide the results of simulations regarding the occupation time of the set A for the GRW and both versions of the averaged LL gas.

For the GRW we can recognize two different behaviours. When $\epsilon < 0$ there is a bias away from the origin, and the distribution of the occupation time is represented by a U-shaped curve, meaning that the particle most likely spends all the time in one of the two sets. When $\epsilon > 0$ there is a bias towards the origin, so we expect an higher contribution from walks which spend an equal amount of time in the two sets. This is confirmed by the plots in Fig. 4.2, where we consider the cases $\epsilon = -0.2$ and $\epsilon = 0.2$.

When the bias towards the origin becomes sufficiently strong, i.e., for $\epsilon \geq \frac{1}{2}$, the outer values of the distribution cease to be the most probable. The process enters in an ergodic regime where the fraction of time spent in a set converges to its expected value, which in our case is $\eta = \frac{1}{2}$. In other words, the distribution is a Dirac delta function centred around η. Fig. 4.3 shows the behaviour of the distribution as the number of steps grows, for $\epsilon = 0.8$, confirming the convergence to a Dirac delta distribution.

For the averaged LL gas, the behaviour of the distribution depends on which version of the model we are considering. In the superdiffusive case the reflection probability decays as a power-law with the distance from the origin, $\mathfrak{r}(k) \sim |k|^{-(1-\alpha)}$, therefore a particle tends to preserve its direction of motion as the distance from the starting point increases. As α varies in $(0, 1)$, the Lamperti parameter varies in $\left(0, \frac{1}{2}\right)$, see Eq. (4.49). In the subdiffusive case instead the reflection probability converges to 1 as the distance from the origin increases, with the transmission coefficient decaying as a power-law. The Lamperti parameter is in the range $\frac{1}{2} < \rho < \frac{2}{3}$. The behaviour of both models is presented in Fig. 4.4, for $\alpha = 0.7$ in the superdiffusive case and $\alpha = 0.3$ in the subdiffusive one. We point out that for both versions of the model we never enter

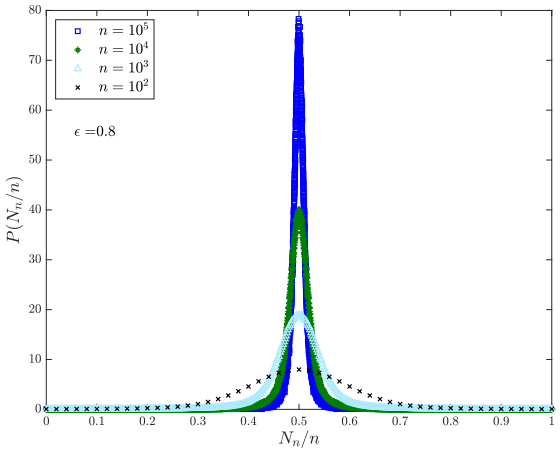

FIGURE 4.3: Distribution of the fraction of time spent in the positive axis for the Gillis random walk, ergodic case, with $\epsilon = 0.8$. Data are obtained simulating 10^6 walks of different numbers of steps. As the maximum number of steps grows, the distribution converges to a Dirac delta, centred around $N_n/n = 1/2$.

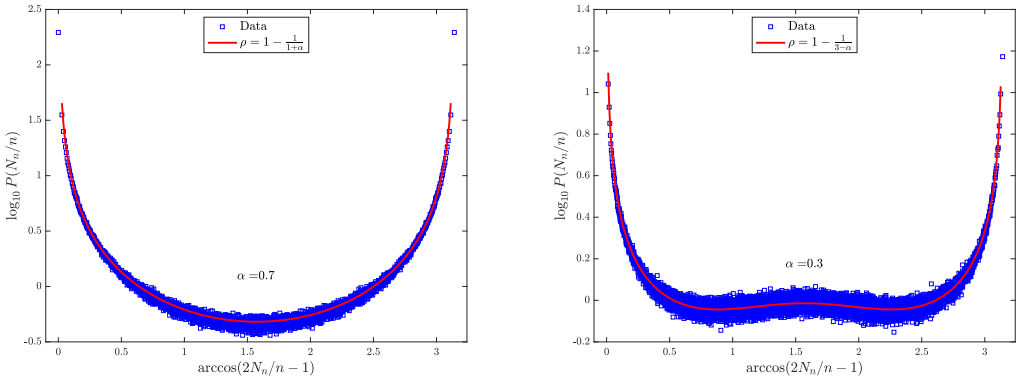

FIGURE 4.4: Distribution of the fraction of time spent in the positive axis for the averaged Lévy-Lorentz gas, in semi-logarithmic scale. To enhance readability of the outer values, it has been performed the transformation $x \to \arccos(2x - 1)$ on the x-axis. The left panel displays the superdiffusive case, with $\alpha = 0.7$. Data are obtained simulating 10^6 walks of 10^4 steps. The right panel displays the subdiffusive version, with $\alpha = 0.3$. In this case data are obtained simulating 10^7 walks of 10^5 steps.

the ergodic regime, as $\rho \neq 1$ for any value of α.

4.5.2 Occupation time of the origin

As we have already shown, the distribution of the occupation time of the origin follows a Mittag-Leffler distribution of the same parameter characterizing the Lamperti

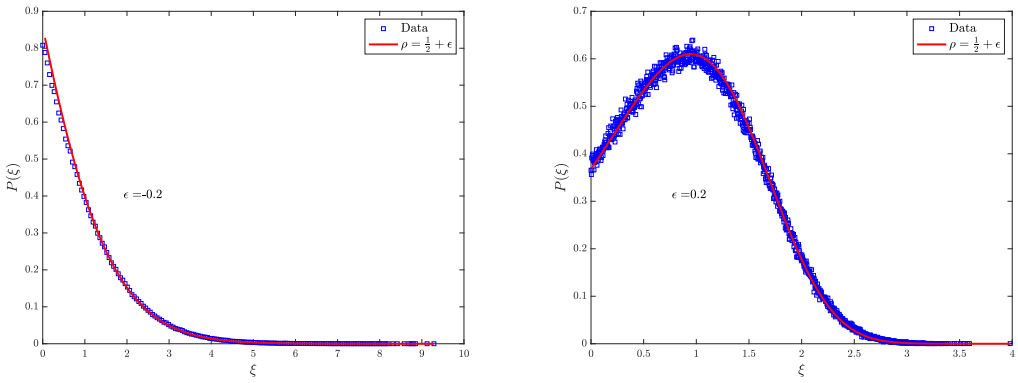

FIGURE 4.5: Distribution of the random variable ξ representing the rescaled number of steps in which the process occupies the origin. The left panel displays the case $\epsilon = -0.2$, the right panel $\epsilon = 0.2$. In both cases the results are obtained simulating 10^6 walks of 10^4 steps.

distribution. We consider the random variable

$$\xi = \lim_{n\to\infty} \frac{1}{\Gamma(1+\rho)} \frac{M_n}{\langle M_n \rangle}. \tag{4.51}$$

Once again the GRW is the model displaying the richest behaviour. As shown in Fig. 4.5, for $\epsilon < 0$ the distribution of ξ is monotonically decreasing, reflecting the fact that the particle is biased away from the origin. Indeed, the walks that do not return to the starting point have the highest probability. For $\epsilon > 0$, instead, the bias is towards the origin, therefore the probability of returning increases. The shape of the distribution is quite different, and we have a pronounced peak close to $\xi_0 = 1$. For values $\epsilon \geq \frac{1}{2}$ we enter in the ergodic regime and the distribution converges to a Dirac delta function centred around $\xi_0 = 1$, Fig. 4.6.

We can recognize a similar behaviour for the averaged LL gas, as shown in Fig. 4.7. Here the shape of the distribution depends on which version of the model is considered: for the superdiffusive case we have a monotonically decreasing curve, while for the subdiffusive one the distribution presents a peak close to $\xi_0 = 1$. The values of α chosen for the two systems are $\alpha = 0.7$ for the superdiffusive version and $\alpha = 0.3$ for the subdiffusive one.

4.5.3 Decay of the survival and persistence probabilities

For both models we also provide simulations regarding the asymptotic decay of the survival and persistence probabilities. As we have seen, we expect both quantities to decay as $n^{-\rho}$, where ρ depends on a parameter characterizing the model (ϵ for Gillis, α for Lévy-Lorentz). We confirm our prediction by plotting the exponent of the asymptotic decay of Q_n and U_n, obtained from simulations, versus the characteristic parameter.

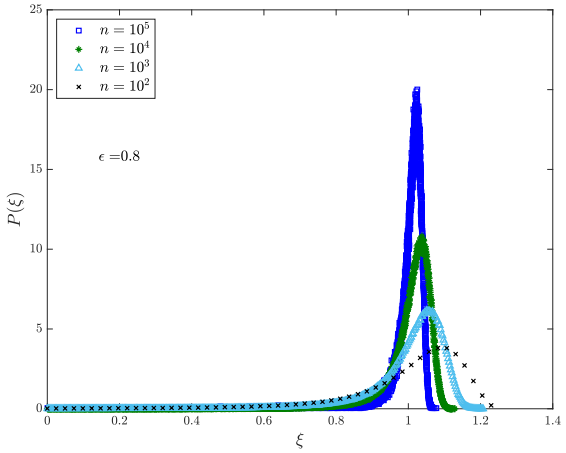

FIGURE 4.6: Distribution of the random variable ξ representing the rescaled number of steps in which the process occupies the origin, ergodic case, with $\epsilon = 0.8$. Data are obtained simulating 10^6 walks of different numbers of steps. As the maximum number of steps grows, the distribution converges to a Dirac delta, centred around $\xi_0 = 1$.

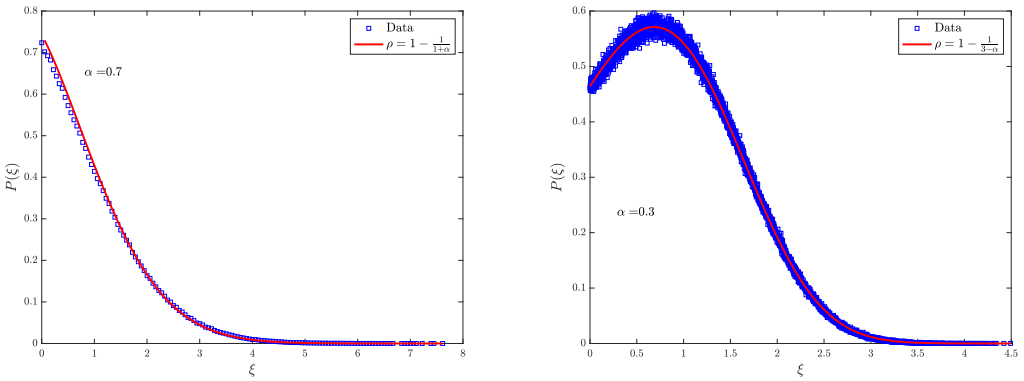

FIGURE 4.7: Distribution of the random variable ξ representing the rescaled number of steps in which the process occupies the origin. The left panel displays the superdiffusive case, with $\alpha = 0.7$. The results are obtained simulating 10^6 walks of 10^4 steps. The right panel corresponds to the subdiffusive version, with $\alpha = 0.3$. Data are obtained simulating 10^7 walks of 10^5 steps.

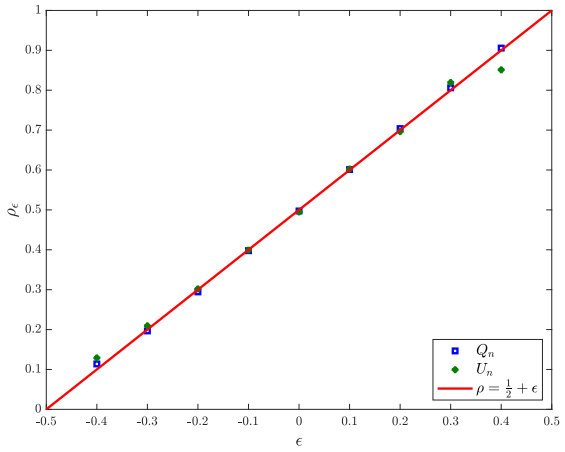

FIGURE 4.8: Exponents of the asymptotic power-law decay of the persistence and survival probabilities for the Gillis random walk. Data are obtained simulating 10^7 walks of 10^5 steps.

For the GRW we have good agreement between the two computed exponents and the theoretical values, Fig. 4.8. We point out that ϵ is taken in the range $\left(-\frac{1}{2}, \frac{1}{2}\right)$, so that $0 < \rho < 1$. We observe that the agreement gets worse when ϵ gets closer to the boundaries of the considered interval: we can explain this fact by considering that as $\epsilon \to -\frac{1}{2}$ convergence to the theoretical values becomes slower, while in the opposite case, $\epsilon \to \frac{1}{2}$, the system is getting closer to the regime $\rho = 1$, where Q_n and U_n are not guaranteed to decay in the same way.

For the superdiffusive averaged LL gas we have good agreement when $\alpha \geq 0.4$, while for lower values of the parameter we observe a non-negligible difference between the two computed exponents. However, we point out that this is due to the fact that the continuum limit used to describe the long-time properties of the system becomes effective after a preasymptotic regime, which depends on α, and the diffusive asymptotic regime is not yet captured at the number of steps of our simulations. Indeed, we observed in Chapter 3 the same discrepancies, in the same range of α, in the evaluation of the moments. For the subdiffusive version instead the difficulties to capture the asymptotic regime may be traced back to the fact that in order to observe cleanly the decay of the quantities of interest we need a larger number of steps with respect to the superdiffusive version. However, for both versions of the model we have in general a good agreement with the theoretical predictions, Fig. 4.9.

4.5.4 Comparison of different systems with the same Lamperti parameter

From the discussion made so far it should be clear that the Lamperti parameter ρ, characterizing the distributions of the observables we have considered in this chapter,

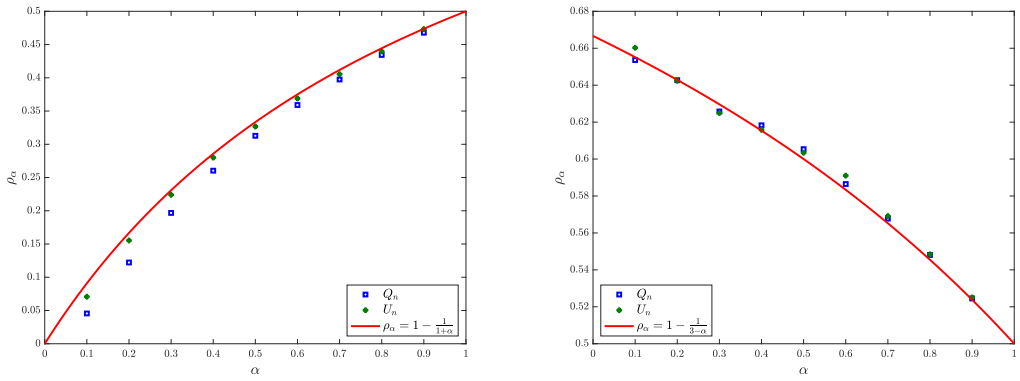

FIGURE 4.9: Exponents of the asymptotic power-law decay of the persistence and survival probabilities for the averaged Lèvy-Lorentz gas. The left panel displays the superdiffusive version, the right panel the subdiffusive one. In both cases data are obtained simulating 10^7 walks of 10^5 steps.

only depends on a local property of the PDF of the process, namely the probability P_n of occupying the origin at time n. It can happen that two stochastic processes are described by two different sets of evolution laws, but share the same asymptotic power-law decay for the distribution of the occupation time of the origin, i.e., the P_n decay with the same exponent. As a consequence, the distributions of the occupation time of the positive axis and the number of returns to the origin will be the same.

In order to show this, we compare the two distributions for the GRW and both versions of the averaged LL gas. For the latter system we consider the values of α already chosen in the previous sections, viz. $\alpha = 0.7$ for the superdiffusive version and $\alpha = 0.3$ for the subdiffusive one. The two corresponding values of the Lamperti parameter are $\rho = \frac{7}{17}$ (superdiffusive) and $\rho = \frac{17}{27}$ (subdiffusive), which are obtained in the case of the GRW for $\epsilon = -0.0882$ and $\epsilon = 0.1296$, respectively. The results are presented in Figs. 4.10 and 4.11. In both cases the simulations agree with the theoretical predictions.

4.6 Extension to Continuous Time Random Walk models

The results we have presented previously rely on the validity of the fundamental relation between the generating functions $P(z)$ and $F(z)$, Eq. (4.15). In general, however, the quantities we have dealt with are defined by the first-passage exponent, as expressed by Theorem 2 and widely discussed in the literature [52, 74, 89, 107]. This, in particular, has been intensively studied in the context of CTRW models with diverging mean waiting time between steps [6, 10, 11], where indeed there is not a relation analogous to Eq. (4.15) between the probability of occupying the origin and the first return probability, see for example [63]. Nevertheless, we will show in the following that also

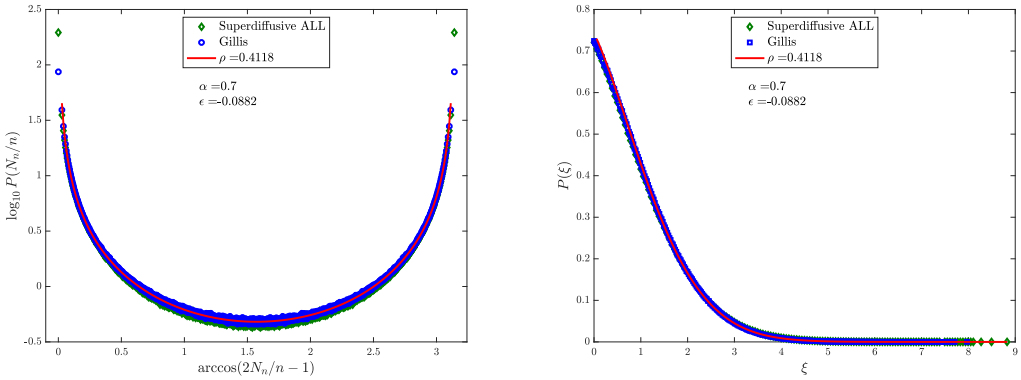

FIGURE 4.10: Distributions of the occupation time (left) and the number of returns (right) for the averaged Lévy-Lorentz gas, superdiffusive version (green asterisks), and the Gillis random walk (blue squares), compared to the theoretic result. The values of the corresponding parameters are $\alpha = 0.7$ and $\epsilon = -0.0882$, which in both cases yield $\rho = 7/17$. For both systems we considered 10^7 walks evolved for 10^4 steps.

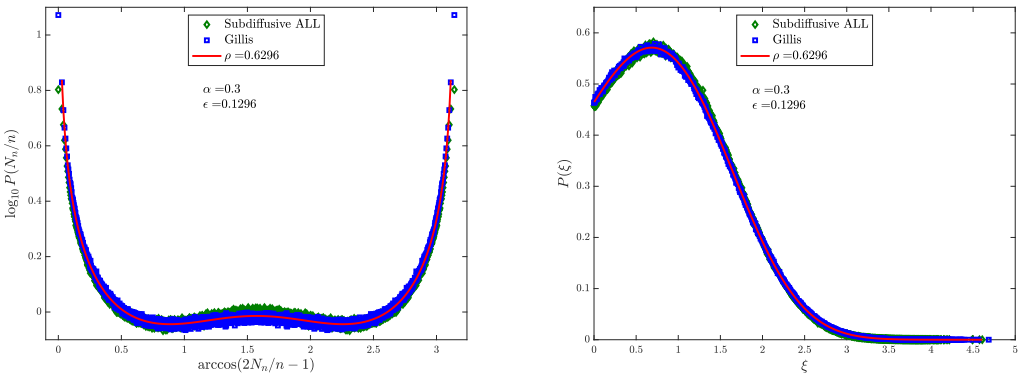

FIGURE 4.11: Distributions of the occupation time (left) and the number of returns (right) for the averaged Lévy-Lorentz gas, subdiffusive version (green asterisks), and the Gillis random walk (blue squares), compared to the theoretic result. The values of the corresponding parameters are $\alpha = 0.3$ and $\epsilon = 0.1296$, which in both cases yield $\rho = 17/27$. For both systems we considered 10^7 walks evolved for 10^4 steps.

for CTRW Eq. (4.15) can still be useful to determine the correct parameters of the distributions.

Indeed, a CTRW is a stochastic model where the dynamics is ruled by an underlying random walk, with the difference that at each step the particle waits a random amount of time before performing the successive one. For the best-known version of CTRW model, the underlying random walk model is the one-dimensional simple symmetric random walk: a particle on the integer lattice performs nearest-neighbour jumps to the right or left with equal probability, and the waiting times τ between steps are independent random variables drawn from a common distribution $\psi(\tau)$ [63]. In order to study a CTRW the following two quantities are often introduced: the first is the PDF of the occurrence of the n-th step at time t:

$$\psi_n(t) = \text{PDF of the occurrence of the } n\text{-th step at time } t; \tag{4.52}$$

the second is the probability that the particle has performed n steps up to time t, with $n = 0, 1, 2, \ldots$:

$$\chi_n(t) = \text{Pr that the particle has performed } n \text{ steps up to time } t. \tag{4.53}$$

Now let us consider for the underlying random walk a one-dimensional model with nearest-neighbour jumps starting at $k = 0$, and suppose that the return to the origin defines a renewal event. We denote with P_n the probability of being at the origin after n steps and with F_n the probability of returning to the origin for the first time after n steps. Then the probability of finding the particle at the origin at time t for the CTRW is

$$p(t) = \chi_0(t) + \sum_{n=1}^{\infty} \sum_{m=1}^{n} F_m P_{n-m} \chi_n(t). \tag{4.54}$$

We now want to compute the Laplace transform of this quantity. We first need to evaluate the transform of $\chi_n(t)$, which can be expressed in terms of $\psi_n(t)$ as

$$\chi_n(t) = \int_0^t \psi_n(t') \, \chi_0(t - t') \, \mathrm{d}t'. \tag{4.55}$$

Indeed, the probability of performing n steps up to time t is equal to the probability of having performed the n-th step at time $t' < t$ and then waiting for a time $t - t'$. This equation appears in the form of a convolution, hence by Laplace transforming one gets:

$$\tilde{\chi}_n(s) = \tilde{\psi}_n(s) \tilde{\chi}_0(s). \tag{4.56}$$

The PDF of the occurrence of the n-th step at time t can defined recursively:

$$\psi_n(t) = \int_0^t \psi_{n-1}(t') \, \psi(t - t') \, \mathrm{d}t', \tag{4.57}$$

hence its Laplace transform reads:

$$\tilde{\psi}_n(s) = \tilde{\psi}^n(s), \tag{4.58}$$

where $\tilde{\psi}(s)$ is the Laplace transform of the PDF of waiting times between steps. The quantity $\chi_0(t)$ is defined as

$$\chi_0(t) = \int_t^\infty \psi\,(t')\,\mathrm{d}t', \tag{4.59}$$

i.e., it is the probability that the waiting time exceeds t. By Laplace transforming the previous equation, one easily gets:

$$\tilde{\chi}_0(s) = \frac{1-\tilde{\psi}(s)}{s}, \tag{4.60}$$

thus Eq. (4.56) yields

$$\tilde{\chi}_n(s) = \tilde{\psi}^n(s)\frac{1-\tilde{\psi}(s)}{s}. \tag{4.61}$$

We are now ready to compute the Laplace transform of Eq. (4.54). Plugging in Eqs. (4.60) and (4.61) we get:

$$\tilde{p}(s) = \frac{1-\tilde{\psi}(s)}{s}\left[1+\sum_{n=1}^{\infty}\sum_{m=1}^{n} F_m P_{n-m}\tilde{\psi}^n(s)\right] \tag{4.62}$$

$$= \frac{1-\tilde{\psi}(s)}{s}\left[1+\sum_{n=1}^{\infty}\sum_{m=1}^{n} F_m\tilde{\psi}^m(s) P_{n-m}\tilde{\psi}^{n-m}(s)\right] \tag{4.63}$$

$$= \frac{1-\tilde{\psi}(s)}{s}\left[1+F\big(z=\tilde{\psi}(s)\big)P\big(z=\tilde{\psi}(s)\big)\right], \tag{4.64}$$

where $P(z)$ and $F(z)$ are the generating functions of the probability of being at the origin and the first return probability, relative to the underlying random walk. Now, assuming that these two functions are related by Eq. (4.15), one obtains:

$$\tilde{p}(s) = \frac{1-\tilde{\psi}(s)}{s}P\big(z=\tilde{\psi}(s)\big). \tag{4.65}$$

If, moreover, for the underlying random walk Theorem 2 holds, then $P(z)$ and $F(z)$ must assume a precise form. In particular, $P(z)$ has the general structure described by Eq. (4.16), hence we can write

$$\tilde{p}(s) = \frac{\left[1-\tilde{\psi}(s)\right]^{1-\nu}}{s}H\left(\frac{1}{1-\tilde{\psi}(s)}\right), \tag{4.66}$$

where $0 \leq \nu \leq 1$ and $H(x)$ is a slowly-varying function.

We can also compute the Laplace transform of the first return time to the origin, which reads [63]:

$$f(t) = \sum_{n=1}^{\infty} F_n\psi_n(t). \tag{4.67}$$

Indeed, the probability of returning to the origin for the first time at time t is equal to the probability of first return in n steps times the probability of performing the n-th step exactly at time t, summed over all possible values of n. Hence its Laplace transform is

$$\tilde{f}(s) = F\left(z = \tilde{\psi}(s)\right) \tag{4.68}$$

$$= 1 - \frac{1}{P\left(z = \tilde{\psi}(s)\right)} \tag{4.69}$$

$$= 1 - \left[1 - \tilde{\psi}(s)\right]^{\nu} L\left(\frac{1}{1 - \tilde{\psi}(s)}\right), \tag{4.70}$$

where we used the relation between $P(z)$ and $F(z)$, Eq. (4.15). Therefore, we find that the relation between the Laplace transforms $\tilde{f}(s)$ and $\tilde{p}(s)$ is:

$$\tilde{f}(s) = 1 - \frac{1 - \tilde{\psi}(s)}{s\tilde{p}(s)}. \tag{4.71}$$

We now want to use this equation to deduce the relation between the first return exponent and the power-law decay of the probability of being at the origin, but we need to make a distinction: if the distribution of the waiting times possesses a well-defined first moment, i.e., the mean waiting time is finite, then the Laplace transform of $\psi(t)$ admits a small-s expansion of the kind:

$$\tilde{\psi}(s) \sim 1 - \langle\tau\rangle s, \tag{4.72}$$

where $\langle\tau\rangle$ is the mean waiting time between steps. Hence, for $s \to 0$, $\tilde{p}(s)$ and $\tilde{f}(s)$ can be written as:

$$\tilde{p}(s) \sim \frac{\langle\tau\rangle^{1-\nu}}{s^{\nu}} H\left(\frac{1}{\langle\tau\rangle s}\right) \tag{4.73}$$

$$\tilde{f}(s) \sim 1 - \langle\tau\rangle^{\nu} s^{\nu} L\left(\frac{1}{\langle\tau\rangle s}\right). \tag{4.74}$$

The small-s behaviours of $\tilde{p}(s)$ and $\tilde{f}(s)$ are related to the long-time behaviours of $p(t)$ and $f(t)$ by Tauberian theorems [39], which we use to obtain:

$$p(t) \sim \frac{1}{\Gamma(\nu)} \left(\frac{\langle\tau\rangle}{t}\right)^{1-\nu} H(t) \tag{4.75}$$

$$f(t) \sim \frac{\nu}{\Gamma(1-\nu)} \frac{\langle\tau\rangle^{\nu}}{t^{1+\nu}} L(t). \tag{4.76}$$

We observe that the relation between the first return exponent and the power-law of the probability of being at the origin is the same as the one we would obtain without considering the presence of waiting-times between steps. Indeed, when the mean waiting time is finite, the difference between a CTRW and the relative underlying

random walk is just the time scale at which the steps occur, thus we do not expect differences in the asymptotic properties. This could also be deduced by the fact that the variable s appears in the Laplace transforms $\tilde{p}(s)$ and $\tilde{f}(s)$ with the same exponent, which is what happens for random walk models, as discussed previously in this chapter. Hence in this case we do not expect any differences in the statistics of occupation times, as ν is sufficient to determine the distributions.

The situation is marked differently when instead the distribution of waiting times does not posses a finite first moment. The most common example considered in the physical literature is the case of distributions decaying with a fat tail, such as:

$$\psi(t) \sim \frac{\alpha}{\Gamma(1-\alpha)} \frac{\tau^\alpha}{t^{1+\alpha}}, \quad 0 < \alpha < 1. \tag{4.77}$$

The non-existence of a finite time scale for the steps implies that the walker can spend a large amount of time without performing any jumps, leading to a huge difference in the behaviours of the CTRW model and the related underlying random walk. For example, the standard CTRW is subdiffusive with exponent α, while for the related simple symmetric random walk the transport is normal [63]. In this case, Tauberian theorems yield the small-s behaviour of the Laplace transform, which is:

$$\tilde{\psi}(s) \sim 1 - \tau^\alpha s^\alpha, \tag{4.78}$$

hence by plugging this in Eqs. (4.66) and (4.70) we get

$$\tilde{p}(s) \sim \frac{\tau^{\alpha(1-\nu)}}{s^{1-\alpha(1-\nu)}} H\left(\frac{1}{\tau^\alpha s^\alpha}\right) \tag{4.79}$$

$$\tilde{f}(s) \sim 1 - \tau^{\alpha\nu} s^{\alpha\nu} L\left(\frac{1}{\tau^\alpha s^\alpha}\right). \tag{4.80}$$

This reveals that the identity between the two exponents appearing in the Laplace transforms $\tilde{p}(s)$ and $\tilde{f}(s)$ in the case of finite mean waiting time - or in the generating functions $P(z)$ and $F(z)$, for the underlying random walk - does not hold true now. Upon Laplace inversion, we obtain the time decay of the probability of being at the origin and the first return probability:

$$p(t) \sim \frac{1}{\Gamma(1-\alpha+\alpha\nu)} \left(\frac{\tau}{t}\right)^{\alpha(1-\nu)} H^*(t) \tag{4.81}$$

$$f(t) \sim \frac{\alpha\nu}{\Gamma(1-\alpha\nu)} \frac{\tau^{\alpha\nu}}{t^{1+\alpha\nu}} L^*(t), \tag{4.82}$$

where $H^*(x)$ and $L^*(x)$ are slowly-varying functions related to $H(x)$ and $L(x)$, respectively.

Before dealing in detail with the statistics of occupation times, let us consider the example of the standard CTRW, ruled by the dynamics of the simple symmetric random

walk. The generating functions of the underlying model are thus

$$P(z) = \frac{1}{\sqrt{1-z^2}} \tag{4.83}$$

$$F(z) = 1 - \sqrt{1-z^2}, \tag{4.84}$$

which yield the expressions of the Laplace transforms $\tilde{p}(s)$ and $\tilde{f}(s)$, see Eqs. (4.65) and (4.68):

$$\tilde{p}(s) = \frac{1-\tilde{\psi}(s)}{s} \frac{1}{\sqrt{1-\tilde{\psi}^2(s)}} \tag{4.85}$$

$$\tilde{f}(s) = 1 - \sqrt{1-\tilde{\psi}^2(s)}. \tag{4.86}$$

Note that both can be rewritten as

$$\tilde{p}(s) = \frac{\sqrt{1-\tilde{\psi}(s)}}{s} H\left(\frac{1}{1-\tilde{\psi}(s)}\right) \tag{4.87}$$

$$\tilde{f}(s) = 1 - \sqrt{1-\tilde{\psi}(s)} L\left(\frac{1}{1-\tilde{\psi}(s)}\right), \tag{4.88}$$

where

$$H(x) = \sqrt{\frac{x}{2x-1}} \tag{4.89}$$

is indeed a slowly-varying function and $L(x) = 1/H(x)$. In the infinite mean waiting time case, from Eqs. (4.81) and (4.82) we get

$$p(t) \sim \frac{1}{\Gamma(1-\alpha/2)} \left(\frac{\tau}{t}\right)^{\alpha/2} H^*(t) \tag{4.90}$$

$$f(t) \sim \frac{\alpha}{2\Gamma(1-\alpha/2)} \frac{\tau^{\alpha/2}}{t^{1+\alpha/2}} L^*(t), \tag{4.91}$$

with

$$H^*(x) = \sqrt{\frac{x^\alpha}{2x^\alpha - 1}}, \tag{4.92}$$

and $L^*(x) = 1/H^*(x)$, which is a textbook result [63], obtained with a different method.

4.6.1 Lamperti theorem for Continuous Time Random Walks

The extension of Lamperti theorem (Theorem 2) to CTRW models has been considered in many works [6, 10, 11, 45, 64]. The main idea is to consider a two-state process, where the particle either occupies or not a given state. For example, we can call *state* 0

the occupation of the origin and *state* 1 the occupation of any other site. The time spent on state 0 is described by a waiting time distribution $\psi_0(\tau)$, while that spent outside the origin by $\psi_1(\tau)$. Let us suppose that the process starts at time $t_0 = 0$ on state 0; after a random time $t_1 = \tau_1$ drawn from $\psi_0(\tau)$, the state of the particle is changed to 1; the particle remains on 1 for a time τ_2, drawn from $\psi_1(\tau)$, and then at time $t_2 = \tau_1 + \tau_2$ it returns to state 0. The process is then repeated up to time t, which, assuming there are n transitions, can be written as

$$t = t_n + \tau^*, \tag{4.93}$$

where t_n is the time of the last transition and τ^* is the amount of time between t_n and t.

Observe that for even n the process ends on the initial state, while for odd n it ends on the other state. Hence the total times T_0 and T_1 spent by the particle on state 0 and 1 are:

$$T_0 = \sum_{j \text{ odd}}^{n} \tau_j + \vartheta_n \tau^* \tag{4.94}$$

$$T_1 = \sum_{j \text{ even}}^{n} \tau_j + (1 - \vartheta_n)\, \tau^*, \tag{4.95}$$

where

$$\vartheta_n = \begin{cases} 1 & \text{if } n \text{ is even} \\ 0 & \text{if } n \text{ is odd.} \end{cases} \tag{4.96}$$

4.6.1.1 Occupation time of the origin

Let us consider the random time T_0, and let us denote with $g_t\,(T_0)$ its PDF for a process observed up to time t. The function $g_t\,(T_0)$ can be written:

$$g_t\,(T_0) = \sum_{n=0}^{\infty} g_{t,n}\,(T_0)\,, \tag{4.97}$$

where $g_{t,n}\,(T_0)$ is the PDF conditioned to the event that n transitions have occurred up to time t. This can be expressed as:

$$g_{n,t}\,(T_0) = \left\langle \delta\left(T_0 - \sum_{j \text{ odd}}^{n} \tau_j - \vartheta_n \tau^* \right) \theta\,(t - t_n)\, \theta\,(t_{n+1} - t) \right\rangle, \tag{4.98}$$

where

$$\theta(x) = \begin{cases} 1 & \text{if } x > 0 \\ 0 & \text{otherwise,} \end{cases} \tag{4.99}$$

and the brackets denote the average over all time intervals τ_j. This expression is particularly useful to determine the double Laplace transform

$$\tilde{g}_{n,s}(p) = \int_0^\infty e^{-st} \int_0^\infty e^{-pT_0} g_{n,t}\,(T_0)\,\mathrm{d}T_0 \mathrm{d}t, \tag{4.100}$$

so that one finds

$$\tilde{g}_{n,s}(p) = \begin{cases} \dfrac{1-\tilde{\psi}_0(p+s)}{p+s}\left[\tilde{\psi}_0(p+s)\tilde{\psi}_1(s)\right]^{\frac{n}{2}} & n \text{ even} \\ \dfrac{1-\tilde{\psi}_1(s)}{s}\tilde{\psi}_0(p+s)\left[\tilde{\psi}_0(p+s)\tilde{\psi}_1(s)\right]^{\frac{n-1}{2}} & n \text{ odd.} \end{cases} \tag{4.101}$$

Note that when n is even, then $n = 2R$, where R is the number of returns to state 0; similarly, when n is odd, it can be written as $n = 2R + 1$. Therefore the sum over n in Eq. (4.97) can be replaced by a sum over the number of returns, leading to

$$\tilde{g}_s(p) = \left[\tilde{\psi}_0(p+s)\frac{1-\tilde{\psi}_1(s)}{s} + \frac{1-\tilde{\psi}_0(p+s)}{p+s}\right]\sum_{R=0}^{\infty}\left[\tilde{\psi}_0(p+s)\tilde{\psi}_1(s)\right]^R \tag{4.102}$$

$$= \left[\tilde{\psi}_0(p+s)\frac{1-\tilde{\psi}_1(s)}{s} + \frac{1-\tilde{\psi}_0(p+s)}{p+s}\right]\frac{1}{1-\tilde{\psi}_0(p+s)\tilde{\psi}_1(s)}. \tag{4.103}$$

In our setting, the distribution of the waiting times on state 0 is given by the distribution of waiting times between steps, i.e., $\psi_0(\tau) = \psi(\tau)$; the distribution of waiting times on state 1 is related to the distribution of the first return time to the origin by

$$f(t) = \int_0^t \psi_0(t')\psi_1(t-t')\mathrm{d}t'. \tag{4.104}$$

Indeed, since the process starts on state 0, the probability of returning for the first time at time t is equal to the probability of performing the first jump at time $t' < t$, switching to state 1, and then waiting on state 1 for a time $t - t'$. In Laplace space this relation reads:

$$\tilde{\psi}_1(s) = \frac{\tilde{f}(s)}{\tilde{\psi}_0(s)}, \tag{4.105}$$

which, as long as the underlying random walk is not ergodic, viz., $\nu \neq 1$, reveals that the small-s behaviour of $\tilde{\psi}_1(s)$ is the same as $\tilde{f}(s)$. This is not surprising, since the difference between the first return time and the waiting time on state 1 is just the waiting time before performing the first jump; in the non-ergodic case the first return time distribution decays more slowly than the distribution of the waiting times between steps; hence the contribution coming from the first waiting time becomes negligible in the

long-time limit. Therefore for small values of their argument, the Laplace transforms $\tilde{\psi}_0(r)$ and $\tilde{\psi}_1(r)$ behave as:

$$\tilde{\psi}_0(r) \sim 1 - \tau^\alpha r^\alpha \tag{4.106}$$

$$\tilde{\psi}_1(r) \sim 1 - \tau^{\alpha\nu} r^{\alpha\nu} L^*\left(\frac{1}{\tau r}\right), \tag{4.107}$$

and by plugging these expressions in Eq. (4.103) we can obtain the small-p, small-s expansion of $\tilde{g}_s(p)$:

$$\tilde{g}_s(p) \sim \frac{\tau^\alpha (p+s)^{\alpha-1} + \tau^{\alpha\nu} s^{\alpha\nu-1} L^*\left(\frac{1}{s}\right) - \tau^{\alpha(1+\nu)} s^{\alpha\nu-1} (p+s)^\alpha L^*\left(\frac{1}{s}\right)}{\tau^\alpha (p+s)^\alpha + \tau^{\alpha\nu} s^{\alpha\nu} L^*\left(\frac{1}{s}\right) - \tau^{\alpha(1+\nu)} s^{\alpha\nu} (p+s)^\alpha L^*\left(\frac{1}{s}\right)}. \tag{4.108}$$

By expanding in powers of p, one may get the moments of $T_0(s)$ in Laplace space for small s, for instance:

$$\langle T_0(s) \rangle \sim \tau^{\alpha(1-\nu)} H^*\left(\frac{1}{s}\right) s^{\alpha(1-\nu)-2}, \tag{4.109}$$

which can be inverted to the time domain, yielding the $t \to \infty$ limit:

$$\langle T_0(t) \rangle \sim \frac{\tau^{\alpha(1-\nu)}}{\Gamma\big(2 - \alpha\,(1-\nu)\big)} H^*(t) t^{1-\alpha(1-\nu)}. \tag{4.110}$$

Moreover, one can check that the q-th moment of $T_0(t)$ scales as:

$$\left\langle T_0^q(t) \right\rangle \sim t^{q-\alpha(1-\nu)}, \tag{4.111}$$

hence by considering the fraction of time $u(t) = T_0(t)/t$, one has that all the moments of $u(t)$ vanish. This means that the distribution of the fraction of time spent at the origin in the long-time limit converges to a Dirac delta $\delta(u)$, having all mass concentrated at $u = 0$.

We point out this result also holds for random walk models, when the mean return time to the origin is infinite. Indeed, let us consider the particular case where the waiting time between steps is fixed, i.e., $\psi_0(\tau) = \delta(\tau - \tau_0)$, so that $\tilde{\psi}_0(s) = e^{-s\tau_0}$. In this case, as we shown previously in this chapter, the Laplace transform of the first return time for small s is:

$$\tilde{f}(s) \sim 1 - \tau_0^\nu s^\nu L\left(\frac{1}{\tau_0 s}\right), \tag{4.112}$$

with $0 \leq \nu < 1$ (for $\nu = 1$, the mean return time is finite). Hence we can consider Eq. (4.103), with $\tilde{\psi}_1(s) \sim \tilde{f}(s)$, to obtain the moments of $T_0(t)$. We get:

$$\left\langle T_0^q(t) \right\rangle \sim \frac{\Gamma(1+q)}{\Gamma(1+q\nu)} \big[\tau H^*(t)\big]^q \left(\frac{t}{\tau}\right)^{q\nu}, \tag{4.113}$$

which means that also in this case the moments of $u(t)$ converge to 0 for $t \to \infty$. This is due to the fact that when the mean return time is infinite and the waiting time at a point decays faster than the return time, we expect that the fraction of time the process spends at the origin goes to 0 in the long-time limit. However, note that the scaling of the moments shows a huge difference with respect to the previous case: indeed, if in this case we consider the random variable

$$\xi(t) = \frac{T_0(t)}{\tau^{1-\nu} H^*(t) t^\nu}, \tag{4.114}$$

we have

$$\lim_{t\to\infty} \langle \xi^q(t) \rangle = \frac{\Gamma(1+q)}{\Gamma(1+q\nu)}, \tag{4.115}$$

which are the moments of the Mittag-Leffler distribution [99], as anticipated in Sec. 4.3. Hence, there exists a scaling function $h(t)$ such that the rescaled occupation time $\xi(t) = T_0(t)/h(t)$ possesses a limiting distribution - although this random variable does not represent the fraction of time spent at the origin. Note that this is also true for any distribution of waiting times $\psi_0(\tau)$ possessing a finite first moment $\langle\tau\rangle$, and it is consistent with the fact that when a microscopic time scale exists for the steps, the physical time of the process is proportional to the number of steps: $t \approx \langle\tau\rangle n$. Therefore, the distribution of $T_0(t)$ must be the same as the distribution of M_n, where M_n is the number of steps spent at the origin by the underlying random walk up to time n (see Section 4.3). This relation between M_n and $T_0(t)$ is broken when instead the mean waiting time between steps is infinite, and indeed for the variable $T_0(t)$ we do not find a similar convergence to the Mittag-Leffler distribution.

We now consider the case where the underlying random walk is ergodic, i.e., $\nu = 1$. The Laplace transforms $\tilde{\psi}(s)$ and $\tilde{f}(s)$ are characterized by the same exponent; moreover, we recall that in the ergodic case both the slowly-varying functions $H(x)$ and $L(x)$ decay to a constant. Therefore from Eq. (4.105) we have

$$\tilde{\psi}_1(s) \sim 1 - \tau^\alpha \, (L-1) \, s^\alpha. \tag{4.116}$$

In this case the difference between $\tilde{f}(s)$ and $\tilde{\psi}_1(s)$ is not negligible, even in the small-s limit. By plugging the expansion in Eq. (4.103) we get

$$\tilde{g}_s(p) \sim \frac{1}{s} \cdot \frac{\left(1+\frac{p}{s}\right)^{\alpha-1} + L - 1}{\left(1+\frac{p}{s}\right)^{\alpha} + L - 1}, \tag{4.117}$$

which can be inverted, using the method introduced in [45], yielding the limiting distribution of the fraction of time $u(t) = T_0(t)/t$, viz., the Lamperti distribution $\mathscr{G}_{L^{-1},\alpha}(u)$:

$$\mathscr{G}'_{L^{-1},\alpha}(u) = \mathscr{N} \frac{u^\alpha (1-u)^{\alpha-1} + u^{\alpha-1}(1-u)^\alpha}{a^2 u^{2\alpha} + 2au^\alpha (1-u)^\alpha \cos(\pi\alpha) + (1-u)^{2\alpha}}, \tag{4.118}$$

with

$$a = L - 1 \tag{4.119}$$

$$\mathscr{N} = \frac{a \sin(\pi\alpha)}{\pi}. \tag{4.120}$$

We recall that the first parameter of the Lamperti distribution is the expected value of the fraction of time:

$$\eta \equiv \lim_{t\to\infty} \mathbb{E}\left(\frac{T_0(t)}{t}\right) = \frac{1}{L}; \tag{4.121}$$

moreover, L is the mean return time to the origin for the underlying random walk. Indeed, the mean return time is

$$\mathscr{T} = \sum_{n=1}^{\infty} nF_n = \lim_{z\to 1^-} F'(z) = L, \tag{4.122}$$

hence the expected value of the fraction of time spent at the origin by the CTRW is equal to the inverse of the mean return time of the underlying random walk, and we have the following relation between the asymmetry parameter a and $\mathscr{T}$:

$$a = \mathscr{T} - 1. \tag{4.123}$$

Furthermore, as we showed in Chapter 2, when the mean return time is finite, $\mathscr{T}$ is related to the value of the stationary distribution at the origin by

$$\mathscr{T} = \frac{1}{\pi_0}. \tag{4.124}$$

It follows that a can be written in terms of the stationary distribution:

$$a = \frac{1 - \pi_0}{\pi_0} = \frac{\pi_1}{\pi_0}, \tag{4.125}$$

where π_0 and π_1 are the stationary measures of the sets defining state 0 and 1, respectively, as already showed in the literature, see [6, 10, 11, 64].

With these results it is straightforward to obtain the distribution of the fraction $T_1(t)/t$. Indeed, in the non-ergodic case the expected value of $T_0(t)/t$ converges to 0 in the long-time limit, and the distribution is the Dirac delta centred around 0. This implies that the fraction of time spent by the process on state 1 must converge to 1, and the limiting distribution must be the Dirac delta $\delta(u - 1)$. In the ergodic case instead the expected fraction of time spent on 0 in the long-time limit is $\mathbb{E}(T_0(t)/t) = L^{-1}$, hence

$$\mathbb{E}\left(\frac{T_1(t)}{t}\right) = 1 - \mathbb{E}\left(\frac{T_0(t)}{t}\right) = \frac{L-1}{L}. \tag{4.126}$$

Since $\psi_0(\tau)$ and $\psi_1(\tau)$ decay with the same exponent α, the limiting distribution of $T_1(t)/t$ must be the Lamperti distribution of asymmetry parameter $a = (L-1)^{-1}$ and exponent α. One can prove this by observing that the Laplace transform of the distribution of $T_1(t)$, which we call $h_t(T_1)$ can be obtained from Eq. (4.103) by switching the roles of the variables $p+s$ and s, yielding:

$$\tilde{h}_s(p) = \left[\tilde{\psi}_0(s)\frac{1-\tilde{\psi}_1(p+s)}{p+s} + \frac{1-\tilde{\psi}_0(s)}{s}\right]\frac{1}{1-\tilde{\psi}_0(s)\tilde{\psi}_1(p+s)}. \tag{4.127}$$

The small-p, small-s behaviour is

$$\tilde{h}_s(p) \sim \frac{1}{s}\cdot\frac{\left(1+\frac{p}{s}\right)^{\alpha-1}+(L-1)^{-1}}{\left(1+\frac{p}{s}\right)^{\alpha}+(L-1)^{-1}}, \tag{4.128}$$

which, upon Laplace inversion, confirms our expectation.

4.6.1.2 Occupation time of the positive axis

From the result regarding the distribution of $T_1(t)$ we can deduce the distribution of the fraction of time spent, e.g, in the positive axis, in the simple case where the process is symmetric with respect to the origin, as done in Sec. 4.2.

In the non-ergodic case, the fraction of time spent by process away from the origin converges to 1, and this is mainly due to the fact that the distribution of the waiting times on state 1 decays with a lower exponent than $\psi_0(\tau)$. Now suppose that state 1 is split evenly in two sets, say A and B, where the dynamics is the same. Then the waiting time distributions $\psi_A(\tau)$ and $\psi_B(\tau)$ in A and B must decay with the same exponent as $\psi_1(\tau)$, viz., $\alpha\nu$; moreover, we must have $\psi_A(\tau) = \psi_B(\tau)$. Hence, since in the long-time limit the process spends all the time on state 1, we can actually see it as a two-state process defined by the occupation of sets A and B. The limiting distribution of the fraction of time spent on one of the two sets, say A, is thus the symmetric Lamperti distribution of exponent $\alpha\nu$: $\mathscr{G}_{\frac{1}{2},\alpha\nu}(u)$. For $\alpha > 1$, we recover the result valid for the underlying random walk, and the distribution is $\mathscr{G}_{\frac{1}{2},\nu}(u)$.

In the ergodic case $\psi_0(\tau)$ and $\psi_1(\tau)$ decay with the same exponent, hence by splitting state 1 evenly in two sets, the process actually becomes a three-state process. However, by symmetry the expected fraction of time spent in set A must be one half of the expected fraction on state 1. This means that the limiting distribution must be the Lamperti distribution with $\eta = (L-1)/2L$ and exponent α. Recalling that $L = 1/\pi_0$, note that the asymmetry parameter a can be written as

$$a = \frac{1-\pi_A}{\pi_A}, \tag{4.129}$$

hence a^{-1} is equal to the ratio of the stationary measure of the set of interest to the stationary measure of its complement, see also Eq. (4.125). Finally, when $\alpha > 1$, the mean waiting time between steps is finite and thus we must recover the ergodic

behaviour of the underlying random walk. Hence the limiting distribution is a Dirac delta centred around the expected fraction of occupation time. This can be shown by plugging the small-r behaviours of $\tilde{\psi}_0(r)$ and $\tilde{\psi}_1(r)$, see Eq. (4.116), in Eq. (4.127), obtaining the small-p, small-s behaviour

$$\tilde{h}_s(p) \sim \frac{1}{s + 2\eta p}, \tag{4.130}$$

with

$$2\eta = \frac{L-1}{L}. \tag{4.131}$$

Upon Laplace inversion, one gets the distribution of the occupation time $T_1(t)$:

$$h_t\left(T_1\right) = \delta\left(T_1 - 2\eta t\right). \tag{4.132}$$

Therefore, if state 1 is split evenly in two sets, A and B, the distribution of the fraction of time spent in A is a Dirac delta centred around η, with

$$\eta = \frac{L-1}{2L} = \frac{1-\pi_0}{2}. \tag{4.133}$$

4.6.2 Numerical results

To test the results discussed in the previous section we introduce the *Gillis Continuous Time Random Walk* (GCTRW), a CTRW governed by the underlying dynamics of the GRW, see Chapter 2. We recall that the properties of the GRW depend on the value of the parameter $\epsilon \in (-1, 1)$; in particular, the process is ergodic for $\epsilon \geq \frac{1}{2}$. Hence by tuning the value of ϵ we can explore all the different behaviours a CTRW can exhibit regarding the statistics of occupation times.

For the GRW the generating function of the first return time has the form

$$F(z) = 1 - (1-z)^{\nu} L\left(\frac{1}{1-z}\right), \tag{4.134}$$

where

$$\nu = \begin{cases} 0 & \text{for } \epsilon < -\dfrac{1}{2} \\ \dfrac{1}{2} + \epsilon & \text{for } -\dfrac{1}{2} \leq \epsilon < \dfrac{1}{2} \\ 1 & \text{for } \epsilon \geq \dfrac{1}{2}, \end{cases} \tag{4.135}$$

and $L(x)$ is a slowly-varying function. The process is recurrent only for $\epsilon \geq -\frac{1}{2}$, so we will restrict ourselves to this range. In our simulations, the waiting times between steps are taken from the Pareto distribution

$$\psi(\tau) = \frac{\alpha \tau_0^{\alpha}}{\tau^{1+\alpha}}, \quad \tau > \tau_0, \tag{4.136}$$

where τ_0 is a cut-off. Note that for $0 < \alpha \leq 2$ the second moment in infinite and in the restricted range $0 < \alpha \leq 1$ also the first moment is infinite. From the knowledge of ν and the exponent α of the waiting time distribution $\psi(\tau)$ we are able to determine the statistics of occupation times for the related CTRW model.

4.6.2.1 Occupation time of the origin

As we have previously shown, the distribution of the occupation time of the origin depends on both the ergodic properties of the underlying random walk and the waiting time PDF between steps $\psi(\tau)$. In the case of Gillis, the regime $\epsilon \in \left[-\frac{1}{2}, \frac{1}{2}\right)$ is non-ergodic and we have $\nu = \frac{1}{2} + \epsilon$. Hence if $\psi(\tau)$ has a well-defined first moment $\langle\tau\rangle$, the distribution of $T_0(t)$ is the same as the distribution of the number of steps at the origin M_n, which is, upon proper rescaling, a Mittag-Leffler of parameter $\rho = \frac{1}{2} + \epsilon$, see Sec. 4.3. The situation changes drastically if we consider waiting time distributions not possessing a finite first moment: in this case the occupation time of the origin is no longer proportional to the number of steps and since the distribution of the time spent away from the origin decays more slowly, in the long-time limit the the fraction of time $u(t) = T_0(t)/t$ converges to 0.

In Fig. 4.12 we consider the distribution of $T_0(t)$ for the GCTRW with $\epsilon = 0.2$, for both finite-mean and infinite-mean waiting time between steps. In the former case we show data regarding two $\psi(\tau)$ with different exponents: $\alpha = 1.9$ (blue squares) and $\alpha = 3$ (green asterisks). In both cases we take $\tau_0 = 0.1$ and the time of the simulations is $t = 10^3$. The random variable ξ is the occupation time $T_0(t)$ rescaled by its mean value. We see that in both cases it converges to the Mittag-Leffler distribution of parameter $\rho = \frac{1}{2} + \epsilon$. For the infinite-mean case we choose instead $\alpha = 0.5$ and consider the fraction of time $u = T_0/t$. Note that the shape of the distributions is clearly different from the previous case: it displays an asymmetric U-shaped curve with a prominent peak at $u = 0$ and a lower peak at $u = 1$. We consider different values of t: as the total time increases, the peak situated at $u = 1$ decreases while the one at $u = 0$ increases, hinting at the slow convergence to the Dirac delta $\delta(u)$.

In Fig. 4.13 we present our simulations regarding the distribution of the fraction of time $u(t) = T_0(t)/t$ spent at the origin when the underlying random walk is ergodic. Here we fix $\epsilon = 0.9$ and choose different values of $\alpha < 1$. Data agree with the corresponding theoretical Lamperti distributions $\mathscr{G}_{\eta,\alpha}(u)$, with

$$\eta = \pi_0 = \frac{2\epsilon - 1}{2\epsilon}. \tag{4.137}$$

Note that in this case we set $\tau_0 = 1$ and run the simulations for different times depending on α: we take $t = 10^7$ for $\alpha = 0.3, 0.5$ and $t = 10^6$ for $\alpha = 0.68, 0.82$. As already observed in the previous literature, as α approaches 1 the ergodic phase of the underlying random walk is recovered [6, 10, 11]. Indeed, the distribution displays a more and more pronounced peak appearing in proximity of η, i.e., the expected value of $u(t)$ for $t \to \infty$. We recall that for the GRW in the ergodic phase the occupation time of the

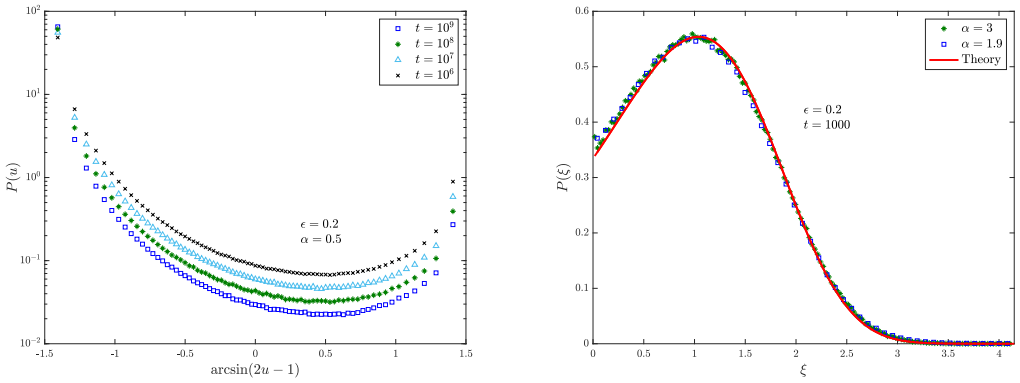

FIGURE 4.12: Distributions of the occupation time of the origin for the Gillis continuous time random walk, with $\epsilon = 0.2$ and waiting time distribution possessing infinite (left) and finite (right) mean. The finite mean case is considered with both infinite and finite variance, with $\alpha = 1.9$ and $\alpha = 3$. The infinite mean is considered for different total times, showing a slow convergence to the Dirac delta $\delta(u)$.

origin converges to the expected value; more precisely, the distribution of

$$\xi \equiv \lim_{n\to\infty} \frac{M_n}{\langle M_n \rangle} \tag{4.138}$$

is a Dirac delta centred around $\xi = 1$, see Sec. 4.3. Since $\langle M_n \rangle$ grows as n, this implies that the fraction of time $u_n \equiv M_n/n$ converges to its expected value

$$\eta \equiv \lim_{n\to\infty} \mathbb{E}\left(\frac{M_n}{n}\right), \tag{4.139}$$

which must be equal to π_0, the value of the stationary distribution at the origin. This is related to the ergodicity of the process. This property is also recovered in the related continuous time model as long as the mean waiting time between steps is finite. When the steps do not possess a finite scale, viz., for $\alpha < 1$, the ergodic behaviour is broken, and we have a proper distribution for the fraction of occupation time. This feature of CTRWs is called in the literature *ergodicity breaking* [6, 10, 11].

4.6.2.2 Occupation time of the positive axis

Due to the symmetry of the GRW, the continuous time model is expected to spend an equal amount of time in the positive and negative axis. Therefore, in the non-ergodic case, viz., $\epsilon < \frac{1}{2}$, the distribution of the fraction of time is the symmetric Lamperti distribution $\mathscr{G}_{\frac{1}{2},\alpha\nu}(u)$. In Fig. 4.14 we consider the non-ergodic case for $\epsilon = -0.2$ and $\epsilon = 0.2$, with waiting time distribution characterized by the exponent $\alpha = 0.3$. Here we take $\tau_0 = 1$ and run the simulations up to $t = 10^{11}$. The effect of introducing a waiting time between steps in this case is limited to the modification of the exponent ρ of the

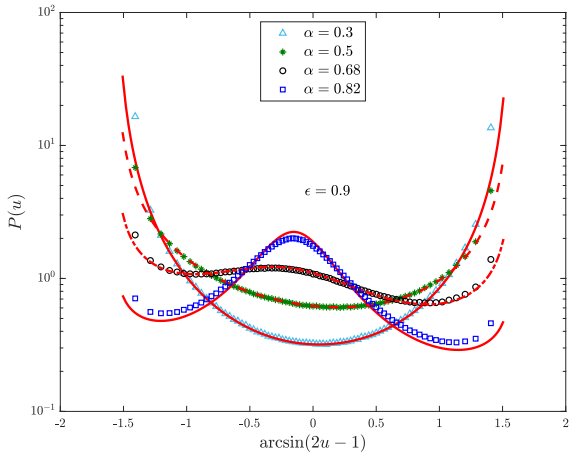

FIGURE 4.13: Distributions of the fraction of time $u(t) = T_0(t)/t$ for the Gillis continuous time random walk, with $\epsilon = 0.9$ and different values of α. Data are compared to the theoretical Lamperti distributions. As α tends to 1, we approach the ergodic phase of the underlying Gillis random walk.

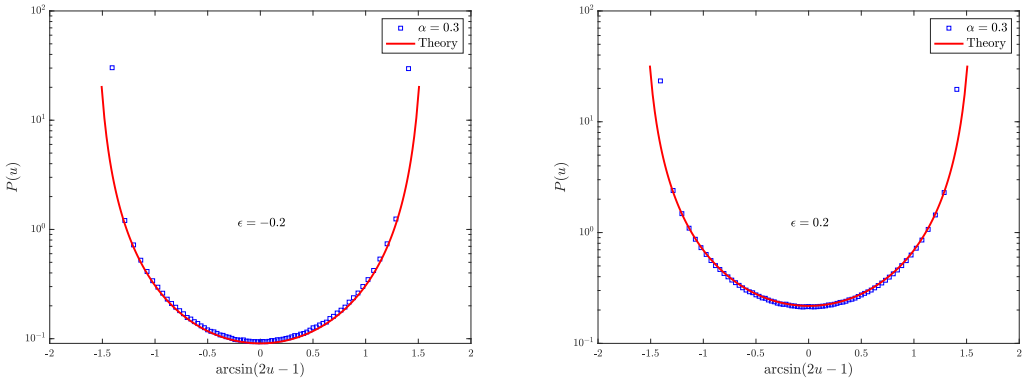

FIGURE 4.14: Distributions of the occupation time of the positive axis for the Gillis continuous time random walk, with waiting time distribution characterized by the exponent $\alpha = 0.3$. Here we choose $\epsilon = -0.2$ (left) and $\epsilon = 0.2$ (right). Data are compared to the corresponding theoretical Lamperti distributions.

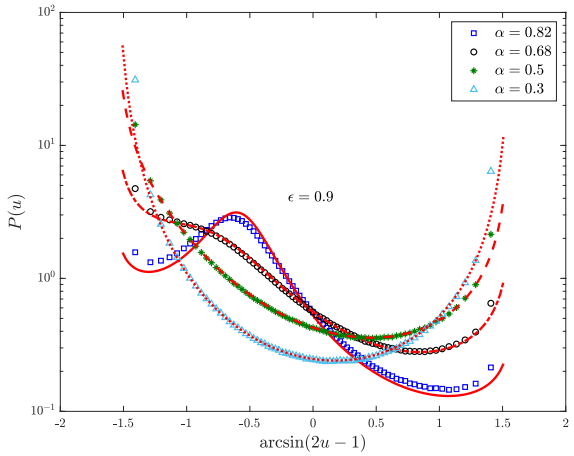

FIGURE 4.15: Distributions of the fraction of time $u(t)$ spent on the positive axis for the Gillis continuous time random walk, with $\epsilon = 0.9$ and different values of α. Data are compared to the theoretical Lamperti distributions. As α tends to 1, we approach the ergodic phase of the underlying Gillis random walk.

Lamperti distribution with respect to the one of the underlying random walk: we have $\rho = \nu$ for the Gillis model and $\rho = \alpha\nu$ for the GCTRW.

The ergodic case is depicted in Fig. 4.15. We choose $\epsilon = 0.9$ and consider different values of α. The parameter τ_0 is taken equal to unity and the simulations are run up to different times depending on α: we took $t = 10^7$ for $\alpha = 0.3, 0.5$ and $t = 10^6$ for $\alpha = 0.68, 0.82$. Data agree with the corresponding theoretical Lamperti distributions $\mathscr{G}_{\eta,\alpha}(u)$, with

$$\eta = \frac{1-\pi_0}{2} = \frac{1}{4\epsilon}. \tag{4.140}$$

Note that the distributions display the same feature of the previous case, namely as α approaches 1 the ergodic phase is recovered, with the appearance of a peak centred around η.

Finally we point out another sign of ergodicity breaking: we recall that in Sec. 4.2 for the GRW the occupation time of the positive axis was counted with the convention that the origin was included or not according to whether the previous step was in the positive or in the negative side. Hence the distribution of the fraction of occupation time of the positive axis in the ergodic regime was a Dirac delta centred around $u = \frac{1}{2}$. One may be tempted to say that by using the same convention, also for the GCTRW the expected fraction of occupation time should be $\frac{1}{2}$. This, however, is not true, because even if the underlying random walk is in the ergodic phase, the related CTRW model is not, and thus the mean return time to the origin is infinite (while the mean return time in the ergodic phase is finite for the GRW). This means that if a particle enters the positive side $A = \{k|k > 1\}$, it rarely returns to the origin and counting or not the origin

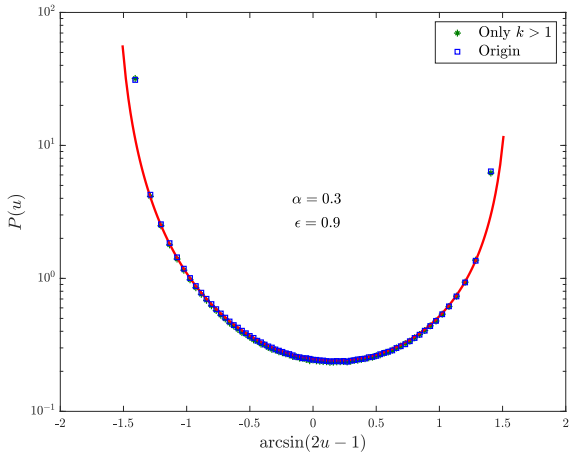

FIGURE 4.16: Comparison between the fraction of occupation time of the positive side by counting (blue squares) or not (green asterisks) the origin with the convention used in Sec. 4.2. Data are obtained by simulating 10^7 walks up to time $t = 10^7$ in both cases.

is therefore inessential in the long-time limit[2] Indeed, we point out that the data shown in Fig. 4.15 are obtained by using the same convention of Sec. 4.2; nevertheless, the limiting distributions are clearly not symmetric and the correct value of the expected fraction of time is $\eta = \frac{1}{4\epsilon}$. In Fig. 4.16 we show that the outcome of the simulations does not change if we consider only the time spent in A or we also count the time spent at the origin according to the convention used in Sec. 4.2, provided that we consider t long enough to reach the limiting distribution.

4.7 Conclusions and discussion

In the first part of this chapter we have shown that for a general class of stochastic processes there is a deep connection between the statistics of the occupation times, the number of visits at the origin and the survival probability. The distributions of these observables can be characterized by the same exponent, which is related to the asymptotic power-law decay of the probability of occupying the origin. We point out that the results of this chapter are also associated with infinite ergodic theory. In particular, let us consider the Darling-Kac theorem, that we used in Sec. 4.3 to obtain the statistics of the occupation time of the origin, in its continuous-time version [28]. The theorem firstly requires that, for a given non-negative and integrable function $V(x)$, one has

$$\lim_{s\to 0} \frac{1}{\pi(s)} \int P_s(x|x_0)V(x)\mathrm{d}x = c, \tag{4.141}$$

[2]However, this may affect the preasymptotic behaviour as well as the speed of convergence to the limiting distribution.

where c is a positive constant, $P_s(x|x_0)$ is the Laplace transform from t to s of the probability of arriving at x starting from x_0 in time t, and $\pi(s)$ is a function such that $\pi(s) \to \infty$ as $s \to 0$. Now suppose that we have

$$\lim_{s\to 0} \frac{P_s(x|x_0)}{\pi(s)} = \mathscr{I}(x), \tag{4.142}$$

where $\mathscr{I}(x)$ is the Infinite Invariant Density [74]. Note that in this case, if $V(x)$ is measurable with respect to the Infinite Invariant Density, the condition given in Eq. (4.141) is satisfied. Therefore, if $\pi(s) = s^{-\rho}H(1/s)$, with $H(u)$ slowly-varying, the Darling-Kac theorem states that the random variable

$$\xi = \lim_{t\to\infty} \frac{1}{c\pi(1/t)} \int_0^t V(x(\tau))\mathrm{d}\tau \tag{4.143}$$

$$= \lim_{t\to\infty} \frac{1}{ct^{\rho}H(t)} \int_0^t V(x(\tau))\mathrm{d}\tau \tag{4.144}$$

follows a Mittag-Leffler distribution of order ρ. Now we observe that using Eq. (4.142) we can say that as $s \to 0$:

$$P_s(x|x_0) \sim \pi(s)\mathscr{I}(x) \tag{4.145}$$

and therefore for the ensemble average of $V(x)$ we have

$$\langle V_s \rangle = \int P_s(x|x_0)V(x)\mathrm{d}x \sim c\pi(s). \tag{4.146}$$

In the case $\pi(s) = s^{-\rho}H(1/s)$, by using the Tauberian theorem [38] we find that the ensemble average in the long-time limit behaves as

$$\langle V_t \rangle \sim \frac{c}{\Gamma(\rho)} t^{\rho-1}H(t) \tag{4.147}$$

and therefore

$$\xi = \lim_{t\to\infty} \frac{1}{\Gamma(\rho)} \frac{\overline{V}_t}{\langle V_t \rangle}, \tag{4.148}$$

where $\overline{V}_t$ indicates the time average of $V(x)$ over a single realization. Such a ratio is a random variable distributed according to a Mittag-Leffler of order ρ. This is the main difference with standard ergodic theory, where instead time averages converge to ensemble averages, and hence ξ is expected to be distributed according to a Dirac delta function centred around $\xi_0 = 1$. Now the important point is that the scaling function $\pi(s)$, which determines the distribution of ξ, i.e., the value of ρ, is a property of the propagator $P_s(x|x_0)$. In other words, for any function which is measurable with respect to the infinite density, the distribution of ξ only depends on the long-time properties of the propagator. Therefore, it is possible to determine the distribution by just evaluating

the long-time behaviour of $P(x,t)$ in a given set, as we have done in the paper by considering the probability of occupying the origin. This fact let us obtain the correct parameter in the case of the averaged LL gas, relying only on the continuum limit, i.e., on the asymptotic properties of the process. Moreover, since the exponent ρ does not depend on x_0, we would have the same Mittag-Leffler distribution even if we considered a different point than the origin (this, however, is not true for the Lamperti law, where the evaluation of the asymmetry parameter depends on how the space is split by the point x_0).

To give an example we can consider the statistics of the occupation time of the origin for the GRW. This is described by the random variable ξ, defined as

$$\xi = \lim_{n\to\infty} \frac{1}{\Gamma(1+\rho)} \frac{M_n}{\langle M_n \rangle}. \tag{4.149}$$

The observable $V(x)$ in this case is the function $V(x) = \delta_{x,0}$, whose time average is

$$\bar{V}_n = \frac{1}{n} \sum_{m=0}^{n} \delta_{x_m,0} = \frac{M_n}{n}, \tag{4.150}$$

while the ensemble-average is

$$\langle V_n \rangle = \sum_{x=-\infty}^{\infty} \delta_{x,0} P_n(x|0) = P_n(0|0) \equiv P_n, \tag{4.151}$$

i.e., the probability of being at the origin. Here we have explicitly used the fact that the walk starts from $k_0 = 0$. The ensemble average can be related to $\langle M_n \rangle$. Indeed, as we showed in the chapter, the generating function of P_n is

$$P(z) = \frac{1}{(1-z)^\rho} H\left(\frac{1}{1-z}\right), \tag{4.152}$$

and the occupation probability can be obtained by Tauberian theorems. However, when we deal with nearest-neighbour random walks, we can not apply directly Tauberian theorems on $P(z)$, because the sequence of the coefficients is not monotonic - P_n is positive for n even, and vanishes for n odd. The corrections to be applied to the result of Tauberian theorems in order to take into account this fact are showed in App. F: it can be proved that one only needs to add a factor 2, hence:

$$P_n \sim \frac{2}{\Gamma(\rho)} n^{\rho-1} H(n), \quad n \text{ even}. \tag{4.153}$$

It follows then from the asymptotic behaviour of $\langle M_n \rangle$, see App. D, that as long as n is even:

$$\langle M_n \rangle \sim \frac{n}{2\rho} P_n. \tag{4.154}$$

For the GRW these quantities can be computed analytically and indeed the expression of P_n was presented in Chap. 2:

$$P_n \sim \frac{2^{\epsilon+1/2}}{\Gamma(1/2-\epsilon)}\frac{\Gamma(1-\epsilon)}{\Gamma(1+\epsilon)}n^{\epsilon-1/2}, \quad n \text{ even} \tag{4.155}$$

The connection with infinite ergodic theory stems from the fact that the infinite density was defined starting from the probability of being at the origin as

$$\frac{1}{2}\lim_{n\to\infty} n^{1/2-\epsilon}P_n = \mathscr{I}(0), \tag{4.156}$$

where the factor $1/2$ was justified previously[3]. It follows that the ensemble-average can be computed as:

$$\langle V_n\rangle = P_n \sim 2\frac{\mathscr{I}(0)}{n^{1/2-\epsilon}}. \tag{4.157}$$

On the other hand, by using Eq. (4.154) with $\rho = \frac{1}{2}+\epsilon$, we can write $\langle M_n\rangle$ in terms of $\mathscr{I}(x)$ as

$$\langle M_n\rangle \sim \frac{n^{1/2+\epsilon}}{1/2+\epsilon}\mathscr{I}(0) = \frac{n^{1/2+\epsilon}}{(1/2+\epsilon)}\frac{2^{\epsilon-1/2}}{\Gamma(1/2-\epsilon)}\frac{\Gamma(1-\epsilon)}{\Gamma(1+\epsilon)}, \tag{4.158}$$

where we used the expression of $\mathscr{I}(0)$ computed in Chap. 2. This expression is consistent with the one we would obtain by using Tauberian theorems, suggested in App. D, hence $\mathscr{I}(x)$ can be effectively used to define the random variable ξ. Indeed

$$\langle M_n\rangle \sim \frac{n\langle V_n\rangle}{2(1/2+\epsilon)}, \tag{4.159}$$

therefore the definition of the random variable ξ can be rewritten in terms of the averages of the observable $V(x)$ as

$$\xi = \lim_{n\to\infty}\frac{2}{\Gamma(1/2+\epsilon)}\frac{\bar{V}_n}{\langle V_n\rangle}, \tag{4.160}$$

and in particular the ensemble average can be computed in terms of the Infinite Invariant Density. Note that this equation differs from the definition of Eq. (4.148) by a factor 2, which is again due to the fact that we have considered a nearest-neighbour random walk.

We remark that the connection between the statistics of the occupation times, the number of visits at the origin, the survival probability and the probability of being at the origin holds true for walks possessing a finite time scale for the steps, and is no longer valid when the time of the process and the total number of steps can not be put in a relation of proportionality. Indeed, studies on the statistics of occupation times have

[3] We recall that it is related to the fact that we are considering a nearest-neighbour random walk

shown that the exponent characterizing the Lamperti law is not related in general to the probability of occupying the starting point. Examples can be found in the contexts of continuous-time random walks [11], fractional diffusion [6] and in the quenched trap model [21], to cite a few. All these cases show that the correct characterization of the Lamperti and Mittag-Leffler distributions is possible by evaluating the first-passage exponent. Nevertheless, we have shown in the second part of the chapter that our general relation is still useful to determine the statistics of occupation time for a CTRW model by applying the results of the first part to the corresponding underlying random walk. In particular, the exponent of the probability of being at the origin and the exponent of the waiting time distribution can be sufficient to determine the correct distributions. We point out once again, however, that in general if one focuses on a point different than the origin, splitting the dynamics in two asymmetric sets, it is also necessary to find the asymmetry parameter.

4.8 Summary

In this chapter we have dealt with the statistics of occupation times for a certain class of stochastic processes. In the first part, based entirely on Ref. [101], we have shown that the exponent of the asymptotic power-law of the occupation probability of the initial state plays a major role to determine the correct limiting distributions. This establishes an important relation between the occupation time of a set, the survival probability and the number of returns to the origin.

However, this result is no longer valid if the process does not posses a finite microscopic time scale, as we have shown in the second part. Nevertheless, in the case of Continuous Time Random Walks one can still use the results of the first part applied to the underlying dynamics, to determine the distribution of the required observables. We point out that the results contained in the second part were mostly proved in the previous literature, see [6, 10, 11, 64]. However, we have rewritten such results in terms of the theory developed in the first part of the chapter. Moreover, we have tested the results by introducing a novel Continuous Time Random Walk model based on the underlying dynamics of the Gillis Random Walk, confirming our expectations both theoretically and numerically.

The hypergeometric function A

A.1 Basic definition

The hypergeometric function, also known as Gaussian hypergeometric function or ordinary hypergeometric function, is defined by the power series

$$ {}_2F_1(a,b;c;z) = \sum_{n=0}^{\infty} \frac{(a)_n (b)_n}{(c)_n} \frac{z^n}{n!}, \tag{A.1} $$

where $(x)_n$ denotes the Pochhammer symbol:

$$ (x)_n = x(x+1)\cdots(x+n-1) = \frac{\Gamma(x+n)}{\Gamma(x)}. \tag{A.2} $$

The series is not defined when c is 0 or a negative integer, provided a or b is not an integer m, with $m < c$ [1]. The series converges for $|z| < 1$, and also on the unit circle $|z| = 1$ if $\Re(c-a-b) > 0$.

A.2 Transformation formulas

To evaluate the behaviour of ${}_2F_1(a,b;c;z)$ as $z \to 1$, it is possible to use the linear transformation formulas [1], valid for $|\arg(1-z)| < \pi$. In the case $c-a-b$ non-integer, the first is

$$ \begin{aligned} {}_2F_1(a,b;c;z) &= \frac{\Gamma(c)\Gamma(c-a-b)}{\Gamma(c-a)\Gamma(c-b)}\ {}_2F_1(a,b;a+b-c+1;1-z) \\ &+ (1-z)^{c-a-b}\frac{\Gamma(c)\Gamma(a+b-c)}{\Gamma(a)\Gamma(b)}\ {}_2F_1(c-a,c-b;c-a-b+1;1-z). \end{aligned} \tag{A.3} $$

Different formulas must be considered in the integer case. When $c = a+b+m$, with $m = 1,2,\ldots$, we have, provided $|1-z| < 1$:

$$ \begin{aligned} {}_2F_1(a,b;a+b+m;z) &= \frac{\Gamma(m)\Gamma(a+b+m)}{\Gamma(a+m)\Gamma(b+m)} \sum_{n=0}^{m-1} \frac{(a)_n (b)_n}{n!(1-m)_n}(1-z)^n \\ &- (z-1)^m \frac{\Gamma(a+b+m)}{\Gamma(a)\Gamma(b)} \sum_{n=0}^{\infty} \frac{(a+m)_n (b+m)_n}{n!(n+m)!}(1-z)^n \times \\ &\times \left[\log(1-z) - \psi(n+1) - \psi(n+m+1) + \psi(a+n+m) + \psi(b+n+m)\right], \end{aligned} \tag{A.4} $$

while for $c = a + b - m$, with $m = 1, 2, \ldots$, and $|1 - z| < 1$:

$$
\begin{aligned}
{}_2F_1(a, b; a + b - m; z) = {} & \frac{\Gamma(m)\Gamma(a + b - m)}{\Gamma(a)\Gamma(b)} \sum_{n=0}^{m-1} \frac{(a - m)_n (b - m)_n}{n!(1 - m)_n} (1 - z)^{n-m} \\
& - (-1)^m \frac{\Gamma(a + b - m)}{\Gamma(a - m)\Gamma(b - m)} \sum_{n=0}^{\infty} \frac{(a)_n (b)_n}{n!(n + m)!} (1 - z)^n \times \\
& \times \left[\log(1 - z) - \psi(n + 1) - \psi(n + m + 1) + \psi(a + n) + \psi(b + n) \right].
\end{aligned}
\tag{A.5}
$$

Finally, for $c = a + b$ and $|1 - z| < 1$:

$$
\begin{aligned}
{}_2F_1(a, b; a + b, z) = {} & \frac{\Gamma(a + b)}{\Gamma(a)\Gamma(b)} \sum_{n=0}^{\infty} \frac{(a)_n (b)_n}{(n!)^2} (1 - z)^n \big[2\psi(n + 1) \\
& - \psi(a + n) - \psi(b + n) - \log(1 - z) \big],
\end{aligned}
\tag{A.6}
$$

where in all the last three formulas, $\psi(x) = \frac{\mathrm{d}}{\mathrm{d}x}\Gamma(x)$ is the digamma function.

A.3 Evaluation of an integral

Let us consider

$$
I = \int_0^{2\pi} \frac{e^{iqk}}{(1 - z \cos q)^{\nu}} \mathrm{d}q, \tag{A.7}
$$

for $|z| < 1$, $k \in \mathbb{Z}$ and $\nu \in \mathbb{R}$. An expansion of the integrand in powers of z yields

$$
I = \sum_{n=0}^{\infty} \frac{(\nu)_n}{n!} z^n \int_0^{2\pi} e^{iqk} \cos^n q \mathrm{d}q. \tag{A.8}
$$

For each value of n, by using the binomial expansion of $\cos^n q$, one deduces that the integral in the n-th terms of the series vanishes unless $n \geq |k|$, and n and k are both even or odd, in which case one gets:

$$
\int_0^{2\pi} e^{ikq} \cos^n q \mathrm{d}q = \frac{2\pi}{2^n} \binom{n}{\frac{n-k}{2}}. \tag{A.9}
$$

Let us first consider the case n even, so that it can be replaced by $2m$. The integral is then transformed into the series

$$I = 2\pi \sum_{m=\frac{|k|}{2}}^{\infty} \frac{(\nu)_{2m}}{2^{2m}} \frac{z^{2m}}{\Gamma\left(m - \frac{k}{2} + 1\right)\Gamma\left(m + \frac{k}{2} + 1\right)}, \tag{A.10}$$

or, by the simple shift of the index $m \to m + \frac{|k|}{2}$:

$$I = \frac{2\pi z^{|k|}}{2^{|k|}} \sum_{m=0}^{\infty} \frac{(\nu)_{2m+|k|}}{2^{2m}} \frac{z^{2m}}{\Gamma(m+1)\Gamma(m+|k|+1)}. \tag{A.11}$$

For n odd, we set $n = 2m + 1$ and obtain a series similar to that in Eq. (A.10), but starting from $m = \frac{|k|-1}{2}$ and with $2m$ replaced by $2m + 1$ in each term. Nevertheless, by shifting the index $m \to m + \frac{|k|-1}{2}$, we obtain the same series as in Eq. (A.11). From the definition of the Pochhammer symbol, we deduce that

$$(\nu)_{2m+|k|} = (\nu)_{|k|}(\nu + |k|)_{2m} = \frac{\Gamma(\nu + |k|)}{\Gamma(\nu)}(\nu + |k|)_{2m} \tag{A.12}$$

and moreover, from the properties of the Gamma function, we have

$$(\nu + |k|)_{2m} = 2^{2m} \left(\frac{\nu + |k|}{2}\right)_m \left(\frac{\nu + |k| + 1}{2}\right)_m. \tag{A.13}$$

Plugging the last two formulas in Eq. (A.11), we finally obtain:

$$I = \frac{2\pi}{|k|!} \left(\frac{z}{2}\right)^{|k|} \frac{\Gamma(\nu + |k|)}{\Gamma(\nu)} \, {}_2F_1\left(\frac{\nu + |k|}{2}, \frac{\nu + |k| + 1}{2}; |k| + 1; z^2\right). \tag{A.14}$$

Tauberian theorems for power series B

Definition 1. We shall say that a real function of a real variable $\mathscr{H}(x)$ is slowly-varying (at infinity) if it is continuous, positive for large-enough x, and $\forall a > 0$ satisfies

$$\lim_{x\to\infty} \frac{\mathscr{H}(ax)}{\mathscr{H}(x)} = 1. \tag{B.1}$$

When considering functions defined by power series, such as generating functions, the following result relates the asymptotic behaviour of the function to the large-n behaviour of the coefficients of the series [39]:

Theorem 5. *Let $g_n \geq 0$ and suppose that*

$$\sum_{n=0}^{\infty} g_n z^n = G(z) \tag{B.2}$$

converges for $0 \leq z < 1$. Then

$$G(z) \sim \frac{1}{(1-z)^\gamma} \mathscr{H}\left(\frac{1}{1-z}\right),\ z \to 1^- \iff$$
$$g_0 + \cdots + g_n \sim \frac{1}{\Gamma(\gamma+1)} n^\gamma \mathscr{H}(n),\ n \to \infty \tag{B.3}$$

where $\mathscr{H}(x)$ is a slowly-varying function and $\gamma \geq 0$.
Furthermore, if the sequence $\{g_n\}$ is ultimately monotonic and $\gamma > 0$, it also holds

$$G(z) \sim \frac{1}{(1-z)^\gamma} \mathscr{H}\left(\frac{1}{1-z}\right),\ z \to 1^- \iff$$
$$g_n \sim \frac{1}{\Gamma(\gamma)} n^{\gamma-1} \mathscr{H}(n),\ n \to \infty. \tag{B.4}$$

Asymptotic values of the probability of having a scatterer at site k for the Lévy-Lorentz gas C

Consider a Lévy-Lorentz gas in nonequilibrium initial condition, with site $k = 0$ occupied by a scatterer. Let $\mu(\xi)$ be the probability of having two nearest-neighbour scatterers at distance ξ, with the following analytical form:

$$\mu(\xi) = \frac{\xi^{-1-\alpha}}{\zeta(1+\alpha)}, \quad 0 < \alpha < 2, \quad \xi = 1, 2, \ldots . \tag{C.1}$$

Then the probability ϖ_k of having a scatterer at distance $|k|$ from the origin is:

$$\begin{aligned} \varpi_k &= \sum_{m=1}^{|k|} \left[\sum_{\sum_{i=1}^{m} \xi_i = |k|} \prod_{i=1}^{m} \mu\left(\xi_i\right) \right] \\ &= \sum_{m=1}^{|k|} \varpi_k^{(m)}, \end{aligned} \tag{C.2}$$

where $\varpi_k^{(m)}$ is the probability of having $m \leq |k|$ scatterers within the distance $|k|$ from the origin, with the last one placed exactly at position k. For example, $\varpi_k^{(1)} = \mu(k)$ and $\varpi_k^{(|k|)} = [\mu(1)]^{|k|}$.

Define the generating function

$$\begin{aligned} \mathscr{L}_\alpha(z) &= \sum_{n=1}^{\infty} \varpi_n^{(1)} z^n \\ &= \sum_{n=1}^{\infty} \mu(n) z^n \\ &= \frac{1}{\zeta(1+\alpha)} \mathrm{Li}_{1+\alpha}(z), \end{aligned} \tag{C.3}$$

where $\mathrm{Li}_s(z)$ denotes the polylogarithm function [78]. The r-th power of $\mathscr{L}_\alpha(z)$ is an analytic function whose coefficient of z^n is the probability of having r scatterers within the distance n from the origin, with the last one placed exactly at position n, hence

$$[\mathscr{L}_\alpha(z)]^r = \sum_{n \geq r} \varpi_n^{(r)} z^n. \tag{C.4}$$

Now consider the generating function of the probabilities ϖ_k:

$$L(z) = 1 + \sum_{k=1}^{\infty} \varpi_k z^k. \tag{C.5}$$

By Eq. (C.2) the series on the right-hand side can be rewritten as:

$$\sum_{k=1}^{\infty} \varpi_k z^k = \sum_{k=1}^{\infty} \sum_{r=1}^{k} \varpi_k^{(r)} z^k$$

or, by setting $\varpi_k^{(r)} = 0$ for $r > k$:

$$\sum_{k=1}^{\infty} \varpi_k z^k = \sum_{r=1}^{\infty} \sum_{k=1}^{\infty} \varpi_k^{(r)} z^k = \sum_{r=1}^{\infty} \left[\mathscr{L}_\alpha(z)\right]^r . \tag{C.6}$$

This means that $L(z)$ can be written as a geometric series with ratio $\mathscr{L}_\alpha(z)$. By the definition of the polylogarithm function it can be verified that for $|z| < 1$ the absolute value of $\mathscr{L}_\alpha(z)$ is always bounded by one, hence the series converges and

$$L(z) = \frac{1}{1 - \mathscr{L}_\alpha(z)}. \tag{C.7}$$

Such an expression enables us to derive analytically the asymptotic expression of ϖ_k by Tauberian theorems for power series, see Appendix B, once we take into account the behaviour of $\mathrm{Li}_{1+\alpha}(z)$ close to $z = 1^-$. To leading order we have

$$\mathscr{L}_\alpha(z) \sim \begin{cases} 1 + \frac{\Gamma(-\alpha)}{\zeta(1+\alpha)}(1-z)^\alpha & 0 < \alpha < 1 \\ 1 - \frac{\zeta(\alpha)}{\zeta(1+\alpha)}(1-z) & \alpha > 1, \end{cases} \tag{C.8}$$

hence the asymptotic values of having a scatter at position k for $|k| \gg 1$ are given by:

$$\varpi_k \sim \pi_k = \begin{cases} \frac{\alpha \sin(\pi\alpha)}{\pi} \frac{\zeta(1+\alpha)}{|k|^{1-\alpha}} & 0 < \alpha < 1 \\ \frac{\zeta(1+\alpha)}{\zeta(\alpha)} & \alpha > 1. \end{cases} \tag{C.9}$$

Meaning of the random variable T_n D

We consider the random variable

$$T_n \equiv \frac{1}{H(n)n^\rho} \sum_{m=0}^{n} \delta_{x_m,0}. \tag{D.1}$$

The sum

$$M_n = \sum_{m=0}^{n} \delta_{x_m,0} \tag{D.2}$$

clearly represents the number of times the random walk has visited the origin up to time n, while it is possible to show that the denominator $n^\rho H(n)$ is connected to the asymptotics of the mean occupation time. Indeed, for $M \geq 1$, let us call $\psi_n(M)$ the probability that the M-th visit occurs at step n, and U_n the probability of observing no returns to the origin up to step n, with the initial conditions $\psi_0(M) = \delta_{M,1}$ and $U_0 = 1$. We have

$$U_n = 1 - \sum_{m=0}^{n} F_m \tag{D.3}$$

$$\psi_n(1) = \delta_{n,0}, \tag{D.4}$$

while for $M \geq 2$ we can write the recurrence relation

$$\psi_n(M) = \sum_{m=0}^{n} F_m \psi_{n-m}(M-1). \tag{D.5}$$

From equations (D.3), (D.4) and (D.5) we can compute the generating functions

$$U(z) = \frac{1 - F(z)}{1 - z} \tag{D.6}$$

$$\psi_z(M) = [F(z)]^{M-1}. \tag{D.7}$$

Now, the probability $\phi_n(M)$ of M visits in n steps is equal to the probability that the M-th visit has occurred at step $k \leq n$, and then no other visit occurs up to time n:

$$\phi_n(M) = \sum_{m=0}^{n} \psi_k(M) U_{n-m}, \tag{D.8}$$

hence its generating function reads

$$\phi_z(M) = F^{M-1}(z)\frac{1-F(z)}{1-z}. \tag{D.9}$$

The generating function of the mean number of visits is

$$\langle M(z)\rangle = \sum_{M=1}^{\infty} M\phi_z(M) = \frac{1}{1-z}\frac{1}{1-F(z)} \tag{D.10}$$

and since we know the relation between $F(z)$ and $P(z)$, Eq. (4.15), and the form that $P(z)$ must assume, Eq. (4.16), we have

$$\langle M(z)\rangle = \frac{1}{(1-z)^{1+\rho}}H\left(\frac{1}{1-z}\right), \tag{D.11}$$

and the Tauberian theorem implies:

$$\langle M_n\rangle \sim \frac{1}{\Gamma(1+\rho)}n^{\rho}H(n), \tag{D.12}$$

which is valid for $0 \leq \rho \leq 1$. We conclude that the random variable T_n represents, up to a constant factor, the asymptotic value of the occupation time of the origin rescaled for its mean value:

$$T_n \sim \frac{1}{\Gamma(1+\rho)}\frac{M_n}{\langle M_n\rangle}. \tag{D.13}$$

The relation between the survival and persistence probabilities and their asymptotic behaviour E

We consider the survival probability in the set of positive integers, A. Define

$$F_n = \Pr\{x_1 \neq 0, x_2 \neq 0, \ldots, x_n = 0 | x_0 = 0\} \tag{E.1}$$

$$Q_n = \Pr\{x_1 \geq 0, x_2 \geq 0, \ldots, x_n \geq 0 | x_0 = 0\} \tag{E.2}$$

$$U_n = \Pr\{x_1 \neq 0, x_2 \neq 0, \ldots, x_n \neq 0 | x_0 = 0\}, \tag{E.3}$$

with the initial conditions $F_0 = 0$, $Q_0 = 1$ and $U_0 = 1$, and the generating functions

$$F(z) = \sum_{n=1}^{\infty} F_n z^n \tag{E.4}$$

$$Q(z) = \sum_{n=0}^{\infty} Q_n z^n \tag{E.5}$$

$$U(z) = \sum_{n=0}^{\infty} U_n z^n. \tag{E.6}$$

It is easy to see that if the process is symmetric with respect to the two sets, the following relation holds:

$$2Q_n = \delta_{n,0} + U_n + \sum_{m=1}^{n} F_m Q_{n-m}. \tag{E.7}$$

By passing to the generating function we get

$$2Q(z) = 1 + U(z) + F(z)Q(z) \tag{E.8}$$

and by using Eq. (D.6) in appendix D, after some algebra we obtain

$$Q(z) = \frac{1 + U(z)}{1 + (1 - z)\, U(z)}. \tag{E.9}$$

To show that $Q(z)$ and $U(z)$ have the same $z \to 1$ behaviour, we use a result by Karamata [61]: if $L(x)$ is a slowly varying function, then for any $\gamma > 0$:

$$\lim_{x \to \infty} x^{-\gamma} L(x) = 0 \tag{E.10}$$

$$\lim_{x \to \infty} x^{\gamma} L(x) = \infty. \tag{E.11}$$

We showed in the main text, Eq. (4.44), that $U(z)$ is of the form:

$$U(z) = \frac{1}{(1-z)^{1-\rho}} L\left(\frac{1}{1-z}\right), \tag{E.12}$$

therefore, as $z \to 1$, $U(z)$ diverges and $(1-z)U(z)$ converges to 0. For $\rho = 0$ we still have the divergence of $U(z)$, but we cannot use the previous result by Karamata for $(1-z)U(z)$, because

$$(1-z)U(z) = L\left(\frac{1}{1-z}\right). \tag{E.13}$$

However, since in this case

$$F(z) = 1 - L\left(\frac{1}{1-z}\right) \tag{E.14}$$

and recurrence implies $F(z) \to 1$, we still have $(1-z)U(z) \to 0$. Hence, it follows from Eq. (E.9) that $Q(z) \sim U(z)$ for any $0 \leq \rho < 1$.

Evaluation of the Lamperti parameter for the Gillis random walk F

The strategy is to make use of the transformation formulas of Appendix A in order to put the generating function $P(z)$, Eq. (4.47) in the main text, in the form:

$$P(z) = \frac{1}{(1-z)^{\nu}} H\left(\frac{1}{1-z}\right), \tag{F.1}$$

where $H(x)$ is a slowly-varying function. Now, since the generating function $P(z)$

$$P(z) = \frac{{}_2F_1\left(\frac{1}{2}\epsilon + 1, \frac{1}{2}\epsilon + \frac{1}{2}; 1; z^2\right)}{{}_2F_1\left(\frac{1}{2}\epsilon, \frac{1}{2}\epsilon + \frac{1}{2}; 1; z^2\right)} \tag{F.2}$$

is a function of z^2, for the sake of simplicity we consider

$$\begin{aligned} P\left(\sqrt{z}\right) \equiv \Pi(z) &= \sum_{n=0}^{\infty} \varpi_n z^n \\ &= \frac{{}_2F_1\left(\frac{1}{2}\epsilon + 1, \frac{1}{2}\epsilon + \frac{1}{2}; 1; z\right)}{{}_2F_1\left(\frac{1}{2}\epsilon, \frac{1}{2}\epsilon + \frac{1}{2}; 1; z\right)}, \end{aligned} \tag{F.3}$$

so that the n-th coefficient ϖ_n corresponds to P_{2n}. It is easy to show that if $P(z)$ is of the form

$$P(z) = \frac{1}{(1-z)^{\rho}} H\left(\frac{1}{1-z}\right), \tag{F.4}$$

then also $\Pi(z)$ can be written as

$$\Pi(z) = \frac{1}{(1-z)^{\rho}} G\left(\frac{1}{1-z}\right), \tag{F.5}$$

where $G(x)$ is slowly-varying and related to $H(x)$ by

$$G(x) = \frac{1}{x^{\rho}\left(1 - \sqrt{1 - \frac{1}{x}}\right)^{\rho}} H\left(\frac{1}{1 - \sqrt{1 - \frac{1}{x}}}\right). \tag{F.6}$$

This means that the transformation does not change the exponent ρ. By using Eq. (F.3) we obtain the following results:

1) In the case $\epsilon = -\frac{1}{2}$ we get

$$\Pi(z) = G\left(\frac{1}{1-z}\right), \tag{F.7}$$

where the slowly-varying function is

$$G(x) = \frac{\sum_{n=0}^{\infty} \frac{(3/4)_n (1/4)_n}{(n!)^2} (x)^{-n} \left[2\psi(n+1) - \psi\left(\frac{3}{4}+n\right) - \psi\left(\frac{1}{4}+n\right) + \log(x)\right]}{4 + \frac{1}{4}\sum_{n=0}^{\infty} \frac{(3/4)_n (5/4)_n}{n!(n+1)!} (x)^{-n-1} \left[\log(x) + \psi(n+1) + \psi(n+2) - \psi\left(\frac{3}{4}+n\right) - \psi\left(\frac{5}{4}+n\right)\right]};$$

2) In the range $\epsilon \in \left(-\frac{1}{2}, \frac{1}{2}\right)$ the generating function has the form

$$\Pi(z) = \frac{1}{(1-z)^{1/2+\epsilon}} G\left(\frac{1}{1-z}\right) \tag{F.8}$$

with

$$G(x) = a_1 \frac{{}_2F_1\left(-\frac{1}{2}\epsilon, \frac{1}{2} - \frac{1}{2}\epsilon; \frac{1}{2} - \epsilon; \frac{1}{x}\right) + a_2 x^{-1/2-\epsilon}\, {}_2F_1\left(\frac{1}{2}\epsilon + 1, \frac{1}{2}\epsilon + \frac{1}{2}; \frac{3}{2} + \epsilon; \frac{1}{x}\right)}{{}_2F_1\left(\frac{1}{2}\epsilon, \frac{1}{2}\epsilon + \frac{1}{2}; \frac{1}{2} + \epsilon; \frac{1}{x}\right) + a_3 x^{-1/2+\epsilon}\, {}_2F_1\left(1 - \frac{1}{2}\epsilon, \frac{1}{2} - \frac{1}{2}\epsilon; \frac{3}{2} - \epsilon; \frac{1}{x}\right)},$$

where a_1, a_2 and a_3 are numerical coefficients (depending on ϵ) which can be determined from formula (**??**);

3) For $\epsilon = \frac{1}{2}$ we have

$$\Pi(z) = \frac{1}{1-z} G\left(\frac{1}{1-z}\right) \tag{F.9}$$

where $G(x)$ has the expression

$$G(x) = \frac{4 - \frac{1}{4}\sum_{n=0}^{\infty} \frac{(5/4)_n (3/4)_n}{n!(n+1)!} (x)^{-n-1} \left[\log(x) + \psi(n+1) + \psi(n+2) - \psi\left(\frac{5}{4}+n\right) - \psi\left(\frac{3}{4}+n\right)\right]}{\sum_{n=0}^{\infty} \frac{(1/4)_n (3/4)_n}{(n!)^2} (x)^{-n} \left[2\psi(n+1) - \psi\left(\frac{1}{4}+n\right) - \psi\left(\frac{3}{4}+n\right) + \log(x)\right]};$$

4) Finally when $\epsilon \in \left(\frac{1}{2}, 1\right)$ the generating function has the same form as the previous case,

$$\Pi(z) = \frac{1}{1-z} G\left(\frac{1}{1-z}\right), \tag{F.10}$$

but with

$$G(x) = b_1 \frac{{}_2F_1\left(-\frac{1}{2}\epsilon, \frac{1}{2} - \frac{1}{2}\epsilon; \frac{1}{2} - \epsilon; \frac{1}{x}\right) + b_2 x^{-1/2-\epsilon}\, {}_2F_1\left(\frac{1}{2}\epsilon + 1, \frac{1}{2}\epsilon + \frac{1}{2}; \frac{3}{2} + \epsilon; \frac{1}{x}\right)}{{}_2F_1\left(1 - \frac{1}{2}\epsilon, \frac{1}{2} - \frac{1}{2}\epsilon; \frac{3}{2} - \epsilon; \frac{1}{x}\right) + b_3 x^{1/2-\epsilon}\, {}_2F_1\left(\frac{1}{2}\epsilon, \frac{1}{2}\epsilon + \frac{1}{2}; \frac{1}{2} + \epsilon; \frac{1}{x}\right)}$$

where once again b_1, b_2 and b_3 can be determined from Eq. (**??**).

We remark that if one wishes to go back to $P(z)$, it is now sufficient to recover the expression of $H(x)$ by using Eq. (F.6).

Bibliography

[1] M. Abramowitz and I. A. Stegun. *Handbook of mathematical functions*. Dover, New York, 1974.

[2] R. Artuso and R. Burioni. Anomalous diffusion: Deterministic and stochastic perspectives. In A. Vulpiani, F. Cecconi, M. Cencini, A. Puglisi, and D. Vergni, editors, *Large Deviations in Physics: The Legacy of the Law of Large Numbers*, pages 263–293. Springer, Berlin, 2014.

[3] R. Artuso, G. Cristadoro, M. Onofri, and M. Radice. Non-homogeneous persistent random walks and Lévy-lorentz gas. *J. Stat. Mech.*, 083209, 2018.

[4] L. Bachelier. Théorie de la spéculation. *Ann. Sci. Éc. Norm. Supér.*, 17:21, 1900.

[5] A. Bar, Y. Kafri, and D. Mukamel. Dynamics of DNA melting. *J. Phys. Condens. Matter*, 21:034110, 2009.

[6] E. Barkai. Residence time statistics for normal and fractional diffusion in a force field. *J. Stat. Phys.*, 123:883, 2006.

[7] E. Barkai, V. Fleurov, and J. Klafter. One-dimensional stochastic Lévy-Lorentz gas. *Phys. Rev. E*, 61:1164, 2000.

[8] P. Barthelemy, J. Bertolotti, and D. S. Wiersma. A Lévy flight for light. *Nature*, 453:495, 2008.

[9] C. W. J. Beenakker, C. W. Groth, and A. R. Akhmerov. Nonalgebraic length dependence of transmission through a chain of barriers with a Lévy spacing distribution. *Phys. Rev. B*, 79:024204, 2009.

[10] G. Bel and E. Barkai. Occupation time and ergodicity breaking in biased continuous time random walks. *J. Phys.: Condens. Matter*, 17:S4287, 2005.

[11] G. Bel and E. Barkai. Weak ergodicity breaking in the continuous-time random walk. *Phys. Rev. Lett.*, 94:240602, 2005.

[12] A. Bianchi, G. Cristadoro, M. Lenci, and M. Ligabò. Random walks in a one-dimensional Lévy random environment. *J. Stat. Phys.*, 163:22, 2016.

[13] A. Bianchi, M. Lenci, and F. Pène. Continuous-time random walk between Lévy-spaced targets in the real line. *Stocastic Process. Appl.*, 130:708, 2020.

[14] R. A. Blythe and A. J. McKane. Stochastic models of evolution in genetics, ecology and linguistics. *J. Stat. Mech.*, P07018, 2007.

[15] F. Bouchet and T. Dauxois. Prediction of anomalous diffusion and algebraic relaxations for long-range interacting systems, using classical statistical mechanics. *Phys. Rev. E*, 72:045103(R), 2005.

[16] A. J. Bray. Random walks in logarithmic and power-law potentials, nonuniversal persistence, and vortex dynamics in the two-dimensional *XY* model. *Phys. Rev. E*, 62:103, 2000.

[17] A. J. Bray, B. Derrida, and C. Godrèche. Non-trivial algebraic decay in a stable model of coarsening. *Europhys. Lett.*, 27:175, 1994.

[18] A. J. Bray, S. N. Majumdar, and G. Schehr. Persistence and first-passage properties in nonequilibrium systems. *Adv. Phys.*, 62:225, 2013.

[19] R. Brown. A brief account of microscopical observations made on the particles contained in the pollen of the plants. *Phil. Mag.*, 4:161, 1828.

[20] R. Burioni, L. Caniparoli, and A. Vezzani. Lévy walks and scaling in quenched disordered media. *Phys. Rev. E*, 81:060101(R), 2010.

[21] S. Burov and E. Barkai. Occupation time statistics in the quenched trap model. *Phys. Rev. Lett.*, 98:250601, 2007.

[22] A. Campa, T. Dauxois, and S. Ruffo. Statistical mechanics and dynamics of solvable models with long-range interactions. *Phys. Rep.*, 480:57, 2009.

[23] A. Caspi, R. Graner, and M. Elbaum. Enhanced diffusion in active intracellular transport. *Phys. Rev. Lett.*, 85:5655, 2000.

[24] P. Castiglione, A. Mazzino, P. Muratore-Ginanneschi, and A. Vulpiani. On strong anomalous diffusion. *Physica D*, 134:75, 1999.

[25] N. I. Chernov and R. Markarian. *Chaotic Billiards*. Providence, RI, American mathematical society, 2006.

[26] G. Cristadoro, T. Gilbert, M. Lenci, and D. P. Sanders. Transport properties of Lévy walks: an analysis in terms of multistate processes. *Europhys. Lett.*, 108:50002, 2014.

[27] P. Cvitanović, R. Artuso, R. Mainieri, G. Tanner, and G. Vattay. *Chaos: classical and quantum*. Niels Bohr Institut, Copenhagen, 2016.

[28] D. A. Darling and M. Kac. On occupation time for Markoff processes. *Trans. Am. Math. Soc.*, 84:444, 1957.

[29] A. Dechant, E. Lutz, E. Barkai, and D. A. Kessler. Solution of the Fokker-Planck equation with a logarithmic potential. *J. Stat. Phys.*, 145:1524, 2011.

[30] M. Dentz, A. Cortis, H. Scher, and B. Berkowitz. Time behavior of solute transport in heterogeneous media: transition from anomalous to normal transport. *Adv. Water Resources*, 27:155, 2004.

[31] C. P. Dettmann. Diffusion in the Lorentz gas. *Commun. Theor. Phys.*, 62:512, 2014.

[32] I. Dornic and C. Godrèche. Large deviations and nontrivial exponents in coarsening systems. *J. Phys. A: Math. Gen.*, 31:5413, 1998.

[33] P. Douglas, S. Gergamini, and F. Renzoni. Tunable Tsallis distributions in dissipative optical lattices. *Phys. Rev. Lett.*, 96:110601, 2006.

[34] J. M. Drouffe and C. Godrèche. Stationary definition of persistence for finite-temperature phase ordering. *J. Phys. A: Math. Gen.*, 31:9801, 1998.

[35] P. Ehrenfest and T Ehrenfest. Über zwei bekannte Einwännde gegen das Boltzamannsche H-Theorem. *Phys. Zeit.*., 8:311, 1907.

[36] A. Einstein. Über die von der molekular-kinetischen Theorie der Wärne geforderte Bewegung von in ruhenden Flüssigkeiten suspendierten Teilchen. *Ann. Phys.*, 322:549, 1905.

[37] W. Feller. Fluctuation theory of recurrent events. *Trans. Am. Math Soc.*, 67:98–119, 1949.

[38] W. Feller. *An introduction to probability theory and its applications*, volume 1. Wiley, New York, 1968.

[39] W. Feller. *An introduction to probability theory and its applications*, volume 2. Wiley, New York, 1971.

[40] R. Fürth. Die Brownsche Bewegung bei Berücksichtigung einer Persistenz der Bewegungsrichtung. Mit Anwendungen auf die Bewegung lebender Infusorien. *Z. Phys.*, 2:244, 1920.

[41] C. W. Gardiner. *Handbook of Stochastic Methods for Physics, Chemistry and the Natural Sciences*. Springer, Berlin, 2003.

[42] J. Gillis. Centrally biased discrete random walk. *Quart. J. Math.*, 7:144, 1956.

[43] M. Giona. Lattice random walks: an old problem with a future ahead. *Phys. Scr.*, 93:095201, 2018.

[44] B. V. Gnedenko and A. N. Kolmogorov. *Limit distributions for sums of independent random variables*. Addison-Wesley, Cambridge, 1954.

[45] C. Godrèche and J. M. Luck. Statistics of the occupation time for renewal processes. *J. Stat. Phys.*, 104:489–524, 2001.

[46] C. Godrèche, S. N. Majumdar, and G. Schehr. Record statistics of a strongly correlated time series: random walks and Lévy flights. *J. Phys. A: Math. Theor.*, 50:333001, 2017.

[47] S. Goldstein. On diffusion by discontinuous movements, and on the telegraph equation. *Q. J. Mech. Appl. Math.*, 4:129, 1951.

[48] M. C.. González, C. A. Hidalgo, and A.-L. Barabási. Understanding individual human mobility patterns. *Nature*, 453:779, 2008.

[49] P. Grassberger. Velocity autocorrelations in a simple model. *Physica A*, 103:558, 1980.

[50] F. Guarnieri, W. Moon, and J. S. Wettlaufer. Solution of the Fokker-Planck equation with a logarithmic potential and mixed eigenvalue spectrum. *J. Math. Phys.*, 58:093301, 2017.

[51] J. W. Haus and K. W. Kehr. Diffusion in regular and disordered lattices. *Phys. Rep.*, 150:263, 1987.

[52] Y. He, S. Burov, R. Metzler, and E. Barkai. Random time-scale invariant diffusion and transport coefficients. *Phys. Rev. Lett.*, 101:058101, 2008.

[53] O. Hirschberg, D. Mukamel, and G. M. Schütz. Approach to equilibrium of diffusion in a logarithmic potential. *Phys. Rev. E*, 84:041111, 2011.

[54] F. Höfling and T. Franosch. Anomalous transport in the crowded world of biological cells. *Rep. Prog. Phys.*, 76:046602, 2013.

[55] O. Hryniv, M. V. Menshikov, and A. R. Wade. Excursions and path functionals for stochastic processes with asymptotically zero drifts. *Stochastic Process. Appl.*, 123:1891, 2013.

[56] B. D. Hughes. On returns to the starting site in lattice random walks. *Physica A*, 134:443–457, 1986.

[57] B. D. Hughes. *Random walks in random environments. Volume 1: Random walks*, volume 1. Clarendon press, Oxford, 1995.

[58] B. D. Hughes. *Random walks in random environments. Volume 2: Random environments*, volume 2. Clarendon press, Oxford, 1996.

[59] M. Kac. Random walk and the theory of Brownian motion. *Am. Math. Mon.*, 54:369, 1947.

[60] M. Kac. A stochastic model related to the telegrapher's equation. *Rocky Mt. J. Math.*, 4:497, 1974.

[61] J. Karamata. Some theorems concerning slowly varying functions. Technical Report 369, Mathematics Research Centre, University of Wisconsin, Madison, 1962.

[62] D. A. Kessler and E. Barkai. Infinite covariant density for diffusion in logarithmic potentials and optical lattices. *Phys. Rev. Lett.*, 105:120602, 2010.

[63] J. Klafter and I. M. Sokolov. *First steps in random walks*. Oxford university press, Oxford, 2011.

[64] N. Korabel and E. Barkai. Anomalous infiltration. *J. Stat. Mech.*, P05022, 2011.

[65] P. L. Krapivsky, E. Ben-Naim, and S. Redner. Kinetics in heterogeneous single-species annihilation. *Phys. Rev. E*, 50:2474, 1994.

[66] J. Krug. Population genetics and evolution. arXiv:1803:08474, 2018.

[67] T. Kühn, T. O. Ihalainen, J. Hyväluoma, N. Dross, S. F. Willman, J. Langowski, M. Vihinen-Ranta, and J. Timonen. Protein diffusion in mammalian cell cytoplasm. *PLoS ONE*, 6:e22962, 2011.

[68] J. Lamperti. An occupation time theorem for a class of stochastic processes. *Trans. Am. Math Soc.*, 88:380–387, 1958.

[69] J. Lamperti. Criteria for the recurrence or transience of stochastic process. I. *J. Math. Anal. and Appl.*, 1:314, 1960.

[70] J. Lamperti. Criteria for stochastic processes II: Passage-time moments. *J. Math. Anal. and Appl.*, 7:127, 1963.

[71] P. Lançon, G. Batrouni, L. Lobry, and N. Ostrowsky. Drift without flux: Brownian walker with a space-dependent diffusion coefficient. *Europhys. Lett.*, 54:28, 2001.

[72] P. Lançon, G. Batrouni, L. Lobry, and N. Ostrowsky. Brownian walker in a confined geometry leading to a space-dependent diffusion coefficient. *Physica A*, 304:65, 2002.

[73] P. Langevin. Sur la théorie du mouvement brownien. *C. R. Acad. Sci. (Paris)*, 146:530, 1908.

[74] N. Leibovich and E. Barkai. Infinite ergodic theory for heterogeneous diffusion processes. *Phys. Rev. E*, 99:042138, 2019.

[75] M. Lenci. Typicality of recurrence for Lorentz gases. *Ergod. Theor. Dynam. Syst.*, 26:799, 2006.

[76] E. Levine, D. Mukamel, and G. M. Schütz. Long-range attraction between probe particles mediated by a driven fluid. *Europhys. Lett.*, 70:565, 2005.

[77] P. Lévy. Sur certains processus stochastiques homogènes. *Compos. Math.*, 7:283, 1939.

[78] L. Lewin. *Polylogarithms and Associated Functions*. Elsevier, New York, 1981.

[79] C.-C. Lo, L. A. Nunes Amaral, S. Havlin, P. Ch. Ivanov, T. Penzel, J.-H. Peter, and H. E. Stanley. Dynamics of sleep-wake transitions during sleep. *Europhys. Lett.*, 57:625, 2002.

[80] H. A. Lorentz. The motion of electrons in metallic bodies I. *KNAW. Proceedings*, 7:438, 1905.

[81] E. Lutz. Power-law tail distributions and nonergodicity. *Phys. Rev. Lett.*, 93:190602, 2004.

[82] M. Magdziarz, H. P. Scheffler, P. Straka, and P. Zebrowski. Limit theorems and governing equations for Lévy walks. *Stochastic Process. Appl.*, 125:4021, 2015.

[83] S. N. Majumdar, A. J. Bray, S. J. Cornell, and C. Sire. Global persistence exponent for nonequilibrium critical dynamics. *Phys. Rev. Lett.*, 77:3704, 1996.

[84] S. N. Majumdar and C. Sire. Survival probability of a gaussian non-Markovian process: application to the $T = 0$ dynamics of the Ising model. *Phys. Rev. Lett.*, 77:1420, 1996.

[85] G. S. Manning. Limiting laws and counterion condensation in polyelectrolyte solutions I. Colligative properties. *J. Chem. Phys.*, 51:924, 1969.

[86] S. Marksteiner, K. Ellinger, and P. Zoller. Anomalous diffusion and lévy walks in optical lattices. *Phys. Rev. A*, 53:3409, 1996.

[87] E. Martin, U. Behn, and G. Germano. First-passage and first-exit times of a bessel-like stochastic process. *Phys. Rev. E*, 83:051115, 2011.

[88] A. Mashanova, T. H. Oliver, and V. A. A. Jansen. Evidence for intermittency and a truncated power law from highly resolved aphid movement data. *J. R. Soc. Interface*, 7:199, 2010.

[89] R. Metzler, J. H. Jeon, A. G. Cherstvy, and E. Barkai. Anomalous diffusion models and their properties: non-stationarity, non-ergodicity, and ageing at the centenary of single particle tracking. *Phys. Chem. Chem. Phys.*, 16:24128, 2014.

[90] R. Metzler and J. Klafter. The random walk' s guide to anomalous diffusion: A fractional dynamics approach. *Phys. Rep.*, 339:1, 2000.

[91] J. Mittal, T. M. Truskett, J. R. Errington, and G. Hummer. Layering and position-dependent diffusive dynamics of confined fluids. *Phys. Rev. Lett.*, 100:145901, 2008.

[92] E. W. Montroll and G. H. Weiss. Random walks on lattices. II. *J. Math. Phys.*, 6:167, 1965.

[93] P. A. P. Moran. Random processes in genetics. *Proc. Camb. Philos. Soc*, 54:60, 1958.

[94] C. St J. A. Nash-Williams. Random walk and electric currents in networks. *Math. Proc. Camb. Philos. Soc*, 55:181, 1959.

[95] K. Oerding, S. J. Cornell, and A. J. Bray. Non-Markovian persistence and nonequilibrium critical dynamics. *Phys. Rev. E*, 56:R25, 1997.

[96] B. Oksendal. *Stochastic Differential Equations: An Introduction with Applications*. Springer science & business media, Berlin, 2013.

[97] M. Onofri, G. Pozzoli, M. Radice, and R. Artuso. Exploring the Gillis model: a discrete approach to diffusion in logarithmic potentials. *J. Stat. Mech.*, 113201, 2020.

[98] A. Pérez-Madrid, J. M. Rubí, and P. Mazur. Brownian motion in the presence of a temperature gradient. *Physica A*, 212:231, 1994.

[99] H. Pollard. The completely monotic characterof the Mittag-Leffler function $E_\alpha(-x)$. *Bull. Amer. Math. Soc.*, 54:1115, 1948.

[100] M. Radice, M. Onofri, R. Artuso, and G. Cristadoro. Transport properties and ageing for the averaged Lévy-lorentz gas. *J. Phys. A: Math. Theor.*, 53:025701, 2019.

[101] M. Radice, M. Onofri, R. Artuso, and G. Pozzoli. Statistics of occupation times and connection to local properties of nonhomogeneous random walks. *Phys. Rev. E*, 101:042103, 2020.

[102] S. Redner. *A guide to first-passage processes*. Cambridge University Press, Cambridge, 2001.

[103] S. Regev, N. Grønbech-Jensen, and O. Farago. Isothermal langevin dynamics in systems with power-law spatially dependent friction. *Phys. Rev. E*, 94:012116, 2016.

[104] E. Renshaw and R. Henderson. The correlated random walk. *J. Appl. Prob.*, 18:403, 1981.

[105] H. Scher and E. W. Montroll. Anomalous transit-time dispersion in amorphous solids. *Phys. Rev. B*, 12:2455, 1975.

[106] H. Scher, G. Morgolin, R. Metzler, J. Klafter, and B. Berkowitz. The dynamical foundation of fractal stream chemistry: The origin of extremely long retention times. *Geophys. Res. Lett.*, 29:1061, 2002.

[107] J. H. P. Schulz, E. Barkai, and R. Metzler. Aging renewal theory and application to random walks. *Phys. Rev. X*, 4:011028, 2014.

[108] M. F.. Shlesinger, B. J. West, and J. Klafter. Lévy dynamics for enhanced diffusion: application to turbulence. *Phys. Rev. Lett.*, 58:1100, 1987.

[109] M. Smoluchowski. Zur kinetischen theorie der Brownsche molekularbewegung und der suspensionen. *Ann. Phys.*, 326:756, 1906.

[110] E. Sparre-Andersen. On the fluctuations of sums of random variables II. *Math. Scand.*, 2:194, 1954.

[111] D. Stauffer. Ising spinodal decomposition at $T = 0$ in one to five dimensions. *J. Phys. A: Math. Gen.*, 27:5029, 1994.

[112] D. Szász and B. Tóth. Persistent random walks in a one-dimensional random environment. *J. Stat. Phys.*, 37:27, 1984.

[113] G. I. Taylor. Diffusion by continuous movements. *Proc. London Math. Soc.*, 20:196, 1922.

[114] M. Thaler and R. Zweimüller. Distributional limit theorems in infinite ergodic theory. *Probab. Theory Relat. Fields*, 135:15, 2006.

[115] Z. Toroczkai, T. J. Newman, and S. Das Sarma. Sign-time distribution for interface growth. *Phys. Rev. E*, 60:R1115(R), 1999.

[116] N. G. van Kampen. *Stochastic Processes in Physics and Chemistry*. Elsevier, Amsterdam, 2007.

[117] C. L. Vestergaard, P. C. Blainey, and H. Flyvbjerg. Single-particle trajectories reveal two-state diffusion-kinetics of hOGG1 proteins on DNA. *Nucleic Acids Res.*, 46:2446, 2018.

[118] A. Vezzani, E. Barkai, and R. Burioni. Single-big-jump principle in physical modeling. *Phys. Rev. E*, 100:012108, 2019.

[119] G. H. Weiss. Some applications of persistent random walks and the telegrapher's equation. *Physica A*, 311:381, 2002.

[120] B. Yurke, A. N. Pargellis, S. N. Majumdar, and C. Sire. Experimental measurement of the persistence exponent of the planar Ising model. *Phys. Rev. E*, 56:R40, 1997.

[121] V. Zaburdaev, S. Denisov, and J. Klafter. Lévy walks. *Rev. Mod. Phys.*, 87:483–530, 2015.

[122] O. Zeitouni. Random walks in random environments. *J. Phys. A: Math. Gen.*, 39:R433, 2006.